University of Southampton

Faculty of Engineering and Physical Sciences

School of Chemistry

On the Cross-Correlated Relaxation of Homonuclear Spin Pairs

by

James William Whipham

ORCiD: 0000-0001-8283-2959

A thesis submitted for the degree of

Doctor of Philosophy

January 2023

UNIVERSITY OF SOUTHAMPTON

Abstract

FACULTY OF ENGINEERING AND PHYSICAL SCIENCES
SCHOOL OF CHEMISTRY

Doctor of Philosophy

On the cross-correlated relaxation of homonuclear spin pairs

by James William Whipham

When a spin ensemble is perturbed from thermal equilibrium, it may return to such a state via a variety of incoherent mechanisms. This process is referred to as relaxation, the theory of which has been of intense interest in the fields of nuclear magnetic resonance (NMR), among others. This thesis considers the cross-correlated mechanisms of second-rank interactions, restricting the treatment to the intrapair dipole-dipole and symmetric chemical shift anisotropy.

After reviewing the mathematical and quantum mechanical requirements, our focus is directed to spin relaxation theory, and specifically on how one may describe the effects of anisotropic rotational diffusion of the host molecule has on the spin system. This is applied to the description of spectral line shape in a near-equivalent system exhibiting asymmetric broadening in its NMR spectrum. This leads naturally to consider longitudinal and singlet-order relaxation.

Contents

Abbreviation/Symbol	Definition
$\|V\rangle$	Ket-vector in a Hilbert space
$\langle V\|$	Bra-vector in a Hilbert space
$\forall$	*forall*
$\in$	*belongs to*
i	$\sqrt{-1}$
$*$	Complex conjugate
$\dagger$	Adjoint operation
$\mathbb{C}$	Set of complex numbers
$\mathbb{R}$	Set of real numbers
$\mathcal{H}_d$	Hilbert space of dimension d
$\mathcal{L}_D$	Liouville space of dimension D
$\|Q)$	Ket-vector in Liouville space
$(Q\|$	Bra-vector in Liouville space
$\hat{A}$	Superoperator in Liouville space
NMR	Nuclear magnetic resonance
QM	Quantum mechanics
Y_{lm}	Spherical harmonics
ρ	A density operator
ω_0	Larmor frequency
$R_\phi(\theta)$	Rotation operator with phase ϕ and angle θ
$D^{(k)}_{qq'}(\Omega)$	Wigner function parameterised by the set Ω
γ	Magnetogyric ratio
I_ζ	Spin operator for component ζ
T_{kq}	Irreducible spherical tensor operator of rank-k and order-q
$C^{jj'k}_{mm'q}$	Clebsch-Gordan coefficients
$\{\alpha, \beta, \gamma\}$	The set of Euler angles
Λ	Spin interaction
H_Λ	Spin Hamiltonian for interaction Λ
$\hat{L}$	Liouvillian
$\tilde{A}$	Operator in the interaction picture
$\mathcal{D}[S_j, S_k]$	Dissipator involving operators S_j and S_k
A^Λ_{kq}	Spatial component of interaction Λ
X_{kq}	Spin component of interaction Λ
$G^k_{qm}(\tau)$	time-correlation function
$J^{\Lambda\Lambda'}_{kq}(\omega_0)$	Spectral density function

Abbreviation/Symbol	**Definition**
P-frame	Principal axis system
D-frame	Diffusion frame
M-frame	Molecular frame
DD	Intrapair dipole-dipole coupling
CSA	Chemical shift anisotropy
b_{ij}	DD coupling constant
δ_{iso}	Isotropic chemical shift
δ_j^{CSA}	Chemical shift anisotropy for spin j
$\tau_\perp$	Correlation time
$D_\perp$, $D_\parallel$	Diffusion tensor components with respect to the z-principal axis
$\hat{\Gamma}$	Relaxation superoperator
$\mathbb{B}_Q$	Singlet-triplet product basis
T_1	Longitudinal relaxation time constant
T_{S}	Singlet-order relaxation time constant
Q_+	$\big\vert\vert T'_0\big\rangle\big\langle T'_{+1}\vert\big)$
Q_-	$\big\vert\vert T'_{-1}\big\rangle\big\langle T'_0\vert\big)$
τ, τ_{LF}	Delay at high- and low-field, respectively.
ZQ	Zero-quantum
$\mathbb{ST}_0$	A set of linearly-independent orthonormal zero-quantum operators

Declaration of Authorship

I declare that this thesis and the work presented in it is my own and has been generated by me as the result of my own original research.

I confirm that:

1. This work was done wholly or mainly while in candidature for a research degree at this University;
2. Where any part of this thesis has previously been submitted for a degree or any other qualification at this University or any other institution, this has been clearly stated;
3. Where I have consulted the published work of others, this is always clearly attributed;
4. Where I have quoted from the work of others, the source is always given. With the exception of such quotations, this thesis is entirely my own work;
5. I have acknowledged all main sources of help;
6. Where the thesis is based on work done by myself jointly with others, I have made clear exactly what was done by others and what I have contributed myself;
7. Parts of this work have been published as:
    - J. W. Whipham, G. A. I. Moustafa, M. Sabba, W. Gong, C. Bengs, M. H. Levitt, *J. Chem. Phys.* **2022**, *157*, 104112.

Signed: Date:

Acknowledgements

I'll begin with my supervisor, colleagues, friends, and lecturers. Firstly, I must thank Malcolm H. Levitt for his supervision throughout the project; he has the mysterious ability to know the answer to a problem before I've even done anything. He has also shown what crystal clear thinking and pedagogical explaining really is; two things I've strived to replicate over the course of my education in Southampton. I must also greatly acknowledge Laurynas Dagys for his friendship, the laughs, technical advice, and making the difficult times much more manageable than they would otherwise be. I thank Christian Bengs for many of the same reasons; his friendship and technical expertise have made the PhD a pleasant experience. And cheers to both for the banter, which is probably too close to the edge to reproduce here. Thank you also to George Bacanu; a friend I have know since our days in Manchester. His infectious enthusiasm never fails to remind one of why we might want to be scientists in the first place. I also thank Mohamed Sabba, for always taking the time to explain theoretical and experimental concepts. He was the one who noticed the aymmetrical line shape in the triyne spectrum in the first place, and ran the $^{13}C_2$-DAND spectrum shown in chapter 4. Acknowledgements are also extended to Gamal Moustafa, for being able to synthesise whatever molecule we conjure up, and synthesising the triyne derivative. The rest of the whole Levitt group is to be acknowledged; Oksana Bondar, Murari Soundararajan, Bonifac Legrady, Harry Harbor Collins, and Urvashi Heramun. I also acknowledge my lecturers Giuseppe Pileio, Marcel Utz, and Joern Werner for creating an intellectually stimulating environment.

I would like to end this with personal acknowledgements. I must express gratitude to my father, Steve, for his immense support from the very beginning of my undergraduate days, and his cheerful nature and perspectives when they're needed the most. It's evident that he is truly proud of each one of his children. I must also thank my late mother, Linda, for always letting us know that we can be the best at whatever we choose to be, and was the reason I had the confidence to drop my pencils and charcoal sticks for the pursuit of science in the first place.

I must mention and thank each one of my siblings; Louise, Tom, and Alex. Louise for always providing thoughtful advice, paying attention when I speak of my work, and listening to me rhapsodise about about my interests (even if she'd take Mendelssohn over Mahler, and Brahms over Bartók). Tom for always expressing enthusiasm in everything – including this thesis – and being the most laid back character one could fathom, whilst having the most deafening – yet infectious – laugh. Alex for being the family man he is, and for always asking what I think when considering complicated matters, whether scientific or not; these moments really do mould one's perspectives. I

must also thank our extended family, Becky and Lauren, for their kind consideration of my schedule. I must mention the kids here; Arlo, Shelby and Noah. They have the wonderful and innate ability to make anyone forget spins even exist... even though Noah has done nothing more than grow his own tooth...

Finally, I cannot express enough appreciation to Catalina, for reasons she already knows.

To Steve, Linda, and myself...

Chapter 1

Mathematical Formalism

As are many works covering linear algebra, this chapter is a flamboyant list of definitions. The beauty of linear algebra lies in elegant mathematics resulting from a set of self-contained and intuitive axioms, which behave as an extension of the basic arithmetic we're all familiar with. In the mathematical description of an NMR experiment, we are effectively exploring a vector space by mapping one vector onto another via unitary transformations. When describing the relaxation dynamics after applying some perturbation to the system, vectors are mapped onto others via non-unitary transformations. With this in mind, we will now briefly review the mathematics of linear vector spaces, with an extension from a state (Hilbert) space to an operator (Liouville) space.

1.1 Linear vector spaces

An *abstract vector space* consists of,

- A set $\mathbb{V}$, with elements called *vectors*
- A set $\mathbb{F}$ of scalars (the *field*)
- Operations addition and multiplication, which are closed[1] and satisfy the following axioms:
  1. $|V\rangle + |W\rangle = |W\rangle + |V\rangle \quad \forall\, |V\rangle, |W\rangle \in \mathbb{V}$ *commutativity*
  2. $|V\rangle + (|W\rangle + |X\rangle) = (|V\rangle + |W\rangle) + |X\rangle \quad \forall\, |V\rangle, |W\rangle, |X\rangle \in \mathbb{V}$ *associativity*
  3. There exists a *null vector* $|0\rangle \in \mathbb{V}$, such that $|V\rangle + |0\rangle = |V\rangle \quad \forall\, |V\rangle \in \mathbb{V}$
  4. $\forall\, |V\rangle \in \mathbb{V}$ there is a vector $|-V\rangle$ such that $|V\rangle + |-V\rangle = |0\rangle$
  5. $c\,(|V\rangle + |W\rangle) = c\,|V\rangle + c\,|W\rangle \quad \forall\, |V\rangle, |W\rangle \in \mathbb{V}$ and $c \in \mathbb{F}$ *distributivity*
  6. $1\,|V\rangle = |V\rangle \quad \forall\, |V\rangle \in \mathbb{V}$ *multiplication by 1*
  7. $(c_1 + c_2)\,|V\rangle = c_1\,|V\rangle + c_2\,|V\rangle$
  8. $(c_1 c_2)\,|V\rangle = c_1\,(c_2\,|V\rangle)$

A set of vectors is said to be *linearly independent* [1] if the only linear relation of the form,

$$\sum_i c_i\,|V_i\rangle = 0, \tag{1.1}$$

is trivial, when all $c_i = 0$. This leads directly to the definition of the *dimension* of the vector space, which is that a vector space with dimension d may accommodate a maximum of d linearly independent vectors. This itself allows us to define the concept of a *basis*; which is that any vector $|V\rangle$ in a d-dimensional space may be written as a linear combination of d linearly independent vectors,

$$|V\rangle = \sum_{i=1}^{d} c_i\,|i\rangle \quad \forall\, |V\rangle, |i\rangle \in \mathbb{V}, \quad c_i \in \mathbb{F} \tag{1.2}$$

where the set of linearly-independent vectors $\{|i\rangle\}_{i=1}^{d}$ is the basis, and scalars $\{c_i\}_{i=1}^{d}$ are components of vector $|V\rangle$ in basis $\{|i\rangle\}_{i=1}^{d}$.

[1] That is, addition and scalar multiplication produce another vector in $\mathbb{V}$.

1.1.1 Hilbert space

For our purposes, we will only be concerned with finite-dimensional spaces. A d-dimensional Hilbert space $\mathcal{H}_d$ is a *complex* linear vector space with a defined *scalar product* [2–4]. $\mathcal{H}_d$ is *complex* in the sense that the *field* is complex; i.e. $\{c_i\}_{i=1}^{d} \in \mathbb{C}$, and the *scalar product* is written as the *bracket*, $\langle\phi|\psi\rangle$, to which is assigned a complex number [5]. As is customary in quantum mechanics, the vectors in $\mathcal{H}_d$ are denoted with Greek letters. Often, the basis vectors will be denoted with Latin letters, particularly when used as an index to sum over. This will be context-dependent. Components will continue to be denoted $c_1, c_2, \cdots, c_d$.

For each *ket* vector in $\mathcal{H}_d$ is a direct correspondence with a *bra* vector in a *dual space*,

$$|\phi\rangle \overset{d.c.}{\longleftrightarrow} \langle\phi| \,, \tag{1.3}$$

and we write,

$$|\phi\rangle = \sum_{i=1}^{d} c_i \,|\phi_i\rangle \overset{d.c.}{\longleftrightarrow} \langle\phi| = \sum_{i=1}^{d} c_i^* \,\langle\phi_i| \,, \tag{1.4}$$

and the vectors $|\phi\rangle$ and $\langle\phi|$ are said to be the *adjoint* of each other. We find that we have, for the scalar product,

1. $\langle\phi|\psi\rangle = \langle\psi|\phi\rangle^*$
2. $\langle\phi| \left(\sum_{i=1}^{d} c_i \,|\psi_i\rangle\right) = \sum_{i}^{d} c_i \,\langle\phi|\psi_i\rangle$
3. $\langle\phi|\phi\rangle \geqslant 0 \quad \forall\, |\phi\rangle \in \mathcal{H}_d$

It follows from the last inequality above that if $\langle\phi|\phi\rangle = 0$ then $|\phi\rangle = |0\rangle$. From the first two, we have,

$$\left(\sum_{i}^{d} c_i^* \,\langle\phi_i|\right) |\psi\rangle = \sum_{i}^{d} c_i^* \,\langle\phi_i|\psi\rangle \,. \tag{1.5}$$

The scalar product vanishes for *orthogonal* vectors, $\langle\phi|\psi\rangle = 0$. For *orthonormal* vectors, we have,

$$\langle \phi_i | \phi_j \rangle = \delta_{ij} \equiv \begin{cases} 1 & \text{if} \quad i = j \\ 0 & \text{if} \quad i \neq j \end{cases}, \tag{1.6}$$

where δ_{ij} is the *Kronecker delta*. The norm of a vector in $\mathcal{H}_d$ is given by the root of the scalar product of a vector with itself,

$$\| \, |\phi\rangle \, \| = \sqrt{\langle \phi | \phi \rangle}. \tag{1.7}$$

Expressing vectors in $\mathcal{H}_d$ in an orthonormal basis $\{|i\rangle\}_{i=1}^{d}$ allows us to write,

$$|\phi\rangle = \sum_{i=1}^{d} |i\rangle\langle i|\phi\rangle \, , \tag{1.8}$$

and we see that the *completeness* relation, $\sum_{i=1}^{d} |i\rangle\langle i| = \mathbb{1}$ is obtained, where $\mathbb{1}$ is the *identity operator*. Taking the adjoint of both sides of eq. (1.8) gives the decomposition of the corresponding vector in the dual space,

$$\begin{aligned} \langle \phi | &= \left(\sum_{i=1}^{d} |i\rangle\langle i|\phi\rangle \right)^{\dagger} \\ &= \sum_{i=1}^{d} \langle \phi|i\rangle\langle i| \, , \end{aligned} \tag{1.9}$$

where $\dagger$ denotes the adjoint operation, and the relation $(|i\rangle\langle j|)^{\dagger} = |j\rangle\langle i|$ is used. Multiplying a vector by unity may seem trivial, and perhaps didn't need to be stated here or indeed expressed as an axiom, but we will see this is a useful tool in numerous scenarios. This leads us to the important topic of *operators*...

An operator maps a vector onto another in $\mathcal{H}_d$ [1]. *Linear operators* have the following properties [1–3]:

1. $A\left(c_1 \, |\phi_1\rangle + c_2 \, |\phi_2\rangle\right) = c_1 A \, |\phi_1\rangle + c_2 A \, |\phi_2\rangle$ *linearity*
2. $(A + B) \, |\phi\rangle = A \, |\phi\rangle + B \, |\phi\rangle$
3. $(AB) \, |\phi\rangle = A \left(B \, |\phi\rangle\right)$

4. $A\,|\phi_a\rangle = a\,|\phi_a\rangle$ eigenvector $|\phi_a\rangle$ *and* eigenvalue a *of* A

5. $\mathbb{1}\,|\phi\rangle = |\phi\rangle$ *identity operator*

and for inverse operators we have, $A^{-1}A = AA^{-1} = \mathbb{1}$. Operators will be represented with upper-case Latin letters.

Equation (1.8) led to the expression for the identity operator as a sum of *dyads* of elements of an orthonormal basis,

$$\mathbb{1} = \sum_{i=1}^{d} |i\rangle\langle i|\,, \tag{1.10}$$

sometimes called the completeness relation.

From this, it follows that all linear operators in $\mathcal{H}_d$ have a dyadic decomposition for the form,

$$\begin{aligned} A &= \sum_{i,j} |i\rangle\langle i|A|j\rangle\langle j| \\ &= \sum_{i,j} A_{ij}\,|i\rangle\langle j|\,, \end{aligned} \tag{1.11}$$

where $A_{ij} = \langle i|A|j\rangle$ are *matrix elements* of A. The adjoint of an operator becomes,

$$A^\dagger = \sum_{i,j} A^*_{ji}\,|j\rangle\langle i|\,, \tag{1.12}$$

and the matrix elements are given by the *complex-transpose* of the matrix representation of A.

An operator N is diagonalisable if there exists an orthonormal basis such that,

$$N|i\rangle = n_i|i\rangle, \quad n_i \in \mathbb{C}, \tag{1.13}$$

and the matrix elements of N may then be written,

$$\begin{aligned} N_{ij} &= \langle i|N|j\rangle \\ &= n_i\delta_{ij}, \end{aligned} \tag{1.14}$$

and from (1.8) and (1.11) N has *spectral decomposition*,

$$N = \sum_i n_i \left|i\right\rangle\!\left\langle i\right|, \quad n_i \in \mathbb{C}. \tag{1.15}$$

Hermitian operators are linear operators which are *self-adjoint*; i.e. $H^\dagger = H$. Hermitian operators have the property of being diagonalisable whilst having real eigenvalues, and thus may be decomposed as,

$$H = \sum_i r_i \left|i\right\rangle\!\left\langle i\right|, \quad r_i \in \mathbb{R}. \tag{1.16}$$

These properties lead to Hermitian operators having a particularly important role in quantum mechanics, and we will encounter them many times, and are often referred to as *observables*. An immensely important theorem of Hermitian operators is as follows: *Hermitian operators commute if, and only if, they have a common orthonormal basis of eigenvectors*. This theorem is integral to quantum mechanics and will be returned to in chapter 2.

A *positive operator* is defined as,

$$\left\langle\phi\right| A \left|\phi\right\rangle \geqslant 0 \quad \forall \left|\phi\right\rangle, \tag{1.17}$$

and the expectation value of operator A is real and non-negative. Then, *every positive operator is Hermitian* and has spectral decomposition,

$$A = \sum_i a_i \left|\phi_i\right\rangle\!\left\langle\phi_i\right|. \tag{1.18}$$

Examples of positive operators relevant to quantum mechanics and NMR are density operators.

Consider the decomposition given by eq. (1.8). We may rewrite this as,

$$\begin{aligned} \left|\phi\right\rangle &= \sum_i P_i \left|\phi\right\rangle \\ &= \sum_i c_i \left|i\right\rangle \end{aligned} \tag{1.19}$$

where $P_i = |i\rangle\langle i|$ is the *projection operator* [6] for ket $|i\rangle$; that is, P_i *projects out* the i^{th} component of a vector. P_i also acts on $\langle\phi|$ in the same way, projecting out component c_i^*. projection operators have the following properties:

1. $P^2 = P$ *idempotent*

2. $P^\dagger = P$ *Hermitian*

Density operators of *pure states* are projection operators [7]; something we will revisit in chapter 2.

A *unitary* linear operator has the property $U^\dagger = U^{-1}$. Unitary operators are diagonalisable and have the spectral decomposition [3],

$$U = \sum_j e^{i\phi_j} |j\rangle\langle j|, \quad \phi_j \in \mathbb{R}, \tag{1.20}$$

with eigenvalues which are *phase factors*, and $i \equiv \sqrt{-1}$ here. From the definition of the exponential of an operator,

$$e^A = \sum_{k=0}^{\infty} \frac{1}{k!} A^k, \tag{1.21}$$

and from (1.16) and (1.20), it follows immediately that $U(t) = e^{iHt}$, $t \in \mathbb{R}$, is unitary when H is Hermitian. Operators of the type $U(t) = e^{iHt}$ are important in quantum mechanics and NMR since *propagators* which act on wavefunctions and density operators take this form [6, 8, 9]. In this case, we also find that,

$$U(t=0) = \mathbb{1} \tag{1.22}$$

$$U(t_1)\, U(t_2) = U(t_1 + t_2), \tag{1.23}$$

when H at t_1 commutes with H at t_2.

The norm of a vector and the trace of an operator are invariant to *unitary transformations* $|\phi'\rangle = U|\phi\rangle$ and $A' = UAU^{-1}$. Using equation (1.7), we have,

$$\begin{aligned}\sqrt{\langle U\phi|U\phi\rangle} &= \sqrt{\langle\phi|\,U^{\dagger}U\,|\phi\rangle} \\ &= \sqrt{\langle\phi|\phi\rangle},\end{aligned} \tag{1.24}$$

and if $U^{\dagger} = U^{-1}$, we have $U^{\dagger}U = \mathbb{1}$. We may also write,

$$\begin{aligned}\mathrm{Tr}\left\{UAU^{-1}\right\} &= \mathrm{Tr}\left\{U^{-1}UA\right\} \\ &= \mathrm{Tr}\left\{A\right\},\end{aligned} \tag{1.25}$$

where the cyclical permutation property of the trace is used.

A *composite system* of state $|\phi\rangle$ and $|\psi\rangle$ is described by the tensor product,

$$\left|\phi^{A},\psi^{B}\right\rangle = \left|\phi^{A}\right\rangle \otimes \left|\psi^{B}\right\rangle \tag{1.26}$$

and belongs to a *composite Hilbert space*,

$$\mathcal{H}_{d}^{AB} = \mathcal{H}_{d_A}^{A} \otimes \mathcal{H}_{d_B}^{B}, \tag{1.27}$$

where $\left|\phi^{A}\right\rangle \in \mathcal{H}_{d_A}^{A}$ and $\left|\psi^{B}\right\rangle \in \mathcal{H}_{d_B}^{B}$. The associated bra vector has the form,

$$\left(\left|\phi^{A},\psi^{B}\right\rangle\right)^{\dagger} = \left\langle\phi^{A},\psi^{B}\right| = \left\langle\phi^{A}\right| \otimes \left\langle\psi^{B}\right|, \tag{1.28}$$

and belongs to the *dual composite space* of $\mathcal{H}_{d}^{AB}$.

If $\{|i\rangle\}_{i=1}^{d_A}$ is a basis for space $\mathcal{H}_{d_A}^{A}$ and $\{|j\rangle\}_{j=1}^{d_B}$ for space $\mathcal{H}_{d_B}^{B}$, then vector $\left|\phi^{AB}\right\rangle \in \mathcal{H}_{d}^{AB}$ may be decomposed as,

$$\left|\phi^{AB}\right\rangle = \sum_{i,j}^{d} c_{ij}\left|i^{A},j^{B}\right\rangle, \tag{1.29}$$

with the basis of $\mathcal{H}^{AB}$ given by $\left\{\left|i^{A},j^{B}\right\rangle\right\}_{i,j=1}^{d} = \left\{\left|i^{A}\right\rangle \otimes \left|j^{B}\right\rangle\right\}_{i,j=1}^{d}$. The dimension d of space $\mathcal{H}_{d}^{AB}$ is then given by $\left(\mathrm{dim}\mathcal{H}_{d_A}^{A}\right) \times \left(\mathrm{dim}\mathcal{H}_{d_B}^{B}\right)$. States which cannot be written as in eq. (1.26), but instead

by a superposition of such vectors, are called *entangled*. These states are of relevance to NMR (and specifically to us), since *singlet states* are entangled states.

The scalar product becomes,

$$\left\langle \phi^A, \psi^B | \theta^A, \chi^B \right\rangle = \left\langle \phi^A | \theta^A \right\rangle \left\langle \psi^B | \chi^B \right\rangle, \tag{1.30}$$

where the product is taken over the individual spaces. It follows that $\left\{ \left| i^A, j^B \right\rangle \right\}_{i,j=1}^{d}$ is an orthonormal basis if,

$$\left\langle i^A, j^B | i'^A, j'^B \right\rangle = \delta_{ii'} \delta_{jj'}; \tag{1.31}$$

i.e., if $\{|i\rangle\}_{i=1}^{d_A}$ and $\{|j\rangle\}_{i=1}^{d_B}$ are orthonormal bases.

If C^A and D^B are linear operators in $\mathcal{H}^A$ and $\mathcal{H}^B$, respectively, then a *product operator* is defined by the tensor product,

$$C^A \otimes D^B \equiv C^A D^B, \tag{1.32}$$

which acts on vectors in individual spaces analogously to the scalar product above. That is,

$$C^A D^B \left| \phi^A, \psi^B \right\rangle = \left| C^A \phi^A, D^B \psi^B \right\rangle, \tag{1.33}$$

which acts linearly in the usual sense and we write,

$$C^A D^B \sum_{i,j} c_{ij} \left| i^A, j^B \right\rangle = \sum_{i,j} c_{ij} \left| C^A i^A, D^B j^B \right\rangle. \tag{1.34}$$

The tensor product of vectors defined by eq. (1.26) is used in the theory of quantum mechanical angular momentum to couple state vectors belonging to different subspaces, and product operators are often used to monitor the spin dynamics of an NMR experiment [6, 9, 10].

1.1.2 Liouville space

The quantum mechanical description of NMR relies on the unitary and non-unitary dynamics of density operators [6, 11]. As such, it is useful to work in *Liouville space*, $\mathcal{L}_D$; the space of linear operators which act on $\mathcal{H}_d$. The vectors of $\mathcal{L}_D$ are denoted $|A)$, $|B)$, $\cdots$, and are the linear operators which act on $\mathcal{H}_d$ described in the previous section.

When working in Liouville space, the dyad decomposition in eq. (1.11) may be written [8],

$$|A) = \sum_{i,j=1}^{d} = A_{ij} \big| \, |i\rangle\langle j| \, \big), \tag{1.35}$$

and the dimension, D, of $\mathcal{L}_D$ is seen to be $(\dim \mathcal{H}_d)^2$.

The scalar product between operators in $\mathcal{L}_D$ is defined,

$$(A|B) = \mathrm{Tr}\left\{A^\dagger B\right\}. \tag{1.36}$$

Every operator may be decomposed in an orthonormal basis, giving the scalar product the following properties:

1. $(Q_i|Q_j) = \delta_{ij}$ *orthonormality*
2. $\sum_{i=1}^{D} |Q_i)\,(Q_i| = \mathbb{1}$ *completeness*
3. $\sum_{i=1}^{D} |Q_i)\,(Q_i|A)$ *spectral decomposition*

In terms of dyads, we have $\big(|i\rangle\langle j| \, \big| \, |i'\rangle\langle j'| \, \big) = \delta_{ii'}\delta_{jj'}$.

As in $\mathcal{H}_d$, we may define linear operators, called *superoperators*, which map vectors of $\mathcal{L}_D$ onto others. That is, superoperators act on the operators in the corresponding Hilbert space. The adjoint, Hermitian, positivity, and unitary properties of operators acting on $\mathcal{H}_d$ extend to $\mathcal{L}_D$.

Important superoperators in our case are the *commutation superoperator*, $\hat{C}\bullet = [C, \bullet]$, and *unitary transformation superoperator*, $\hat{U}\bullet = U \bullet U^{-1}$, which have the properties,

$$\hat{C}\,|Q) = \big[C, Q\big] \tag{1.37}$$

and,

$$\hat{U}\,|Q) = UQU^{-1}. \tag{1.38}$$

The former is important in describing how the spin system in question evolves temporally under coherent and incoherent interactions, whilst the latter is used in describing the rotation of a spin system.

Chapter 2

Quantum Mechanics

The cornerstone of any modern theoretical treatment of NMR is quantum mechanics (QM), and in particular the mathematical framework of *angular momentum* and *spin*. This is necessary, since we often must juggle with the algebra of rotations, of which angular momentum operators are the *generators*. Firstly, however, the postulates of QM are stated with some terseness, treating them as axioms in the sense that they are simply accepted. In NMR, we deal with an *ensemble* of spins; that is, a statistical mixture of spin states. The toolbox of chapter 1 is then used to develop the idea of a *density operator*, allowing us in turn to average populations and coherences over the entire ensemble. These nuclear spins must interact with their environment, though, giving rise to the structure of the NMR spectrum as well as relaxation phenomena. Relevant QM operators and their properties are discussed, and how they relate to these interactions. After these prerequisites, we close this chapter how we initially intended; with a thorough discussion of rotations, leaving us with relations used throughout the following chapters.

2.1 Postulates

The postulates presented here are those of non-relativistic QM, and consider a single particle only [2–4, 12].

Postulate 1 *The state of an isolated quantum system may be described by a normalised ket* $|\psi\rangle$ *in a complex Hilbert space* $\mathcal{H}_d$*. Such a state is referred to as a pure state.*

From this, the basis elements are all possible states of the system, as are superpositions of basis elements so long as the resultant ket is normalised.

Postulate 2 *All possible measurements in a quantum system are described by a Hermitian operator, called an observable, which may be time-dependent. The possible measured values of observable* A *are the associated eigenvalues* a_i *in orthonormal basis* $\{|u_i^g\rangle\}_{i=1}^d$*, defined by the eigenvalue equation,*

$$A\,|u_i^g\rangle = a_i\,|u_i^g\rangle\,, \tag{2.1}$$

where the superscript g *denotes the degree of degeneracy. That is, states associated with equal eigenvalues,* a_i*.*

The probability $p(a_i)$ of obtaining a_i when measuring A in a system of state $|\psi\rangle$ is equal to,

$$p(a_i) = \langle\psi|P_i|\psi\rangle\,, \tag{2.2}$$

where $P_i = \sum_g |u_i^g\rangle\langle u_i^g|$ is the projection operator which projects onto the *eigenspace* with eigenvalue a_i. Since $\sum_i P_i = \mathbb{1}$, it follows that the total probability equals unity, $\sum_i p(a_i) = \langle\psi|\psi\rangle = 1$, as expected. The *expectation value* for observable A is,

$$\begin{aligned}\langle A\rangle &= \sum_i p(a_i)a_i \\ &= \langle\psi|A|\psi\rangle\,.\end{aligned} \tag{2.3}$$

As eluded to in chapter 1, if observables $A, B, C, \cdots$ commute, they have a common set of eigenvectors. Thus, all observables may be measured to arbitrary precision. The set $A, B, C, \cdots$ is then called a *complete set of commuting observables.*

Postulate 3 *The state ket* $|\psi(t)\rangle$ *evolves in time according to the* time-dependent Schödinger equation*,*

$$i\hbar\frac{d}{dt}|\psi(t)\rangle = H(t)|\psi(t)\rangle, \tag{2.4}$$

where $H(t)$ *is the* Hamiltonian *(energy operator) of the quantum system, and* $i \equiv \sqrt{-1}$*.*

$|\psi(t)\rangle$ evolves via a unitary transformation between arbitrary times t_0 and t_1 according to,

$$|\psi(t)\rangle = U(t,t_0)|\psi(0)\rangle \tag{2.5}$$

,

where $U^\dagger(t,t_0) = U^{-1}(t,t_0)$, and has the properties, $U(t_0,t_0) = \mathbb{1}$ and $U(t_2,t_1)U(t_1,t_0) = U(t_2,t_0)$. The dynamic equation for this operator is,

$$i\hbar\frac{d}{dt}U(t,t_0) = H(t)U(t,t_0). \tag{2.6}$$

$\hbar$ in equations (2.4) and (2.6) is the *reduced Planck's constant*, having the value, $\hbar \simeq 1.05\times10^{-34}$ J s. From here on, this will be defined as $\hbar \equiv 1$.

2.2 The density operator

Up until now, the description of the state of the spin system has been to use pure states; that is, by vectors in the Hilbert space. A more general formalism to describe a quantum state would allow us to describe *mixed states*. Density operators allow such a treatment, and lead to a statistical description of an ensemble of states [7].

2.2.1 Pure states

The density operator for a pure state is defined as,

$$\rho \equiv |\psi\rangle\langle\psi|. \tag{2.7}$$

The following properties may be deduced immediately from this:

1. ρ is positive; i.e. $\langle\phi|\,\rho\,|\phi\rangle \geqslant 0\ \forall\,|\phi\rangle \in \mathcal{H}_d$

2. $\mathrm{Tr}\,\{\rho\} = 1$

3. ρ is idempotent; i.e. $\rho^2 = \rho$

As a consequence of the above properties, it follows that ρ is Hermitian, as well as $\mathrm{Tr}\left\{\rho^2\right\} = 1$, and the density operator for pure states is a projection operator. Making use of the decomposition $|\psi\rangle = \sum_i c_i\,|i\rangle$, we find,

$$\rho = \sum_{i,j=1}^{d} \rho_{ij}\,|i\rangle\langle j| \tag{2.8}$$

,

where $\rho_{ii} = |c_i|^2 \in \mathbb{R}_0^+$ are called *populations* and, from properties 1 and 2, are positive and sum to unity. $\rho_{ij} = c_i c_j^* \in \mathbb{C}$ $(i \neq j)$ are called *coherences*, and $\rho_{ij} = \rho_{ji}^*$ due to the Hermiticity of ρ.

We may obtain the expectation value of operator O using the orthonormal basis $\{|i\rangle\}$ of $\mathcal{H}_d$,

$$\begin{aligned}
\langle O\rangle &= \langle\psi|\,O\,|\psi\rangle \\
&= \sum_{i,j=1}^{d} \langle\psi|i\rangle\langle i|O|j\rangle\langle j|\psi\rangle \\
&= \sum_{i,j=1}^{d} \langle j|\,\rho\,|i\rangle\langle i|\,O\,|j\rangle \\
&= \sum_{j=1}^{d} \langle j|\,\rho O\,|j\rangle \\
&= \mathrm{Tr}\{\rho O\},
\end{aligned} \tag{2.9}$$

where the closure relation, $\sum_i |i\rangle\langle i| = \mathbb{1}$ has been used extensively, with $\mathbb{1}$ the identity operator.

The pure state is an idealisation, whereby all spin systems of the ensemble are in the same state. Thus, they may be described by the same state function, $|\psi_i\rangle$. This is different for mixed states.

2.2.2 Mixed states

For an ensemble in thermal equilibrium, we have a *mixed state*, and we may only be able to assign a probability p_k that a spin system in the ensemble is in state $|\psi_k\rangle$. The density operator for a mixed state becomes [6],

$$\rho \equiv \sum_k p_k \left|\psi_k\right\rangle\left\langle\psi_k\right|, \tag{2.10}$$

with $\sum_k p_k = 1$.

For a time-dependent $|\psi_k(t)\rangle$, (2.10) expands as,

$$\begin{aligned}\rho(t) &= \sum_k p_k \left|\psi_k(t)\right\rangle\left\langle\psi_k(t)\right| \\ &= \sum_k p_k \sum_{i,j} \rho_{ij}^{(k)}(t) \left|i\right\rangle\left\langle j\right| \\ &= \sum_{i,j} \overline{c_i(t) c_j^*(t)} \left|i\right\rangle\left\langle j\right|\end{aligned} \tag{2.11}$$

where the overbar denotes an ensemble average. The density operator of a mixed states has two of the three properties outlined above for a pure state:

1. ρ is positive for pure and mixed states
2. $\mathrm{Tr}\{\rho\} = 1$ for pure and mixed states

It follows that an operator must fulfill these two conditions to be a *density operator*. However, density operators of mixed states are not idempotent and,

$$\mathrm{Tr}\left\{\rho^2\right\} < 1. \tag{2.12}$$

We see that the density operator of a mixed state is no longer a projection operator due to lacking idempotency.

2.2.3 Equation of motion

Using the time-dependent Schrödinger equation, the unitary dynamics of $\rho(t)$ become,

$$\begin{aligned}\frac{d}{dt}\rho(t) &= \frac{d}{dt}U\rho(t_0)U^{-1} \\ &= -iHU\rho(t_0)U^{-1} + iU\rho(t_0)U^{-1}H \\ &= -i\big[H, \rho(t)\big],\end{aligned} \tag{2.13}$$

where $U \equiv U(t, t_0)$ and $\rho(t) = U(t, t_0)\rho(t_0)U^{-1}(t, t_0)$ have been used. Eq. (2.13) is often referred to as the *Liouville-von Neumann equation*. In Liouville space we write this as,

$$\frac{d}{dt}\big|\rho(t)\big) = \hat{L}\big|\rho(t)\big), \tag{2.14}$$

with $\hat{L}\bullet \equiv -i\big[H, \bullet\big]$, referred to as the *Liouvillian superoperator.*

2.2.4 Thermal equilibrium

At *thermal equilibrium* at temperature T, the populations obey the *Boltzmann distribution*, and the density operator may be written,

$$\rho_0 = \frac{1}{Z}e^{-\hbar H/k_B T}, \tag{2.15}$$

where,

$$Z = \mathrm{Tr}\{e^{-\hbar H/k_B T}\}, \tag{2.16}$$

is the *partition function* of the system, H the Hamiltonian of the system, and k_B is Boltzmann's constant. Evaluating ρ_0 in the eigenbasis $\{|i\rangle\}_{i=1}^{d}$ of H, we see that the expression for the populations is given by,

$$\rho_{ii} = \frac{1}{Z}e^{-\hbar E_i/k_B T}, \tag{2.17}$$

where E_i is the energy associated with state $|i\rangle$, and all coherences vanish at thermal equilibrium ($\rho_{ij} = 0 \; \forall \; i \neq j$). Note, in equations (2.15)-(2.17), $\hbar$ is reintroduced, and will be so when required in an exponent.

2.3 Angular momentum and spin

Thus far, quantum states and systems have been spoken about in a general and abstract way. We will, however, be exclusively concerned with *spin states*; that is, quantum states associated with an intrinsic property of subatomic particles, called *spin*. Spin behaves much in the same way as angular momentum does in the quantum realm, at least in terms of the mathematics. Therefore, we will cover the basic relations of angular momentum here and extend them to describe spin states and their dynamics.

2.3.1 Angular momentum operators and their properties

Classically, a particle of mass m and velocity $\mathbf{v}$ located at position $\mathbf{r}$ from some origin has linear momentum $\mathbf{p} = m\mathbf{v}$ and angular momentum,

$$\mathbf{L}^{(\mathrm{cl})} = \mathbf{r} \times \mathbf{p}, \tag{2.18}$$

where the superscript (cl) denotes a *classical* property. To obtain the QM operator, the substitution $\mathbf{p} \rightarrow -i\boldsymbol{\nabla}$ is made [13, 14], with $\boldsymbol{\nabla}$ the gradient operator, which takes the form,

$$\boldsymbol{\nabla} = \frac{\partial}{\partial x}\mathbf{e}_x + \frac{\partial}{\partial y}\mathbf{e}_y + \frac{\partial}{\partial z}\mathbf{e}_z, \tag{2.19}$$

in Cartesian form, with $\mathbf{e}_x$, $\mathbf{e}_y$, and $\mathbf{e}_z$ the Cartesian basis vectors of $\mathbb{R}^3$. The Cartesian components of $\mathbf{p}$ are then,

$$p_x = -i\frac{\partial}{\partial x}, \quad p_y = -i\frac{\partial}{\partial y}, \quad \text{and} \quad p_z = -i\frac{\partial}{\partial z}, \tag{2.20}$$

and those of $\mathbf{L}$ are,

$$L_x = yp_z - zp_y = -i\left(y\frac{\partial}{\partial z} - z\frac{\partial}{\partial y}\right),$$

$$L_y = zp_x - xp_z = -i\left(z\frac{\partial}{\partial x} - x\frac{\partial}{\partial z}\right), \tag{2.21}$$

$$L_z = xp_y - yp_x = -i\left(x\frac{\partial}{\partial y} - y\frac{\partial}{\partial x}\right),$$

where $i \equiv \sqrt{-1}$. From these definitions, we have,

$$\left[x_j, p_k\right] = i\delta_{jk}, \tag{2.22}$$

and we see that position and momentum along the same direction cannot be measured to arbitrary precision [13].

The fundamental angular momentum commutation relation is [2, 13, 14],

$$\left[L_j, L_k\right] = i\epsilon_{jkl}L_l \quad \forall j,k,l \in \{x,y,z\} \tag{2.23}$$

where ϵ_{jkl} is the Levi-Civita symbol defined by $\epsilon_{jkl} = 1$ if $\{j,k,l\}$ is a *cyclic permutation*, -1 if $\{j,k,l\}$ is an *anti-cyclic permutation*, and 0 otherwise.

The total angular momentum is defined,

$$\mathbf{L}^2 = L_x^2 + L_y^2 + L_z^2, \tag{2.24}$$

and although the components of angular momentum do not commute, each commutes with $\mathbf{L}^2$,

$$\left[\mathbf{L}^2, L_j\right] = 0 \quad \forall j \in \{x,y,z\}, \tag{2.25}$$

and there exists a simultaneous eigenbasis for $\mathbf{L}^2$ and each component L_j independently. By convention, the eigenbasis considered is that associated with L_z, and satisfies the relations,

$$\mathbf{L}^2 |lm\rangle = l(l+1) |lm\rangle \tag{2.26}$$

$$L_z |lm\rangle = m |lm\rangle , \tag{2.27}$$

where l is an integer and $m \in \{l, l-1, \cdots, -l\}$, giving $2l+1$ values m may take, and $|lm\rangle$ are the *spherical harmonics*, $Y_{lm}(x,y,z)$ [13], tabulated in table 2.1 for $l = 0, 1, 2$.

In this case, when l takes integer values and operators the form (2.21), we are dealing with *orbital angular momentum*. To generalise this and account for half-integer angular momentum, we define general angular momentum operator $\mathbf{J}$ which obeys the commutation rules [13, 14],

$$\left[J_i, J_j\right] = i\epsilon_{ijk} J_k \quad \forall i,j,k \in \{x,y,z\} , \tag{2.28}$$

for which $\left[\mathbf{J}^2, J_i\right] = 0 \ \forall i \in \{x,y,z\}$ is a consequence. Introducing the *ladder* operators,

$$\begin{aligned} J_+ &= J_x + iJ_y \\ J_- &= J_x - iJ_y, \end{aligned} \tag{2.29}$$

the following commutation properties may be deduced:

$$\begin{aligned} \left[\mathbf{J}^2, J_\pm\right] &= 0 \\ \left[J_z, J_\pm^k\right] &= \pm k J_\pm \\ \left[J_+, J_-\right] &= 2J_z. \end{aligned} \tag{2.30}$$

And since the general operators in eq. (2.28) are defined to be Hermitian, from definition (2.29) the ladder operators are adjoints of each other. Matrix elements of the angular momentum operators in a basis for which $\mathbf{J}^2$ and J_z are diagonal are given by,

l	m	$Y_{lm}(x,y,z)$
0	0	$1/\sqrt{4\pi}$
1	0	$\sqrt{\frac{3}{4\pi}}\frac{z}{r}$
	±1	$\mp\sqrt{\frac{3}{8\pi}}\frac{x\pm iy}{r}$
2	0	$\sqrt{\frac{5}{16\pi}}\frac{2z^2-x^2-y^2}{r^2}$
	±1	$\mp\sqrt{\frac{15}{16\pi}}\frac{(x\pm iy)z}{r^2}$
	±2	$\sqrt{\frac{15}{32\pi}}\frac{(x\pm iy)^2}{r^2}$

TABLE 2.1: The spherical harmonics in Cartesian coordinates for $l = 0, 1, 2$ [13], where $r = \sqrt{x^2+y^2+z^2}$

$$
\begin{aligned}
\left\langle jm|\mathbf{J}^2|j'm'\right\rangle &= j\left(j+1\right)\delta_{jj'}\delta_{mm'} \\
\left\langle jm|J_z|j'm'\right\rangle &= m'\delta_{jj'}\delta_{mm'} \\
\left\langle jm|J_x|j'm'\right\rangle &= \frac{1}{2}\left\{j\left(j+1\right)-m'\left(m'\pm1\right)\right\}^{\frac{1}{2}}\delta_{jj'}\delta_{m,m'\pm1} \\
\left\langle jm|J_y|j'm'\right\rangle &= \mp i\frac{1}{2}\left\{j\left(j+1\right)-m'\left(m'\pm1\right)\right\}^{\frac{1}{2}}\delta_{jj'}\delta_{m,m'\pm1} \\
\left\langle jm|J_\pm|j'm'\right\rangle &= \left\{j\left(j+1\right)-m'\left(m'\pm1\right)\right\}^{\frac{1}{2}}\delta_{jj'}\delta_{m,m'\pm1}.
\end{aligned}
\tag{2.31}
$$

2.3.2 Coupling of angular momenta

The sum of two angular momenta,

$$\mathbf{J} = \mathbf{J}_1 + \mathbf{J}_2, \tag{2.32}$$

is also a QM angular momentum operator and satisfies the commutation property (2.28), and has Cartesian components,

$$\begin{aligned} J_x &= J_{1x} + J_{2x} \\ J_y &= J_{1y} + J_{2y} \\ J_z &= J_{1z} + J_{2z}. \end{aligned} \tag{2.33}$$

This implies immediately that,

$$m = m_1 + m_2. \tag{2.34}$$

Consider the two sets of commuting operators $\left\{\mathbf{J}_1^2, J_{1z}, \mathbf{J}_2^2, J_{2z}, \Gamma\right\}$ and $\left\{\mathbf{J}_1^2, \mathbf{J}_2^2, \mathbf{J}^2, J_z, \Gamma\right\}$, where Γ represents operators in the set invariant to unitary transformation (and, thus, rotation) [14]. The simultaneous eigenvectors of the first set are denoted, $|j_1 m_1, j_2 m_2\rangle \equiv |j_1 m_1\rangle \otimes |j_2 m_2\rangle$, and obey the relations,

$$\begin{aligned} \mathbf{J}_1^2 \, |j_1 m_1, j_2 m_2\rangle &= j_1 \left(j_1 + 1\right) |j_1 m_1, j_2 m_2\rangle \\ J_{1z} \, |j_1 m_1, j_2 m_2\rangle &= m_1 \, |j_1 m_1, j_2 m_2\rangle \\ \mathbf{J}_2^2 \, |j_1 m_1, j_2 m_2\rangle &= j_2 \left(j_2 + 1\right) |j_1 m_1, j_2 m_2\rangle \\ J_{2z} \, |j_1 m_1, j_2 m_2\rangle &= m_2 \, |j_1 m_1, j_2 m_2\rangle . \end{aligned} \tag{2.35}$$

States $|j_1 m_1, j_2 m_2\rangle$ span a space of dimension $(2j_1 + 1)(2j_2 + 1)$ and are referred to as the *uncoupled representation*. States $|jm\rangle$ are simultaneous eigenvectors of the latter set of operators, and obey the relations,

$$\begin{aligned} \mathbf{J}_1^2 \, |jm\rangle &= j_1 \left(j_1 + 1\right) |jm\rangle \\ \mathbf{J}_2^2 \, |jm\rangle &= j_2 \left(j_2 + 1\right) |jm\rangle \\ \mathbf{J}^2 \, |jm\rangle &= j \left(j + 1\right) |jm\rangle \\ J_z \, |jm\rangle &= m \, |jm\rangle . \end{aligned} \tag{2.36}$$

States $|jm\rangle$ span a space of dimension $2j+1$, and are called the *coupled representation*. To transform between bases, a unitary transformation is performed. This is obtained using the completeness relation over the basis $\{|j_1 m_1, j_2 m_2\rangle\}$,

$$|jm\rangle = \sum_{m_1,m_2} |j_1 m_1, j_2 m_2\rangle\langle j_1 m_1, j_2 m_2|jm\rangle\,. \tag{2.37}$$

Thus, the two bases are connected by,

$$|jm\rangle = \sum_{m_1,m_2} C^{jj_1j_2}_{mm_1m_2}\,|j_1 m_1, j_2 m_2\rangle\,, \tag{2.38}$$

where $C^{jj_1j_2}_{mm_1m_2}$ are the *Clebsch-Gordan coefficients* [13], which are matrix elements of the unitary transformation which connects the $\{|jm\rangle\}$ and $\{|j_1 m_1, j_2 m_2\rangle\}$ bases. They are defined as,

$$C^{jj_1j_2}_{mm_1m_2} \equiv \langle j_1 m_1, j_2 m_2|jm\rangle\,, \tag{2.39}$$

and chosen to be real by convention. Clebsch-Gordan coefficients vanish unless,

$$m = m_1 + m_2 \tag{2.40}$$

and

$$|j_1 + j_2| \geqslant j \geqslant |j_1 - j_2|\,. \tag{2.41}$$

Expressions for Clebsh-Gordan coefficients are tabulated in many texts [13–16], but will not be used explicitly. However, they will be used in the construction of the rank-1 and 2 chemical shift anisotropy Hamiltonians in the irreducible spherical tensor formalism (see sections 2.4 and 2.5.2).

2.3.3 Angular momentum operators as generators of infinitesimal rotations

Consider the rotation of particle coordinates by infinitesimal angle $\delta\phi$ in the xy-plane. In polar coordinates, this transformation then takes the system through $\phi \to \phi + \delta\phi$ and, hence, the angle $\phi \to \phi - \delta\phi$ in the coordinates frame. This is written,

$$R_z(\delta\phi)\,|\psi(r,\theta,\phi)\rangle = |\psi(r,\theta,\phi-\delta\phi)\rangle\,. \tag{2.42}$$

Since $\delta\phi$ is defined to be infinitesimal, $|\psi(r,\theta,\phi-\delta\phi)\rangle$ may be expanded in the Taylor series,

$$|\psi(r,\theta,\phi-\delta\phi)\rangle \simeq |\psi(r,\theta,\phi)\rangle - \delta\phi\frac{\delta}{\delta\phi}|\psi(r,\theta,\phi)\rangle + \mathcal{O}\left[(\delta\phi)^2\right] + \cdots . \tag{2.43}$$

Truncating at first-order,

$$|\psi(r,\theta,\phi-\delta\phi)\rangle \simeq \left(1-\delta\phi\frac{\delta}{\delta\phi}\right)|\psi(r,\theta,\phi)\rangle , \tag{2.44}$$

shows us that,

$$R_z(\delta\phi) = 1 - i\delta\phi L_z, \tag{2.45}$$

where it is recognised that the z-component orbital angular momentum operator in eq. (2.21) takes the form, $L_z = -i\,(\delta/\delta\phi)$ in polar coordinates for infinitesial changes in ϕ. The general relation for a spatial rotation through $\delta\phi$ about arbitrary axis with unit vector $\mathbf{n}$ is,

$$R_n(\delta\phi) = 1 - i\delta\phi\mathbf{n}\cdot\mathbf{L}, \tag{2.46}$$

and it is said that orbital angular momentum operators are the *generators* of infinitesimal rotations.

The operator for *finite* rotations over angle ϕ may be constructed in term of successive rotations by $\delta\phi$. Writing $\phi = N\delta\phi$, it follows that,

$$\begin{aligned} R_n(\phi) &= \lim_{N\to\infty}\left(1 - i\frac{\phi}{N}\mathbf{n}\cdot\mathbf{L}\right)^N \\ &= e^{-i\phi\mathbf{n}\cdot\mathbf{L}}, \end{aligned} \tag{2.47}$$

where the relation, $\lim_{N\to\infty}(1+x/N)^N = e^x$ is used. The properties of a function of an operator are determined by the operator itself. Thus, the operator in eq. (2.47) obeys the commutation properties of $\mathbf{L}$ and the corresponding components. To involve rotations of spin angular momentum, the substitution $\mathbf{L} \to \mathbf{J}$ is made, and the general form of a rotation operator for finite angle of rotation ϕ is,

$$R_n(\phi) = e^{-i\phi \mathbf{n}\cdot\mathbf{J}}, \tag{2.48}$$

with Cartesian components,

$$R_\zeta(\phi) = e^{-i\phi J_\zeta} \quad \forall \zeta \in \{x, y, z\}\,. \tag{2.49}$$

From eq. (2.48), it follows that the rotation operator is a unitary operator, and maps one vector onto another in $\mathcal{H}_d$, with the property,

$$R_\zeta^\dagger(\phi) = R_\zeta^{-1}(\phi) = e^{i\phi J_\zeta} = R_\zeta(-\phi). \tag{2.50}$$

It follows that the adjoint or – equivalently – the inverse of the rotation operator performs a rotation also of angle ϕ but in reverse. That is, successive application of $R_\zeta(\phi)$ with its adjoint leaves the system unchanged, as expected.

As noted above, the algebraic properties of an operator are reflected in those of a function of the operator. Thus, the rotation operator in (2.49) commutes with $\mathbf{J}^2$, and so will a rotation operator which is a product of rotation operators about the Cartesian axes. Therefore, the total angular momentum is conserved under rotation, and state $|jm\rangle$ may be decomposed into a linear combination of states of varying m upon upon application of $R_n(\phi)$. We write,

$$\begin{aligned} R_n(\phi)|jm\rangle &= \sum_{m'=-j}^{j} |jm'\rangle\langle jm'|R_n(\phi)|jm\rangle \\ &= \sum_{m'=-j}^{j} D^{(j)}_{m'm}(\phi)|jm'\rangle, \end{aligned} \tag{2.51}$$

where $D^{(j)}_{m'm}(\phi)$ are the matrix elements of $R_n(\phi)$ in the eigenbasis of $\mathbf{J}^2$, of which there are $(2j + 1) \times (2j + 1)$ entries [13, 14, 17]. These matrix elements are known as *Wigner functions*, and will be returned to countless times; they are fundamental to the description of time-dependent molecular rotations and the consequences these have on spin relaxation.

2.3.4 Spin angular momentum

It is an experimental fact that many particles possess an *intrinsic angular momentum*, which we call *spin* [18–20]. The spin angular momentum operator $\mathbf{I}$ is related to the magnetic moment $\boldsymbol{\mu}$ of the particle proportionally;

$$\boldsymbol{\mu} = \gamma \mathbf{I}, \tag{2.52}$$

where γ is the *magnetogyric ratio* of the spin in question. The angular momentum operator referred to thus far may be written,

$$\mathbf{J} = \mathbf{L} + \mathbf{I}, \tag{2.53}$$

where $\mathbf{I}$ is the total spin angular momentum operator with Cartesian component operators which obey the commutation relations,

$$\left[I_j, I_k\right] = i\epsilon_{jkl} I_l \quad \forall j,k,l \in \{x,y,z\}\,, \tag{2.54}$$

as well as,

$$\left[\mathbf{I}^2, I_j\right] = 0 \quad \forall j \in \{x,y,z\}. \tag{2.55}$$

Again, convention is to work in the eigenbasis associated with I_z, and satisfies the relations,

$$\begin{aligned} \mathbf{I}^2 \left|Im_I\right\rangle &= I\left(I+1\right)\left|Im_I\right\rangle \\ I_z \left|Im_I\right\rangle &= m_I \left|Im_I\right\rangle. \end{aligned} \tag{2.56}$$

This time, though, I may be a half-integer, unlike l. Still, $m_I \in \{I, I-1, \cdots, -I\}$, giving $2I+1$ values m_I may take.

The particularly important case for us is that when $I = j = 1/2$, and $m_I = m$ takes values $+1/2$ and $-1/2$; that is,

$$\mathbf{I}^2 \left|\frac{1}{2}, \pm\frac{1}{2}\right\rangle = \frac{3}{4}\left|\frac{1}{2}, \pm\frac{1}{2}\right\rangle$$

$$I_z \left|\frac{1}{2}, \pm\frac{1}{2}\right\rangle = \pm\frac{1}{2}\left|\frac{1}{2}, \pm\frac{1}{2}\right\rangle.$$

Using the general expressions for the matrix elements of an angular momentum operator in (2.31), the spin vector $\mathbf{I}$ may be written,

$$\mathbf{I} = \frac{1}{2}\boldsymbol{\sigma}, \tag{2.57}$$

where the matrix representations of the Cartesian components of $\boldsymbol{\sigma}$ are the *Pauli matrices* [2, 17], given by,

$$\sigma_x = \begin{pmatrix} 0 & 1 \\ 1 & 0 \end{pmatrix}; \quad \sigma_y = \begin{pmatrix} 0 & -i \\ i & 0 \end{pmatrix}; \quad \sigma_z = \begin{pmatrix} 1 & 0 \\ 0 & -1 \end{pmatrix}. \tag{2.58}$$

The Pauli matrices satisfy the cyclic commutation relation,

$$\left[\sigma_j, \sigma_k\right] = 2i\epsilon_{jkl}\sigma_l \quad \forall j,k,l \in \{x,y,z\}, \tag{2.59}$$

and the anticommutation relation,

$$\left\{\sigma_j, \sigma_k\right\} = 2\mathbb{1}\delta_{jk} \quad \forall j,k \in \{x,y,z\}, \tag{2.60}$$

which leads to, $\sigma_j^2 = \mathbb{1}$. The Pauli matrices are Hermitian and traceless.

The ladder operators $I_\pm = I_x \pm iI_y$ have the matrix representations,

$$I_+ = \begin{pmatrix} 0 & 1 \\ 0 & 0 \end{pmatrix}; \quad I_- = \begin{pmatrix} 0 & 0 \\ 1 & 0 \end{pmatrix}. \tag{2.61}$$

By convention in NMR, we will write $\left|\frac{1}{2}, +\frac{1}{2}\right\rangle \equiv |\alpha\rangle$ and $\left|\frac{1}{2}, -\frac{1}{2}\right\rangle \equiv |\beta\rangle$. From the discussion thus far, the column vector representations are,

$$|\alpha\rangle = \begin{pmatrix} 1 \\ 0 \end{pmatrix}; \quad |\beta\rangle = \begin{pmatrix} 0 \\ 1 \end{pmatrix}, \tag{2.62}$$

and we're left with the relations,

$$\begin{aligned} I_+ |\alpha\rangle &= 0 \\ I_+ |\beta\rangle &= |\alpha\rangle \\ I_- |\alpha\rangle &= |\beta\rangle \\ I_- |\beta\rangle &= 0. \end{aligned} \tag{2.63}$$

We see that the ladder operators $I_\pm$ shift m_I by ± 1 wherever possible, returning zero otherwise.

2.4 Spin Hamiltonian

In the description of magnetic resonance experiments, we have the luxury of dealing only with the *nuclear spin Hamiltonian* of the system, rather than the full molecular Hamiltonian [21–24]. A total spin Hamiltonian may be written as a sum of Hamiltonians, each describing a different interaction Λ the spin system is experiencing with its environment [25, 26]. We write,

$$H_{\text{spin}}(t) = \sum_{\Lambda} H_\Lambda(t) \tag{2.64}$$

These interactions may be split into two categories; *coherent* and *incoherent* interactions [27]. Coherent interactions are those which are uniform over the spin ensemble, whilst incoherent interactions differ instantaneously for ensemble members. With some hindsight, we will denote these as H_0 and H_1, respectively, where H_1 is interpreted as a small *perturbation* on H_0. We write,

$$\begin{aligned} H_{\text{spin}}(t) &= \sum_{\Lambda} H_\Lambda(t) \\ &= H_0(t) + H_1(t). \end{aligned} \tag{2.65}$$

Each spin Hamiltonian $H_\Lambda(t)$ may be written as a dot product,

$$H_\Lambda(t) = c_\Lambda \mathbf{I} \cdot \mathbf{A}_\Lambda(t) \cdot \mathbf{S}_\Lambda, \tag{2.66}$$

where c_Λ is an interaction-specific constant, $\mathbf{I}$ is a spin-vector, $\mathbf{A}_\Lambda$ is a rank-2 Cartesian tensor with nine independent components, and $\mathbf{S}_\Lambda$ is a second vector, which may be the same spin-vector as the first, a different spin-vector, a static magnetic field vector, or the molecular angular momentum vector, depending on the interaction in question. Due to this, the interactions also divide themselves among three other categories; *linear*, *bilinear*, and *quadratic* in the spin operators.

2.4.1 The Zeeman interaction

The Zeeman interaction describes the intearction of a spin with a static magnetic field, such as that of an NMR spectrometer, and is thus linear in spin operators. The classical expression for the energy of interaction between a dipole and magnetic field is,

$$E_\mathrm{Z} = -\boldsymbol{\mu} \cdot \mathbf{B}, \tag{2.67}$$

where $\boldsymbol{\mu}$ is the classical dipole moment and B is the magnetic field vector. Substitution of $\boldsymbol{\mu}$ with its QM analogue, $\boldsymbol{\mu} \rightarrow \hbar\gamma\mathbf{I}$, gives us the Zeeman hamiltonian, and introducing the identity operator casts it into the form in equation (2.66) to give (while setting $\hbar \equiv 1$ again),

$$H_\mathrm{Z} = -\gamma \mathbf{I} \cdot \mathbb{1} \cdot \mathbf{B}_0, \tag{2.68}$$

where γ is the magnetogyric ratio of the spin, and $\mathbf{B}_0$ is the static magnetic field vector of the spectrometer and defined in the z-component of the vector; i.e., $\mathbf{B}_0 = (0, 0, B_0)$. Performing the tensor product in (2.68) and summing over all spins i,

$$H_\mathrm{Z} = \sum_i \omega_{0i} I_{iz}, \tag{2.69}$$

where $\omega_{0i} = -\gamma_i B_0$ is the Larmor frequency of spin i.

Note that inclusion of $\mathbb{1}$ in (2.68) was trivial, and included only to conform to the formalism expressed by (2.66). This emphasises that there are no spatial coordinates of the nucleus associated

with the spin in question. Thus, the Zeeman interaction is uniform over ensemble members and is a coherent interaction, which does not cause relaxation.

2.4.2 The chemical shift interaction

Another interaction linear in spin is the *chemical shift*, which has coherent and incoherent components. In the presence of an external static magnetic field, the motion of the electron cloud surrounding a nucleus generates a localised magnetic field which also interacts with the spins. For a spin in the system, a magnetic field $\mathbf{B}' = -\boldsymbol{\delta} \cdot \mathbf{B}_0$ is induced, where $\boldsymbol{\delta}$ is the *chemical shift tensor*. Using (2.67),

$$\begin{aligned} E_{\mathrm{CS}} &= -\boldsymbol{\mu} \cdot \mathbf{B}' \\ &= \boldsymbol{\mu} \cdot \boldsymbol{\delta} \cdot \mathbf{B}_0. \end{aligned} \tag{2.70}$$

Again, making the substitution, $\boldsymbol{\mu} \rightarrow \gamma \mathbf{I}$ and summing over all spins i gives,

$$H_{\mathrm{CS}} = \sum_i \gamma_i \mathbf{I}_i \cdot \boldsymbol{\delta}_i \cdot \mathbf{B}_0. \tag{2.71}$$

The chemical shift tensor (like all rank-2 tensors) may be written as a linear combination of *isotropic*, *antisymmetric*, and *symmetric* components. These are given, respectively, by,

$$\boldsymbol{\delta}^{(0)} = \mathbb{1}\delta_{\mathrm{iso}} \tag{2.72}$$

$$\boldsymbol{\delta}^{(-)} = \frac{1}{2}\left(\boldsymbol{\delta} - \boldsymbol{\delta}^{\mathrm{T}}\right) \tag{2.73}$$

$$\boldsymbol{\delta}^{(+)} = \frac{1}{2}\left(\boldsymbol{\delta} + \boldsymbol{\delta}^{\mathrm{T}}\right) - \boldsymbol{\delta}^{(0)}, \tag{2.74}$$

where $\delta_{\mathrm{iso}} = \frac{1}{3}\mathrm{Tr}\{\boldsymbol{\delta}\}$, T denotes the transpose operation, and $\boldsymbol{\delta} = \boldsymbol{\delta}^{(0)} + \boldsymbol{\delta}^{(-)} + \boldsymbol{\delta}^{(+)}$. In solution NMR, the Hamiltonian associated with $\boldsymbol{\delta}^{(0)}$ describes a coherent interaction, and is a term in H_0, whilst those Hamiltonians associated with $\boldsymbol{\delta}^{(-)}$ and $\boldsymbol{\delta}^{(+)}$ are incoherent interactions and contained in H_1.

2.4.3 Spin-spin coupling interaction

The *spin-spin coupling* is an indirect interaction between two spin moments, mediated by electrons in chemical bonds [28]. Since two spins are involved, the interaction will be bilinear in the spin operators. The treatment here follows that in Smith et al. (1992) [25]. The classical energy is,

$$E_{\mathrm{J}} = \frac{\boldsymbol{\mu}_i \cdot \boldsymbol{\mu}'_j}{r_{ij}^3}, \tag{2.75}$$

where $\boldsymbol{\mu}'_j$ is the *effective magnetic moment* of spin j. Defining the coupling tensor $\mathbf{J}'^{(ij)}$ as that which acts on $\boldsymbol{\mu}_j$ to give,

$$\mathbf{J}'^{(ij)} \cdot \boldsymbol{\mu}_j = \frac{1}{r_{ij}^3}\boldsymbol{\mu}'_j, \tag{2.76}$$

the spin-spin coupling interaction energy between spins i and j becomes,

$$E_{\mathrm{J}} = \boldsymbol{\mu}_i \cdot \mathbf{J}'^{(ij)} \cdot \boldsymbol{\mu}_j. \tag{2.77}$$

As in all cases in this section, the Hamiltonian is obtained by making the substitution $\boldsymbol{\mu} \rightarrow \gamma\mathbf{I}$. By convention, the coupling tensor is written in units of Hz and the Hamiltonian reads,

$$H_{\mathrm{J}} = 2\pi \sum_{i<j} \mathbf{I}_i \cdot \mathbf{J}^{(ij)} \cdot \mathbf{I}_j, \tag{2.78}$$

where $\gamma_{i(j)}$ are absorded into $\mathbf{J}^{(ij)}$, and is related to $\mathbf{J}'^{(ij)}$ by a constant.

2.4.4 Intrapair dipole-dipole interaction

Consider two dipoles, $\boldsymbol{\mu}_i$ and $\boldsymbol{\mu}_j$, connected by a vector $\mathbf{r}_{ij} = \boldsymbol{r}_j - \boldsymbol{r}_i$. The classical interaction energy is,

$$E_{\mathrm{DD}} = \frac{\boldsymbol{\mu}_i \cdot \boldsymbol{\mu}_j}{r_{ij}^3} - \frac{3\left(\boldsymbol{\mu}_i \cdot \mathbf{r}\right)\left(\boldsymbol{\mu}_j \cdot \mathbf{r}\right)}{r_{ij}^5}, \tag{2.79}$$

and the Hamiltonian for all spins becomes [6],

$$H_{\mathrm{DD}} = \sum_{i<j} b_{ij} \left\{ \mathbf{I}_i \cdot \mathbf{I}_j - \frac{3\left(\mathbf{I}_i \cdot \mathbf{r}_{ij}\right)\left(\mathbf{I}_j \cdot \mathbf{r}_{ij}\right)}{r_{ij}^2} \right\}, \tag{2.80}$$

where $b_{ij} = \mu_0 \gamma_i \gamma_j \hbar / (4\pi r_{ij}^3)$ is the dipolar coupling constant for spins i and j. Eq (2.80) may be written,

$$H_{\mathrm{DD}} = \sum_{i<j} b_{ij} \mathbf{I}_i \cdot \mathbf{D}^{(ij)} \cdot \mathbf{I}_j, \tag{2.81}$$

where elements of $\mathbf{D}^{(ij)}$ are given by,

$$D_{pq}^{(ij)} = \delta_{pq} - 3 e_p^{(j)} e_q^{(i)}, \tag{2.82}$$

where $p, q \in \{x, y, z\}$, δ_{pq} is the Kronecker delta defined by eq (1.6) in chapter 1, and e_p and e_q are components along coordinates p and q. From (2.81), the intrapair dipole-dipole interaction is bilinear in spin operators.

2.4.5 Spin-rotation interaction

Consider a charged particle orbiting some origin, with mass m and at radius r. The magnetic field induced is given by the classical expression,

$$\mathbf{B} = \frac{\mu_0}{4\pi} \frac{\mathbf{v} \times \mathbf{r}}{r^3} q, \tag{2.83}$$

where q is the charge of the particle and $\mathbf{v}$ the velocity. Writing this in terms of the classical angular momentum about the origin, $\mathbf{L}^{(\mathrm{cl})} = \mathbf{r} \times \mathbf{p}$ with $\mathbf{p} = m\mathbf{v}$ as in eq. (2.18), the induced field is,

$$\mathbf{B} = -\frac{\mu_0}{4\pi} \frac{q}{m r^3} \mathbf{L}^{(\mathrm{cl})}. \tag{2.84}$$

Now consider a collection of particles, each with charge q_j orbiting at a radius $\mathbf{r}_j$ of their own about the same origin. One can imagine that if a spin is at or close to this origin, it will experience the induced field as the sum of all contributions,

$$\mathbf{B} = -\frac{\mu_0}{4\pi}\sum_j \frac{q_j}{m_j r_j^3}\mathbf{L}_j^{(\mathrm{cl})}. \tag{2.85}$$

Using $E_{\mathrm{SR}} = -\boldsymbol{\mu}\cdot\mathbf{B}$ for a single particle, substitution of $\mathbf{L}^{(\mathrm{cl})}$ and $\boldsymbol{\mu}$ for their QM counterparts, and summing over all spins i, the Hamiltonian may be written,

$$\begin{aligned} H_{\mathrm{SR}} &= -\sum_i \gamma_i \mathbf{I}_i \cdot \mathbf{B} \\ &= \frac{\mu_0}{4\pi}\sum_{i,j}\gamma_i \frac{q_j}{m_j r_j^3}\mathbf{I}_i \cdot \mathbf{L}_j. \end{aligned} \tag{2.86}$$

This is often written in the formalism of the tensor product as [29],

$$H_{\mathrm{SR}} = \sum_i \mathbf{I}_i \cdot \mathbf{C}^{(i)} \cdot \mathbf{L}, \tag{2.87}$$

where $\mathbf{L}$ is the angular momentum of the molecule which hosts the spin system, and $\mathbf{C}^{(i)}$ is a tensor describing the spatial aspects of the interaction for spin i and is usually determined experimentally.

The spin-rotation mechanism will not be considered explicitly in any theoretical treatment that follows. Here, then, it will be stated that the spin-rotation mechanism is incoherent, and spin relaxation results from molecular collisions, which cause molecular reorientation, which in turn modulates the magnetic field created by the molecular rotations.

2.4.6 Random field interaction

The last Hamiltonian to be considered here is that associated with spins experiencing random fluctuating fields [26]. This occurs when magnetic moments close to the spin system generate small, time-dependent magnetic fields. These small fields may be generated from paramagnetic impurities in solution, molecular geometry fluctuations, solvent molecules, etc. The spin system, therefore, experiences a local field which is random in magnitude and direction.

Recall eq. (2.67) and substitude $\mathbf{B} \rightarrow \mathbf{B}^{\mathrm{rand}}(t)$, where $\mathbf{B}^{\mathrm{rand}}(t)$ is the time-dependent fluctuating random field vector the spin experiences. The relevant Hamiltonian becomes,

$$H_{\text{rand}}(t) = -\sum_i \gamma_i \mathbf{I}_i \cdot \mathbf{B}_i^{\text{rand}}(t). \tag{2.88}$$

In an isotropic medium, the field produced is isotropic, since the mechanisms responsible for the fluctuating field will have no preferred orientation. Then, $\left\langle B_\zeta^{\text{rand}}(t)^2 \right\rangle \ \forall \zeta \in \{x, y, z\}$ are equivalent, where B_ζ is the component of $\mathbf{B}^{\text{rand}}(t)$ along $\mathbf{B}_\zeta^{\text{rand}}$.

2.4.7 Coherent and incoherent interactions

In solution state NMR, whereby the molecule hosting the spin system tumbles in an isotropic medium, the coherent interactions are the Zeeman, isotropic chemical shift, and isotropic spin-spin coupling interactions [6, 9, 11]. We write,

$$\begin{aligned} H_0 &= H_{\text{Z}} + H_{\text{CS}} + H_{\text{J}} \\ &= \sum_i \omega_{0i} \left(1 - \delta_{\text{iso}}\right) + \sum_{i<j} J_{ij} \mathbf{I}_i \cdot \mathbf{I}_j \end{aligned} \tag{2.89}$$

where H_{CS} is the *isotropic* chemical shift Hamiltonian, and $J_{ij} = \langle \text{Tr}\{\mathbf{J}_{ij}\} \rangle$.

The remaining interactions are incoherent, and H_1 is given by,

$$H_1(t) = H_{\text{DD}}(t) + H_{\text{CSA}}(t) + H_{\text{SR}}(t) + H'_{\text{J}}(t) + H_{\text{rand}}(t) \tag{2.90}$$

where $H_{\text{CSA}}(t)$ is the *chemical shift anisotropy* Hamiltonian [30–32] and may be split into anti-symmetric and symmetric terms, $H_{\text{CSA}} = H_{\text{CSA}}^{(-)} + H_{\text{CSA}}^{(+)}$, and H'_{J} contains the antisymmetric and symmetric terms for the spin-spin coupling [33], $H'_{\text{J}} = H_{\text{J}}^{(1)} + H_{\text{J}}^{(2)}$. Each Hamiltonian is left without expansion in eq. (2.90), since the most convenient representation is in terms of *irreducible spherical tensor components*; their properties under rotation are known and convenient (see section 2.5.2).

Other interactions may also be active which aren't covered here, particularly spin relaxation by paramagnetic agents [34–39] and quadrupolar relaxation [34, 40–42].

2.5 Tensor operators

As eluded to in section 2.4, a tensor may often be decomposed into a linear combination of tensors which cannot be decomposed further. A tensor which may be decomposed in such a way is termed *reducible*, and those which cannot are *irreducible*. Generally, a tensor of rank-k has d^k components, where d is the dimension of the space. Thus, for a three-dimensional Cartesian tensor, there are 9 components.

2.5.1 Reducible tensors

A Cartesian tensor may be decomposed into tensors of rank-0, 1, and 2 as,

$$\mathbf{A} = \mathbf{A}^{(0)} + \mathbf{A}^{(1)} + \mathbf{A}^{(2)}, \tag{2.91}$$

with,

$$\begin{aligned} \mathbf{A}^{(0)} &= \mathbb{1}\,\mathrm{Tr}\,\{\mathbf{A}\} \\ \mathbf{A}^{(1)} &= \frac{1}{2}\left(\mathbf{A} - \mathbf{A}^{\mathrm{T}}\right) \\ \mathbf{A}^{(2)} &= \frac{1}{2}\left(\mathbf{A} + \mathbf{A}^{\mathrm{T}}\right) - \mathbf{A}^{(0)}, \end{aligned} \tag{2.92}$$

where the superscript T denotes the transpose operation. In terms of components,

$$\begin{aligned} A^{(0)}_{ij} &= \frac{1}{3}\sum_{i,j} A_{ij}\delta_{ij} \\ A^{(1)}_{ij} &= \frac{1}{2}\left(A_{ij} - A_{ji}\right) \\ A^{(2)}_{ij} &= \frac{1}{2}\left(A_{ij} + A_{ji}\right) - A^{(0)}_{ij}. \end{aligned} \tag{2.93}$$

The tensor $\mathbf{A}^{(0)}$ in eq. (2.92) has only one *independent* component, and transforms as does a scalar under rotation; i.e. invariant to such transformations. Tensor $\mathbf{A}^{(1)}$ is an *antisymmetric* tensor of rank-1, which transforms as does a vector under rotation and has three independent components. The tensor $\mathbf{A}^{(2)}$ is a *symmetric*, *traceless* tensor of rank-2, which has five independent components. $\mathbf{A}^{(2)}$ may not be reduced further and the five independent components define an irreducible tensor.

2.5.2 Irreducible spherical tensors and rotations

Cartesian tensors become unsuitable for theoretical treatments in NMR since they are reducible under rotation. However, spherical tensors are irreducible and transform linearly among themselves under rotation. An *irreducible spherical tensor* (IST) of rank k is defined to be a set of $2k+1$ operators T_{kq}, with $q \in \{k, k-1, \cdots, -k\}$, which transform analogously to angular momentum under rotation of coordinate frame [13, 17, 43, 44]. That is,

$$\hat{R}_n(\phi) T_{kq} = \sum_{q'=-k}^{+k} D^{(k)}_{q'q}(\phi) T_{kq'}, \tag{2.94}$$

where $\hat{R}_n(\phi)$ is rotation superoperator for finite rotation ϕ, and defined by $\hat{R}_n(\phi)\bullet \equiv R_n(\phi) \bullet R_n^\dagger(\phi)$. Like $Y^*_{lm}(\theta,\phi) = (-1)^m Y_{l-m}(\theta,\phi)$, IST have the property,

$$T^\dagger_{kq} = (-1)^q T^\dagger_{k-q}. \tag{2.95}$$

Defining commutation superoperators $\hat{J}_z \equiv \big[J_z, \bullet\big]$ and $\hat{J}_\pm \equiv \big[J_\pm, \bullet\big]$, we may write the commutation relations of IST operators as,

$$\hat{J}_z T_{kq} = q T_{kq}, \tag{2.96}$$

and,

$$\hat{J}_\pm T_{kq} = \{k(k+1) - q(q\pm 1)\}^{\frac{1}{2}} T_{k,q\pm 1}. \tag{2.97}$$

Note how the eigenvalues in (2.96) and (2.97) take analogous form to the matrix elements of J_z and $J_\pm$ in the eigenbasis $\{|kq\rangle\}$ of $\mathbf{J}^2$ and J_z.

To find the matrix elements of T_{kq}, (2.96) may be used to write,

$$\begin{aligned} \big\langle jm\big|\hat{J}_z T_{kq} - q T_{kq}\big|j'm'\big\rangle &= 0 \\ \Rightarrow \big(m - m' - q\big)\big\langle jm\big|T_{kq}\big|j'm'\big\rangle &= 0, \end{aligned} \tag{2.98}$$

and $\langle jm|\, T_{kq}\, |j'm'\rangle$ vanishes unless $m = m' + q$, suggesting it to be proportional to the Clebsch-Gordan coefficients. This leads to the *Wigner-Eckart theorem*, which states: *The matrix elements of spherical tensor operators T_{kq}, with respect to the eigenbasis of $\mathbf{J}^2$ and J_z, are given by,*

$$\big\langle jm\big|T_{kq}\big|j'm'\big\rangle = C^{jj'k}_{mm'q}\big\langle j\big\|T_{kq}\big\|j'\big\rangle, \tag{2.99}$$

where $C^{jj'k}_{mm'q} = \big\langle j'm', kq|jm\big\rangle$ is a Clebsch-Gordan coefficient and $\big\langle j\big\|T_{kq}\big\|j'\big\rangle$ is some value independent of m, m', and q, and is called the reduced matrix element. This theorem has been used to show that *singlet-* and *triplet-states* do not mix under the influence of H_{DD} [45], generalising the findings of early singlet-NMR experiments [46]; a topic we return to in section 3.3.

The IST operator basis forms a matrix basis for the decomposition of Cartesian tensors, with elements given by,

$$\begin{aligned}
\mathbf{T}_{00} &= -\frac{1}{\sqrt{3}}\left(\mathbf{T}_{xx} + \mathbf{T}_{yy} + \mathbf{T}_{zz}\right) \\
\mathbf{T}_{10} &= -\frac{i}{\sqrt{2}}\left(\mathbf{T}_{xy} - \mathbf{T}_{yx}\right) \\
\mathbf{T}_{1\pm1} &= -\frac{1}{2}\left[\mathbf{T}_{zx} - \mathbf{T}_{xz} \pm i\left(\mathbf{T}_{zy} - \mathbf{T}_{yz}\right)\right] \\
\mathbf{T}_{20} &= \frac{1}{\sqrt{6}}\left[3\mathbf{T}_{zz} - \left(\mathbf{T}_{xx} + \mathbf{T}_{yy} + \mathbf{T}_{zz}\right)\right] \\
\mathbf{T}_{2\pm1} &= \mp\frac{1}{2}\left[\mathbf{T}_{xz} + \mathbf{T}_{zx} \pm i\left(\mathbf{T}_{yz} + \mathbf{T}_{zy}\right)\right] \\
\mathbf{T}_{2\pm2} &= \frac{1}{2}\left[\mathbf{T}_{xx} - \mathbf{T}_{yy} \pm i\left(\mathbf{T}_{xy} + \mathbf{T}_{yx}\right)\right],
\end{aligned} \tag{2.100}$$

where $\mathbf{T}_{xx}$ has entry 1 for component $\{\mathbf{T}_{xx}\}_{11}$ and 0 elsewhere, $\mathbf{T}_{xy}$ has entry 1 for component $\{\mathbf{T}_{xy}\}_{12}$ and 0 elsewhere, and so on. A Cartesian tensor $\mathbf{A}$ decomposition in this basis takes the form,

$$\mathbf{A} = \sum_{k=0}^{2}\sum_{q=-k}^{+k} A_{kq}\mathbf{T}_{kq}. \tag{2.101}$$

This basis is orthonormal,

$$\mathrm{Tr}\left\{\mathbf{T}^{\dagger}_{kq}\mathbf{T}_{k'q'}\right\} = \delta_{kk'}\delta_{qq'}, \tag{2.102}$$

and, thus, coefficients A_{kq} may be obtained by,

$$A_{kq} = \mathrm{Tr}\left\{\mathbf{T}^{\dagger}_{kq}\mathbf{A}\right\}. \tag{2.103}$$

These components have a similar form to tensors in (2.100) with some minor sign changes. They are,

$$\begin{aligned}
A_{00} &= -\frac{1}{\sqrt{3}}\left(A_{xx}+A_{yy}+A_{zz}\right)\\
A_{10} &= \frac{i}{\sqrt{2}}\left(A_{xy}-A_{yx}\right)\\
A_{1\pm1} &= -\frac{1}{2}\left[A_{zx}-A_{xz}\mp i\left(A_{zy}-A_{yz}\right)\right]\\
A_{20} &= \frac{1}{\sqrt{6}}\left[3A_{zz}-\left(A_{xx}+A_{yy}+A_{zz}\right)\right]\\
A_{2\pm1} &= \mp\frac{1}{2}\left[A_{xz}+A_{zx}\mp i\left(A_{yz}+A_{zy}\right)\right]\\
A_{2\pm2} &= \left[A_{xx}-A_{yy}\mp i\left(A_{xy}+A_{yx}\right)\right].
\end{aligned} \tag{2.104}$$

Explicit forms for these coefficients are considered on a case-by-case basis for some of those Cartesian tensors in section 2.4.

In general, a spin Hamiltonian may be written in terms of IST operator components by decomposing the spatial Cartesian tensor. We write, for interaction Λ,

$$\begin{aligned}
H_{\Lambda} &= c_{\Lambda}\mathbf{I}\cdot\mathbf{A}_{\Lambda}(t)\cdot\mathbf{S}_{\Lambda}\\
&= c_{\Lambda}\mathrm{Tr}\left\{\mathbf{A}_{\Lambda}(t)\mathbf{X}_{\Lambda}\right\}\\
&= c_{\Lambda}\mathrm{Tr}\left\{\sum_{k=0}^{2}\sum_{q=-k}^{+k}A^{\Lambda}_{kq}(t)\mathbf{T}^{\Lambda}_{kq}\sum_{k'=0}^{2}\sum_{q'=-k'}^{+k'}X^{\Lambda}_{k'q'}\mathbf{T}^{\Lambda}_{k'q'}\right\}\\
&= c_{\Lambda}\sum_{k=0}^{2}\sum_{q=-k}^{+k}(-1)^{q}A^{\Lambda}_{k-q}X^{\Lambda}_{kq},
\end{aligned} \tag{2.105}$$

where $\mathbf{X}_{\Lambda} = \mathbf{S}_{\Lambda}\otimes\mathbf{I}$ is a dyad which has analogous components to $\mathbf{A}_{\Lambda}$ in the IST operator basis, and are given by,

$$
\begin{aligned}
X_{00} &= -\frac{1}{\sqrt{3}}\left(S_x I_x + S_y I_y + S_z I_z\right) \\
X_{10} &= \frac{i}{\sqrt{2}}\left(S_x I_y - S_y I_x\right) \\
X_{1\pm1} &= -\frac{1}{2}\left[S_z I_x - S_x I_z \mp i\left(S_z I_y - S_y I_z\right)\right] \\
X_{20} &= \frac{1}{\sqrt{6}}\left[3S_z I_z - \left(S_x I_x + S_y I_y + S_z I_z\right)\right] \\
X_{2\pm1} &= \mp\frac{1}{2}\left[S_x I_z + S_z I_x \mp i\left(S_y I_z + S_z I_y\right)\right] \\
X_{2\pm2} &= \frac{1}{2}\left[S_x I_x - S_y I_y \mp i\left(S_x I_y + S_y I_x\right)\right],
\end{aligned}
\tag{2.106}
$$

and the relation $\mathbf{T}^{\dagger}_{kq} = (-1)^q \mathbf{T}_{k-q}$ has been used, along with $\mathrm{Tr}\left\{\mathbf{T}^{\dagger}_{kq}\mathbf{T}_{k'q'}\right\} = \delta_{kk'}\delta_{qq'}$.

2.5.3 Active and passive rotations

Upon describing the relaxation properties of a spin system in solution, time-dependent rotations of the spatial part of the Hamiltonian are used to describe the effects of stochastic tumbling of the molecule in space. Rotations may be described in one of two ways, which both rely on the use of observer- and body-fixed frames of reference, and the meaning of equation (2.94) is determined by which point of view is taken. These are the active and passive points of view. The mathematical formalism of rotations has been studied strictly and presented in detail in the literature[43, 44, 47, 48]. Here, inspiration is taken from the work and reviews by Bouten (1968), Mueller (2011), Man (2014), and Millot and Man (2012), and the relations are used extensively throughout the following chapters.

Before giving the details of active and passive rotations, a convention must be chosen for the angles which parameterise them. Consider a *fixed* reference frame, O^F_{xyz}, and a *rotated* reference frame, O^R_{xyz}. The orientation of the rotated frame with respect to the fixed one may be parameterised by the *Euler angles*, $\Omega = \{\alpha, \beta, \gamma\}$. Suppose these two frames are initially coincident. Then, these angles describe successive rotations which transform O^R_{xyz} from its initial orientation coincident with O^F_{xyz} to its final orientation. They are:

1. A rotation about the z^F-axis by angle α
2. A rotation about the transformed y^R-axis by angle β
3. A rotation about the transformed z^R-axis by angle γ

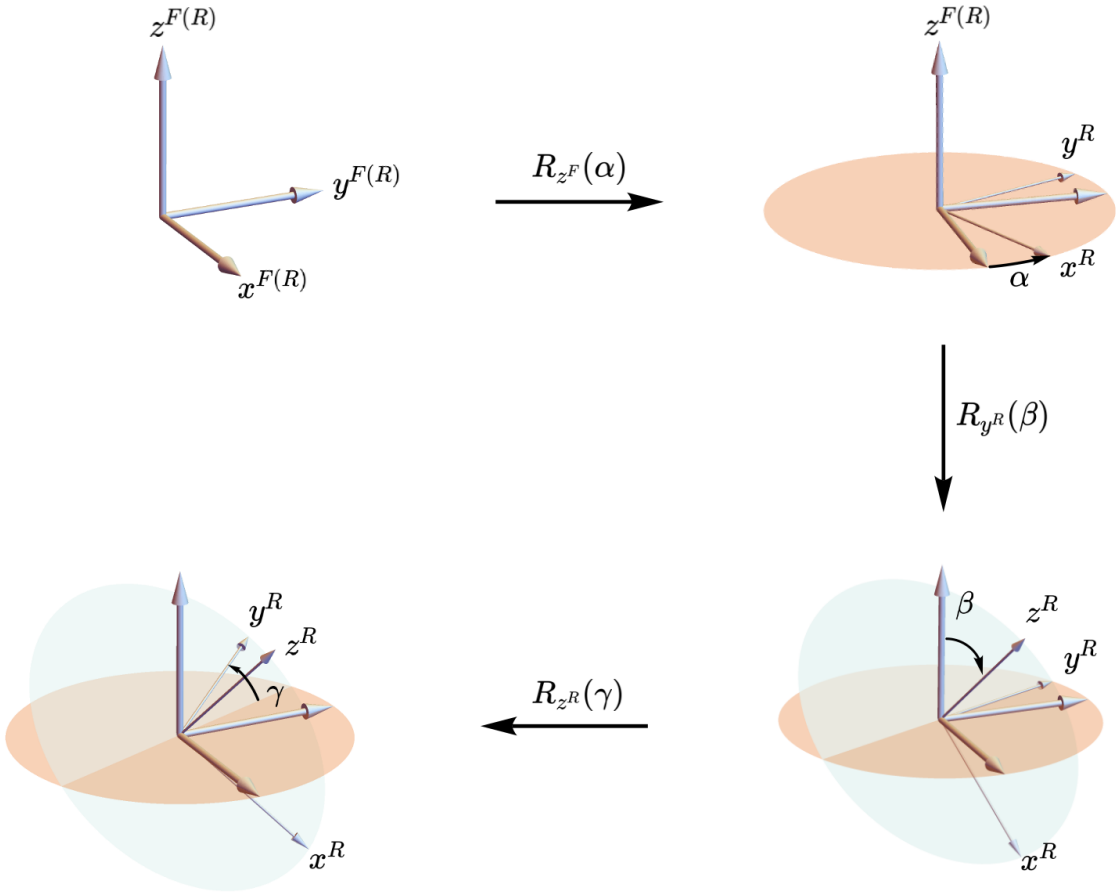

FIGURE 2.1: Euler-angle parameterisation for a rotation in which the fixed and rotated reference frames are initailly coincident; Euler-angles $\Omega = \{\alpha, \beta, \gamma\}$ parameterise the orientation of the rotated in the fixed reference frame.

The above transformations are depicted in figure 2.1. Note that each of the operations are performed using the right-hand rule.

Under the *active* rotation formalism, a body may be rotated about a fixed origin O relative to an observer-fixed frame O_{xyz}. The orientation of the body is then determined by the orientation of the body-fixed O^R_{xyz} frame relative to the observer-fixed O^F_{xyz} frame. In the *passive* rotation formalism, O^R_{xyz} is the observer-fixed frame, whilst O^F_{xyz} is the body-fixed frame. Then, the observer-fixed frame is rotated with respect to the body and its fixed frame under a passive rotation. Further, in both contexts, the coordinates of the body are expressed in the observer-fixed reference frame.

Without further ado, Bouten derives the active rotation operator as,

$$R_{\mathrm{A}}(\Omega) = e^{-i\alpha L_z} e^{-i\beta L_y} e^{-i\gamma L_z}, \tag{2.107}$$

and the passive rotation operator as,

$$R_{\mathrm{P}}(\Omega) = e^{i\gamma L_z} e^{i\beta L_y} e^{i\alpha L_z}, \tag{2.108}$$

and we take the liberty of making the substitution $L_\zeta \to I_\zeta$ in the following discussion. From eq. (2.107) and (2.108), the two operators are unitary as well as each other's inverse, and we may write,

$$R_{\mathrm{A}}(\Omega) = R_{\mathrm{P}}^{-1}(\Omega) = R_{\mathrm{P}}^{\dagger}(\Omega), \tag{2.109}$$

or simply,

$$R_{\mathrm{A}}(\Omega) R_{\mathrm{P}}(\Omega) = \mathbb{1}. \tag{2.110}$$

The physical consequence is that if one were to perform an active rotation on a body, followed by a passive one using the same set of Euler angles, the body would be appear unchanged in the observer-fixed frame. That is, the passive rotation restores the body to its original position.

The distinction between active and passive rotations is important, since the associated QM operators clearly have differing matrix elements. For an active rotation, these matrix elements (Wigner functions, see section 2.3.3) may be written,

$$D^{(k)}_{qq'}(\Omega) = e^{-i\alpha q} e^{-i\gamma q'} d^{(k)}_{qq'}(\beta), \tag{2.111}$$

and for a passive rotation,

$$D^{(k)}_{qq'}(\Omega) = e^{i\gamma q} e^{i\alpha q'} d^{(k)}_{qq'}(-\beta). \tag{2.112}$$

For both types of rotation, $d^{(0)}_{00}(\pm\beta) = 1$. The remaining values for $d^{(k)}_{qq'}(\beta)$ with $k = 1, 2$ are gathered in tables 2.2 and 2.3, respectively. These entries correspond to the active point of view, and substitution $\beta \to -\beta$ will correspond to the passive one.

q, q'	$+1$	0	-1
$+1$	$\cos^2\frac{\beta}{2}$	$-\frac{1}{\sqrt{2}}\sin\beta$	$\sin^2\frac{\beta}{2}$
0	$\frac{1}{\sqrt{2}}\sin\beta$	$\cos\beta$	$-\frac{1}{\sqrt{2}}\sin\beta$
-1	$\sin^2\frac{\beta}{2}$	$\frac{1}{\sqrt{2}}\sin\beta$	$\cos^2\frac{\beta}{2}$

TABLE 2.2: Reduced Wigner functions, $d^{(1)}_{qq'}(\beta)\ \forall\ q, q' \in \{+1, 0, -1\}$. Using these, the Wigner functions for an active rotation are constructed with eq. (2.111). For a passive rotation, substitution $\beta \to -\beta$ is made and eq. (2.112) is used.

q, q'	$+2$	$+1$	0	-1	-2
$+2$	$\cos^4\frac{\beta}{2}$	$-\frac{1}{2}\sin\beta\,(\cos\beta+1)$	$\sqrt{\frac{3}{8}}\sin^2\beta$	$\frac{1}{2}\sin\beta\,(\cos\beta-1)$	$\sin^4\frac{\beta}{2}$
$+1$	$\frac{1}{2}\sin\beta\,(\cos\beta+1)$	$\frac{1}{2}\,(2\cos\beta-1)\,(\cos\beta+1)$	$-\sqrt{\frac{3}{2}}\sin\beta\cos\beta$	$\frac{1}{2}\,(2\cos\beta+1)\,(\cos\beta-1)$	$\frac{1}{2}\sin\beta\,(\cos\beta-1)$
0	$\sqrt{\frac{3}{8}}\sin^2\beta$	$\sqrt{\frac{3}{2}}\sin\beta\cos\beta$	$\frac{1}{2}\left(3\cos^2\beta-1\right)$	$-\sqrt{\frac{3}{2}}\sin\beta\cos\beta$	$\sqrt{\frac{3}{8}}\sin^2\beta$
-1	$\frac{1}{2}\sin\beta\,(\cos\beta-1)$	$\frac{1}{2}\,(2\cos\beta+1)\,(1-\cos\beta)$	$\sqrt{\frac{3}{2}}\sin\beta\cos\beta$	$\frac{1}{2}\,(2\cos\beta-1)\,(\cos\beta+1)$	$\frac{1}{2}\sin\beta\,(\cos\beta+1)$
-2	$\sin^4\frac{\beta}{2}$	$\frac{1}{2}\sin\beta\,(1-\cos\beta)$	$\sqrt{\frac{3}{8}}\sin^2\beta$	$\frac{1}{2}\sin\beta\,(\cos\beta+1)$	$\cos^4\frac{\beta}{2}$

TABLE 2.3: Reduced Wigner functions, $d^{(2)}_{qq'}(\beta)\ \forall\ q, q' \in \{+2, +1, 0, -1, -2\}$. The same applies here as in caption 2.2 to construct the Wigner functions for active and passive rotations.

In the theoretical description of spin rotation, we are concerned with the way in which the spatial tensors of spin Hamiltonians associated with incoherent interactions rotate. These spatial tensors are outlined in section 2.4, and include the intrapair dipole-dipole, first- and second-rank chemical shift, and spin-rotation tensors, among others. From the rotational properties of IST operators and the decompositon of Cartesian tensors in such a basis (recall eq. (2.94) and (2.101)), an alluring means to achieve such a rotation is to first decompose a Cartesian tensor in the IST operator basis, and use the linearity of the rotation superoperator to rotate the decompostion component-wise. Then,

$$\begin{aligned}\hat{R}_n(\Omega)\mathbf{A} &= \hat{R}_n(\Omega)\sum_{k=0}^{2}\sum_{q=-k}^{+k} A_{kq}\mathbf{T}_{kq} \\ &= \sum_{k=0}^{2}\sum_{q=-k}^{+k} A_{kq}\sum_{q'=-k}^{+k} D^{(k)}_{q'q}(\Omega)\mathbf{T}_{kq'} \\ &= \sum_{k=0}^{2}\sum_{q=-k}^{+k}\sum_{q'=-k}^{+k} D^{(k)}_{q'q}(\Omega)A_{kq}\mathbf{T}_{kq'},\end{aligned} \tag{2.113}$$

and the coefficient of component q' of the transformed rank-k tensor is given by,

$$A'_{kq'} = \sum_{q=-k}^{+k} D^{(k)}_{q'q}(\Omega)A_{kq}. \tag{2.114}$$

Note the difference between eq. (2.94) (rotation of an IST operator) and (2.114). The former describes the transformation of a component of a tensor of a specific rank, while the latter gives the coefficient of a specific tensor component after transformation.

With some hindsight, we will be using a *covariant* spherical tensor basis, writing the decomposition of a tensor $\mathbf{T}$ as,

$$\mathbf{T} = \sum_{k=0}^{2}\sum_{q=-k}^{+k} B_{kq}\mathbf{T}_{kq}, \tag{2.115}$$

where $B_{kq} = A^*_{kq}$ is a *covariant spherical tensor component*. Then, eq (2.114) becomes,

$$B'^*_{kq'} = \sum_{q=-k}^{+k} D^{(k)}_{q'q}(\Omega)B^*_{kq}, \tag{2.116}$$

or, equivalently,

$$B'_{kq'} = \sum_{q=-k}^{+k} D^{(k)*}_{q'q}(\Omega) B_{kq}, \tag{2.117}$$

which is the relation used throughout the following chapters. The reason for the use of the covariant basis is due to being that which is implemented in the *SpinDynamica* [49] software package, which is consistent with the definition of a covariant basis in Man [43], and that used in Mehring [50]. The active rotation formalism, covariant basis, and transformation in eq. (2.117) are also used implicitly throughout Smith et al. [25, 26].

2.6 Measurement and NMR

Solution-state NMR samples host highly mixed states. We thus turn to the density operator formalism to interpret experiments, and observables are averaged over the ensemble [11]. The solution to the Liouville-von Neumann equation in which the density operator evolves under coherent interactions only may be written,

$$\big|\rho(t)\big) = \hat{U}(t, t_0)\big|\rho(t_0)\big), \tag{2.118}$$

where $\hat{U}(t, t_0)$ is a unitary transformation superoperator (see section 1.1.2, eq. (1.38)). Incorporating incoherent interactions, evolution is no longer unitary, and we write eq. 2.118 in terms of the so-called *Liouvillian superoperator*, $\hat{L}$, as,

$$\big|\rho(t)\big) = \hat{V}(t, t_0)\big|\rho(t_0)\big), \tag{2.119}$$

with solution,

$$\hat{V}(t, t_0) \equiv e^{\hat{L}(t-t_0)}, \tag{2.120}$$

for a time-independent $\hat{L}$.[1] Working in an eigenoperator basis $\{Q_q\}_{q=1}^{D}$ of $\hat{L}$, we find,

$$\big|\rho(t)\big) = \sum_q \big|Q_q\big)\big(Q_q\big|\rho(t_0)\big) e^{\Lambda_q (t-t_0)}, \tag{2.121}$$

[1] We will see in chapter 3 that $\hat{L}$ is indeed time-independent, and will be so throughout chapters 4 and 5, too.

where Λ_q is an eigenvalue of $\hat{L}$ associated with operator $\big|Q_q\big)$.

In NMR, the detection method is most often *quadrature detection* [6, 9, 51], and the observables are (-1)-quanatum coherences, represented by the operator, $-\frac{i}{2}\big|I_-\big)e^{i\phi_{\rm rec}}$ with $\phi_{\rm rec}$ the receiver phase. Setting $\phi_{\rm rec} = 0$, the signal may then be written,

$$\begin{aligned} s(t) &= \frac{i}{2}\big(I_-\big|\rho(t)\big) \\ &= \sum_q a_q e^{\Lambda_q(t-t_0)} \end{aligned} \tag{2.122}$$

,

with a_q the peak amplitude given by,

$$a_q = \frac{i}{2}\big(I_-\big|Q_q\big)\big(Q_q\big|\rho(t_0)\big). \tag{2.123}$$

Density operator $\big|\rho(t_0)\big)$ corresponds to the state of the ensemble at the beginning of the detection period, and is created via a *pulse-sequence*. This is returned to in chapters 4 and 5 when considering spectral line-shapes and longitudinal relaxation processes.

Chapter 3

Spin Relaxation

Following some perturbation, our spin system returns to thermal equilibrium via a complicated set of processes catalysed by molecular collisions. Collectively, this set constitutes *spin relaxation*. Each of these processes is *Markovian* in nature, and the task of describing a given process is forwarded to a *master equation*.

The history of theoretical spin relaxation is a rich one, and two prominent frameworks are considered here; that attributed to Wangsness, Bloch, and Redfield, and that to Lindblad (and others). In the former, it is well documented that positivity of the density operator isn't always conserved. The latter remedies this by invoking the *secular approximation*, whereby sufficiently oscillating terms are neglected, resulting in *trace-preserving* dynamics.

Here, though, no approximation will be invoked other than the agreed starting point; that the molecule hosting the spin system maintains a rigid geometry as it tumbles stochastically in a homogeneous medium. Then, secular terms only survive as a natural mathematical consequence for a molecule of arbirary geometry. This in itself suggests translation to Lindbladian form offers a valid master equation.

3.1 The Markovian master equations

A Markovian process is one which is *memoryless* and *stochastic*. These processes are described by the temporal evolution of the density operator of the system; i.e. a *master equation*. Sparing the reader of the mathematical details,[1] the general form of a QM Markovian master equation is [52, 53],

$$\frac{d}{dt}\rho(t) = L\rho(t), \tag{3.1}$$

where L is the *generator* of a *quantum-dynamical semigroup*; i.e. generates the propagator with semigroup property,

$$V(t_1)V(t_2) = V(t_1 + t_2), \tag{3.2}$$

where the initial time t_0 is set to 0, and $t_1, t_2 \geqslant 0$. We see immediately that our generator satisfies the solution,

$$V(t) = e^{Lt}, \tag{3.3}$$

and, therefore, must be time-independent.

When describing relaxation in Liouville space, we see that $L \equiv \hat{L}$ is the Liouvillian superoperator, and superoperator $\hat{V}(t)$ preserves the trace of the density operator.

The intention behind the theory of open quantum systems is to disentangle the dynamics of the quantum system from the environment. After a brief discussion of the interaction picture and its practical consequences, we see how just how this is achieved, allowing us to follow this up with two theoretical treatments describing a Markovian process.

[1] The original derivation for a quantum Markovian master equation utilises mathematics outside the scope of this thesis; the interested reader is deferred elsewhere, and to references therein.

3.1.1 Quantum dynamics in the interaction picture

As described in section 2.4, interactions may be categorised as coherent or incoherent, described, respectively, by Hamiltonians H_0 and H_1. The Liouville-von Neumann equation becomes,

$$\frac{d}{dt}\rho(t) = -i\big[H_0 + H_1, \rho(t)\big]. \tag{3.4}$$

To remove the influence of the coherent Hamiltonian, we move to the interaction picture [11] using,

$$\tilde{Q}(t) = e^{+iH_0 t} Q e^{-iH_0 t}, \tag{3.5}$$

for an arbitrary operator, Q, and the time-dependence of $\tilde{Q}(t)$ is contained in the exponents for time-independent operators. The (t) has been dropped from $H_0(t)$ for brevity. Eq. (3.4) in the interaction picture becomes,

$$\frac{d}{dt}\tilde{\rho}(t) = -i\big[\tilde{H}_1(t), \tilde{\rho}(t)\big]. \tag{3.6}$$

Formal integration gives,

$$\tilde{\rho}(t) = \tilde{\rho}(0) - i\int_0^t dt' \big[\tilde{H}_1(t'), \tilde{\rho}(t')\big], \tag{3.7}$$

which offers approximate solutions via perturbative treatments, such as *Wangsness-Bloch-Redfield (WBR) relaxation theory* [11, 54–58].

3.1.2 Open quantum systems

A spin system will inevitably interact with its environment. When the environment is in thermal equilibrium we refer to it as the *bath*. Then, we describe the Hilbert space of the total system $\mathcal{H}_\mathrm{T}$ as the composite Hilbert space,

$$\mathcal{H}_\mathrm{T} = \mathcal{H}_\mathrm{S} \otimes \mathcal{H}_\mathrm{B}, \tag{3.8}$$

where $\mathcal{H}_{\mathrm{S}}$ and $\mathcal{H}_{\mathrm{B}}$ are the Hilbert spaces of the system and bath, respectively. Then, the total Hamiltonian may be written,

$$H_{\mathrm{T}}(t) = H_{\mathrm{S}} \otimes \mathbb{1}_{\mathrm{B}} + \mathbb{1}_{\mathrm{S}} \otimes H_{\mathrm{B}} + H_{\mathrm{int}}(t), \tag{3.9}$$

where H_{S} and H_{B} are Hamiltonians of the system and bath, respectively, and $H_{\mathrm{int}}(t)$ is the Hamiltonian describing the interaction between the two. H_{S} and H_{B} may or may not be time-dependent depending on the physical problem at hand, but are written not to be so here to draw analogy with the situation in solution NMR. Eq. (3.9) illustrates the motivation behind the theory of open quantum systems; the dynamics of the bath and spin system are separated, and the evolution of the latter is inferred from those of the total system.

The dynamics of the spin system density operator ρ_{S} are studied by application of the *partial trace* over the bath degree of freedom to density operator of the whole system [3, 52, 57]. That is,

$$\rho_{\mathrm{S}} = \mathrm{Tr}_{\mathrm{B}}\{\rho_{\mathrm{T}}\}, \tag{3.10}$$

which may be appreciated by noting that the trace of a density operator equates to unity. ρ_{S} is referred to as the *reduced density operator*, and the equation of motion becomes,

$$\frac{d}{dt}\rho_{\mathrm{S}}(t) = -i\mathrm{Tr}_{\mathrm{B}}\big[H_{\mathrm{T}}, \rho_{\mathrm{T}}(t)\big]. \tag{3.11}$$

The most popular master equation used in NMR to date is that referred to as the *Redfield equation*, and, recently, interest has been sparked by integration of a *Lindbladian* formalism in the treatment of long-lived states.

3.1.3 WBR as standard repertoire

As mentioned in section 3.1.1, semiclassical WBR theory offers an approximate perturbative solution to the Liouville-von Neumann equation. Stated explicitly in the introduction of the 1965 paper by Redfield, this theory concerns a system interacting *weakly* with the bath [57]. Here, H_0 is time-independent, and the state vector of each member of the ensemble may be written in terms of its eigenvectors. H_1, however, is a time-dependent, stochastic, and Hermitian perturbation.

Starting from eq. (3.7), substitution back into the Liouville-von Neumann equation and successive integration to second-order yields,

$$\frac{d}{dt}\tilde{\rho}(t) = -i\big[\tilde{H}_1(t), \tilde{\rho}(0)\big] - \int_0^t dt' \big[\tilde{H}_1(t), \big[\tilde{H}_1(t'), \tilde{\rho}(t')\big], \tag{3.12}$$

where $\rho(t)$ is the density operator of the spin system only, and gives no information on the bath. An ensemble averaging of all terms is taken, since remote parts of the spin ensemble relax independently, leading to differing *local* density operators. From here, a stream of assumptions are introduced to perform an ensemble averaging;

1. $\overline{H_1(t)} = 0$; more precisely, all matrix elements vanish under ensemble averaging
2. The quantity $\langle Q \rangle$ evolves slowly on the timescale of the correlation time τ_c
3. It is permissable to make the substitution $\tilde{\rho}(t') \to \tilde{\rho}(t)$ on the RHS of eq. (3.12)
4. The upper limit of integration may be extended to infinity
5. Higher-order terms may be neglected in eq. (3.12); a consequence of WBR theory being a weak collision theory.

Assumption 1 holds immediately, since any interactions which have non-vanishing Hamiltonian matrix elements under averaging may simply be included in a redefined H_0, and are not considered perturbations. Then, since all remote parts of the ensemble have equivalent $\rho(0)$, the first term in eq. (3.12) vanishes. If we assume the expectation value of some observable Q varies slowly on the timescale of τ_c, then so does $\tilde{\rho}(t)$, and we choose $t \gg \tau_c$. This leads directly into assumption 3, since only values of t differing from t' by a small factor of τ_c will contribute to the integral. Eq. (3.12) is then *local* in time, in the sense that time evolution of the system depends only on $\rho(t)$, but is not yet Markovian since it depends on the initial preparation of the system. Further, introducing the integration variable, $\tau = t - t'$, we may extend the integral to infinity as a consequence of $t \gg \tau_c$. The semiclassical Markovian master equation has finally become,

$$\frac{d}{dt}\tilde{\rho}(t) = -\int_0^\infty d\tau \overline{\big[\tilde{H}_1(t), \big[\tilde{H}_1(t-\tau), \tilde{\rho}(t)\big]\big]}, \tag{3.13}$$

where the overbar has been dropped from the LHS for clarity.

Eq. (3.13) is the celebrated *Redfield equation*, which has been the master equation utilised with great success in the NMR literature and elsewhere. However, there are some caveats which one must bear in mind. Firstly, the semiclassical theory predicts the system will evolve to equal populations of all states, which corresponds to a bath of infinite temperature on thermodynamic grounds. This is remedied in the original literature with the *ad hoc* correction, $\rho(t) \rightarrow \rho(t) - \rho_{eq}$ on the RHS of eq. (3.13). In fact, it has been shown theoretically [59, 60] that eq. (3.13) predicts unphysical behaviour along the way when a system prepared "in an unusual way" returns to thermal equilibrium.

Although eq. (3.13) is the more practical form of the Redfield equation, a purely quantum mechanical form of the equation was also derived [11, 57], which considers the bath explicitly and utilises the partial trace to isolate the spin system dynamics rather than take an ensemble average. This also considers only the *weak-coupling limit*, and the Hamiltonian of the full system is assumed to be of the form,

$$H_{\mathrm{T}} = H_{\mathrm{S}} + H_{\mathrm{B}} + H_{\mathrm{int}}, \tag{3.14}$$

where H_{int} here is a time-independent perturbation loosely coupling the spin system to the bath. In this limit, it is assumed the bath – and hence its density operator – is influenced by the system in a negligible way. The total density operator may be approximated as,

$$\rho_{\mathrm{T}}(t) \simeq \rho_{\mathrm{S}}(t) \otimes \rho_{\mathrm{B}}, \tag{3.15}$$

where the time-dependence of the total density operator is contained in the spin system.

From here, derivation is analogous to that leading to eq. (3.12), but the partial trace over bath degrees of freedom is introduced to give,

$$\frac{d}{dt}\tilde{\rho}_{\mathrm{S}}(t) = -i\mathrm{Tr}_{\mathrm{B}}\big[\tilde{H}_{\mathrm{int}}(t), \tilde{\rho}_{\mathrm{S}}(0) \otimes \tilde{\rho}_{\mathrm{B}}\big] - \int_0^t dt' \mathrm{Tr}_{\mathrm{B}}\big[\tilde{H}_{\mathrm{int}}(t), \big[\tilde{H}_{\mathrm{int}}(t'), \tilde{\rho}_{\mathrm{S}}(t') \otimes \tilde{\rho}_{\mathrm{B}}\big]\big], \tag{3.16}$$

where the notation $\tilde{\rho}_{\mathrm{T}}(t) = \tilde{\rho}_{\mathrm{S}}(t) \otimes \tilde{\rho}_{\mathrm{B}}$ is used. The same assumptions are made as above, but the correlation time considered is that associated with the bath correlation functions. That is,

1. $\mathrm{Tr}_{\mathrm{B}}\big[\tilde{H}_{\mathrm{int}}(t), \tilde{\rho}_{\mathrm{S}}(0) \otimes \tilde{\rho}_{\mathrm{B}}\big] = 0$

2. If the time scale in consideration is large compared to that which the correlation of the bath decays ($t \gg \tau_{\mathrm{B}}$), then we may again make the substitution $\rho_{\mathrm{S}}(t') \to \rho_{\mathrm{S}}(t)$, and the quantum mechanical Redfield equation is *local* in time

3. The substitution $t' \to t - \tau$ is again made with the upper limit of integration taken to infinity, since the QM Redfield equation still depends on the initial preparation of the system and is non-Markovian otherwise; since $t \gg \tau_{\mathrm{B}}$, the integrand vanishes sufficiently fast

The QM Markovian master equation becomes,

$$\frac{d}{dt}\tilde{\rho}_{\mathrm{S}}(t) = -\int_0^t d\tau \mathrm{Tr}_{\mathrm{B}}\big[\tilde{H}_{\mathrm{int}}(t), \big[\tilde{H}_{\mathrm{int}}(t-\tau), \tilde{\rho}_{\mathrm{S}}(t) \otimes \tilde{\rho}_{\mathrm{B}}\big]\big]. \tag{3.17}$$

Although eq. (3.17) is Markovian, it does not always preserve the positivity of the density operator [61–64], and as such the operator describing the final state may not fulfill the requirements of a density operator. To rectify this, the secular approsimation is made, which amounts to averaging over large oscillating terms in the master equation. This in turn leads to the Gorini-Kossakowski-Sudarshan-Lindblad (or, simply, *Lindblad*) master equation...

3.1.4 The Lindblad master equation

In order to secularise eq. (3.17) and put it in Lindbladian form, the perturbing Hamiltonian is written in *operator form*. The transformation to the interaction frame provides a master equation written with oscillating terms, which are then averaged out [52, 53]. This serves as a pedagogical precursor to the treatment given to the semiclassical equation in section 3.2.

The Hamiltonian H_{int} may be written in the Schroödinger picture as,

$$H_{\mathrm{int}} = \sum_j S_j \otimes B_j, \tag{3.18}$$

where $S_j \in \mathcal{H}_{\mathrm{S}}$ and $B_j \in \mathcal{H}_{\mathrm{B}}$ are operators. The secular approximation is achieved by choosing S_j to be eigenoperators of $\hat{H}_{\mathrm{S}}\bullet = \big[H_{\mathrm{S}}, \bullet\big]$ which satisfy,

$$\big[H_{\mathrm{S}}, S_j\big] = -\omega_j S_j. \tag{3.19}$$

In the interaction picture of the spin system, these operators become,

$$\tilde{S}_j(t) = e^{iH_{\rm S}t} S_j e^{iH_{\rm S}t} = e^{-i\omega_j t} S_j \tag{3.20}$$

which immediately implies,

$$\left[H_{\rm S}, S_j^\dagger\right] = +\omega_j S_j^\dagger. \tag{3.21}$$

We then write,

$$\tilde{H}_{\rm int}(t) = \sum_j e^{-i\omega_j t} S_j \otimes \tilde{B}_j(t), \tag{3.22}$$

where $\tilde{B}_j(t)$ are interaction picture operators of the bath. From the requirement, $\mathrm{Tr}_{\rm B}\big[\tilde{H}_{\rm int}(t), \tilde{\rho}_{\rm S}(0) \otimes \tilde{\rho}_{\rm B}\big] = 0$, we note,

$$\left\langle \tilde{B}_j(t) \right\rangle \equiv \mathrm{Tr}_{\rm B}\left\{\tilde{B}_j(t)\tilde{\rho}_{\rm B}\right\} = 0, \tag{3.23}$$

and bath averages vanish for all $\tilde{B}_j(t)$. Note that the spectrum $\{\omega_i\}$ is discrete and is in general degenerate. Substitution of eq. (3.22) into the master equation (3.17) yields,

$$\frac{d}{dt}\tilde{\rho}_{\rm S}(t) = \sum_{j,k} e^{i(\omega_k - \omega_j)t} \Gamma_{jk}(\omega_j) \left(S_j \tilde{\rho}_{\rm S}(t) S_k^\dagger - S_k^\dagger S_j \tilde{\rho}_{\rm S(t)} \right) + \text{h.c.}, \tag{3.24}$$

where h.c. means Hermitian-conjugated terms of those already expressed, and $\Gamma_{ij}(\omega_i)$ are the Fourier transforms of bath correlation functions; i.e. *quantum mechanical spectral density functions*,

$$\Gamma_{jk}(\omega_j) \equiv \int_0^\infty d\tau \left\langle \tilde{B}_j^\dagger(t) \tilde{B}_k(t-\tau) \right\rangle e^{i\omega_j \tau}, \tag{3.25}$$

with $\Gamma_{jk}^\dagger(\omega_j) = \Gamma_{kj}^*(\omega_k)$, and $\left\langle B_j^\dagger(t) B_k(t-\tau) \right\rangle \equiv \mathrm{Tr}_{\rm B}\left\{B_j^\dagger(t) B_k(t-\tau)\rho_{\rm B}\right\}$.

The timescale on which the open system evolves is defined by a typical value of $\tau_{\rm S} = |\omega_j - \omega_k|^{-1}$, with $\omega_j \neq \omega_k$. If this is large compared to the relaxation time of the open system, the terms for

which $\omega_j \neq \omega_k$ may be assumed to average to zero much more rapidly than relaxation occurs. That is, terms proportional to $e^{i(\omega_k - \omega_j)}$, where $\omega_j \neq \omega_k$ are neglected. We're then left with,

$$\frac{d}{dt}\rho_{\rm S}(t) = \sum_{j,k}\Gamma_{jk}(\omega_j)\left(S_j\rho_{\rm S}(t)S_k^\dagger - S_k^\dagger S_j\rho_{\rm S(t)}\right) + \text{h.c.}, \tag{3.26}$$

and although different operators S_j and S_k are involved, they are to account for degeneracy, and both correspond to eigenfrequency ω_j of $\hat{H}_{\rm S}\bullet$.

In a final step, we may obtain the Lindblad form of the QM master equation by decomposing $\Gamma_{jk}(\omega_j)$ into Hermitian and non-Hermitian parts,

$$\Gamma_{jk}(\omega_j) = \frac{1}{2}\gamma_{jk}(\omega_j) + i\epsilon_{jk}(\omega_j), \tag{3.27}$$

with,

$$\gamma_{jk}(\omega_j) = \Gamma_{jk}(\omega_j) + \Gamma_{jk}^\dagger(\omega_j) = \int_{-\infty}^{+\infty} d\tau \left\langle \tilde{B}_j^\dagger(t)\tilde{B}_k(t-\tau)\right\rangle e^{i\omega_j\tau} \tag{3.28}$$

$$\epsilon_{jk}(\omega_j) = \frac{1}{2i}\left(\Gamma_{jk}(\omega_j) - \Gamma_{jk}^\dagger(\omega_j)\right). \tag{3.29}$$

The dynamics may then be separated into Hermitian and non-Hermitian, and the master equation in the interaction picture becomes,

$$\frac{d}{dt}\rho_{\rm S}(t) = -i\big[H_{\rm S} + H_{\rm shift}, \rho_{\rm S}(t)\big] + \mathcal{D}\big[S_j, S_k\big]\rho_{\rm S}(t), \tag{3.30}$$

where $H_{\rm shift} = \sum_{jk}\epsilon_{jk}(\omega_j)S_jS_k$ is a Hermitian operator which contributes to the unitary dynamics, and shifts the unperturbed energy levels due to the system-bath coupling. $\mathcal{D}\big[S_j, S_k\big]\bullet$ is the *dissipator* of the master equation, and takes the form,

$$\mathcal{D}\big[S_j, S_k\big]\bullet = \sum_{j,k}\gamma_{jk}(\omega_j)\left(S_j \bullet S_k^\dagger - \frac{1}{2}\left\{S_k^\dagger S_j, \bullet\right\}\right), \tag{3.31}$$

and the QM spectral density functions satisfy,

$$\gamma_{jk}(\omega_j) = \gamma_{kj}(-\omega_j)e^{\beta\omega_j}, \tag{3.32}$$

where $\beta \equiv 1/k_{\mathrm{B}}T$ is the inverse temperature, which is a consequence of $\rho(t)$ reaching thermal equilibrium at $t \to \infty$.

Finally, Suppose, ρ_{B} is a stationary state of H_{B}, then it is permissable to make the substitution $t \to \tau$, and $\Gamma_{jk}(\omega_j)$ are time-independent. Then, the generator in eq. (3.30) satisfies the time-independent solution of the Liouville-von Neumann equation and has the semigroup property defined by eq. (3.2) and (3.3).

A final note to put the Lindblad master equation into the context of NMR: H_{S} and H_{shift} are combined into the coherent dynamics, and a refined coherent Hamiltonian $H_0 = H_{\mathrm{S}} + H_{\mathrm{shift}}$ may thusly be redefined. This is analogous to the *dynamic frequency shift* [65–67], which stem from the imaginary part of the classical spectral density function. Practically, the parameters which define energy levels will be experimentally determined in all following simulations. We, therefore, account for these shifts indirectly in all that follows.

3.2 Relaxation via anisotropic rotational diffusion

The theory of spin relaxation often focuses on the rotational diffusion of the molecules hosting the spin system; that is, molecular tumbling modulates the time-dependent interactions via random reorientation of the molecule, which in turn is brought about by molecular collisions. Here, the tumbling is considered to be entirely anisotropic, implying the molecule is of arbitrary geometry. The derivation of the spectral density function is very much in the vain of Huntress (1968 and 1970) [68, 69].

3.2.1 Operator form of the Redfield Equation

In section 2.5, spin Hamiltonians were written in terms of tensor components in the irreducible spherical tensor (IST) basis, and for interaction Λ we write,

$$\begin{aligned} H_\Lambda(t) &= c_\Lambda \sum_{k=0}^{2} \sum_{q=k}^{+k} (-1)^q A^\Lambda_{k-q}(t) X^\Lambda_{kq} \\ &= c^\Lambda \sum_{k=0}^{2} \sum_{q=-k}^{+k} (-1)^q A^\Lambda_{kq}(t) X^\Lambda_{k-q}, \end{aligned} \tag{3.33}$$

where the Hermiticity $H^\Lambda = H^{\Lambda\dagger}$ is used in the second line. Writing the pertubative Hamiltonian $H_1(t)$ in the form of eq. (3.33), and subsequent substitution into the semiclassical Redfield equation, (3.13), yields,

$$\begin{aligned} \frac{d}{dt}\tilde{\rho} = &- \sum_{\Lambda,\Lambda'} c_\Lambda c_{\Lambda'} \sum_{k,k'} \sum_{q,q'} (-1)^{q+q'} \Big[\tilde{X}^\Lambda_{k-q}, \Big[\tilde{X}^{\Lambda'}_{k'-q'}, \tilde{\rho}(t)\Big]\Big] \\ &\times \int_0^{+\infty} d\tau \overline{A^\Lambda_{kq}(t) A^{\Lambda'}_{k'q'}(t-\tau)}, \end{aligned} \tag{3.34}$$

where $q \in \{k, k-1, \cdots, -k\}$ and similarly for q'. To remove excessive indices in the expressions, the time derivative on the LHS of (3.34) may be written as a sum of terms for which k, k', Λ, and Λ' are kept constant, and linearity of the differential operator is used. We write,

$$\frac{d}{dt}\tilde{\rho} = \sum_{\Lambda,\Lambda'} \sum_{k,k'} \frac{d}{dt}\tilde{\rho}^{\Lambda\Lambda'}_{kk'}, \tag{3.35}$$

where,

$$\begin{aligned} \frac{d}{dt}\tilde{\rho}^{\Lambda,\Lambda'}_{kk'} = &-c^\Lambda c^{\Lambda'} \sum_{q,q'} (-1)^{q+q'} \big[\tilde{X}^\Lambda_{kq}, \big[\tilde{X}^{\Lambda'}_{k'q'}, \tilde{\rho}(t)\big]\big] \\ &\times \int_0^{+\infty} d\tau \overline{A^\Lambda_{k-q}(t) A^{\Lambda'}_{k'-q'}(t-\tau)}. \end{aligned} \tag{3.36}$$

While this is a trivial and seemingly pointless step, it will avoid having six indices to sum over (and even more when Wigner functions are introduced).

To write the equation of motion in the Schrödinger picture, we introduce similar requirements to those of the H_{int} open system operators in eq. (3.9),

$$\begin{aligned} \big[H_0, X_{kq}\big] &= \hat{H}_0 X_{kq} = \omega_q X_{kq} \\ \big[H_0, X^\dagger_{kq}\big] &= \hat{H}_0 X^\dagger_{kq} = -\omega_q X^\dagger_{kq}, \end{aligned} \tag{3.37}$$

with $\omega_{-q} = -\omega_q$. The operator X_{kq} in the interaction picture may be written,

$$\begin{aligned} \tilde{X}_{kq}(t) &= e^{i\hat{H}_0 t} X_{kq} \\ &= e^{i\omega_q t} X_{kq}, \end{aligned} \tag{3.38}$$

where ω_q is an eigenfrequency. The stochastic Hamiltonians then become,

$$\begin{aligned} \tilde{H}_1^\Lambda(t) &= e^{i\hat{H}_0 t} H_1(t) \\ &= c^\Lambda \sum_{k,q} (-1)^q A_{k-q}^\Lambda(t) X_{kq}^\Lambda e^{i\omega_q t}, \end{aligned} \tag{3.39}$$

and,

$$\begin{aligned} \tilde{H}_1^\Lambda(t-\tau) &= e^{i\hat{H}_0 t} H_1^\Lambda(t-\tau) \\ &= c^\Lambda \sum_{k,q} (-1)^q A_{k-q}^\Lambda(t-\tau) X_{kq}^\Lambda e^{i\omega_q t} e^{-i\omega_q \tau}. \end{aligned} \tag{3.40}$$

Inserting (3.39) and (3.40) into (3.36), and utilising $H^\Lambda = H^{\Lambda\dagger}$ gives us,

$$\begin{aligned} \frac{d}{dt}\tilde{\rho}_{k,k'}^{\Lambda,\Lambda'} = -c_\Lambda c_{\Lambda'} \sum_{q,q'} (-1)^{q+q'} e^{i\left(\omega_q - \omega_{q'}\right)t} \left[X_{kq}^\Lambda, \left[X_{k'q'}^{\Lambda'\dagger}, \tilde{\rho}(t)\right]\right] \\ \times J_{kk'qq'}^{\Lambda\Lambda'}\left(\omega_{q'}\right), \end{aligned} \tag{3.41}$$

where $J_{kk'qq'}^{\Lambda\Lambda'}(\omega_{q'})$ is the *classical spectral density function*,

$$J_{kk'qq'}^{\Lambda\Lambda'}(\omega_q) = \mathrm{Re}\int_0^{+\infty} d\tau \overline{A_{k-q}^\Lambda(t) A_{k'-q'}^{\Lambda'*}(t-\tau)} e^{i\omega_{q'}\tau}, \tag{3.42}$$

whereby only the real part is expressed in the master equation, and the ensemble average is taken over the spatial components only since ergodocity of the ensemble is assumed, and they are the components which contain the temporal dependence. The imaginary part is called the *dynamic frequency shift* and may be shown to induce small shifts in the unperturbed energy levels. Then, a refined coherent Hamiltonian H_0 may be considered, accounting for these effects. This is an analogous situation found above when considering H_{shift} in the Lindblad master equation.

We can now write the Redfield equation in operator form in the Schrödinger picture. Hopping into Liouville space from our Hilbert space,

$$\frac{d}{dt}|\rho) = -i\hat{H}_0|\rho(t)) + \hat{\Gamma}|\rho(t) - \rho_{\mathrm{eq}}), \tag{3.43}$$

where $\hat{\Gamma}\bullet$ is the relaxation superoperator defined by,

$$\hat{\Gamma}\bullet = -\sum_{\Lambda,\Lambda'} c^{\Lambda}c^{\Lambda'} \sum_{k,k'}\sum_{q,q'} (-1)^{q+q'} e^{i\left(\omega_q - \omega_{q'}\right)t} J^{\Lambda\Lambda'}_{kk'qq'}(\omega_{q'}) \hat{X}^{\Lambda}_{kq} \hat{X}^{\Lambda'\dagger}_{k'q'} \bullet, \tag{3.44}$$

where $\hat{X}_{kq} \equiv \left[X_{kq}, \bullet\right]$ has been defined, and $|\rho_{\mathrm{eq}})$ is the thermal equlibrium density operator which is included as an *ad hoc* correction in order for the system populations to return to thermal equilibrium described by a Boltzmann equilibrium. Terms for which $\Lambda = \Lambda'$ are called *auto-correlated*, and *cross-correlated* otherwise.

For any mechanism treated in the following chapters, the operators X^{Λ}_{kq} are known. Thus, our task is reduced to finding the spectral density function for the system in question...

3.2.2 Classical spectral density function

For a Hamiltonian of the form in (3.33) to make sense, the spatial and spin tensors must be written in the same reference frame. However, the spin tensors are known in the observer-fixed *laboratory* (L-) *frame* (that which has the z-axis along the static magnetic field) and the spatial tensor a molecule-fixed arbitrary axis system. The latter is easily written in the *principal axis* (P-) *frame* of the interaction, whereby the tensor is diagonal, which is also molecule-fixed.

The tensors $\mathbf{A}_{\Lambda}$ contain the spatial components of the Hamiltonian and, therefore, become time-dependent due to molecular tumbling when expressed relative to the L-frame. We, thus, write the components of $\mathbf{A}_{\Lambda}$ relative to the L-frame as time-dependent stochastic functions in the P-frame. That is, we use the transformation,

$$\left[A^{\Lambda}_{kq}(t)\right]^{\mathrm{L}} = \sum_{q=-k}^{+k} D^{(k)*}_{qp}(\Omega^{\mathrm{PL}}_t)\left[A^{\Lambda}_{kp}\right]^{\mathrm{P}}, \tag{3.45}$$

from section 2.5.3, where the Wigner functions have time-dependent Euler angles as their argument, and PL denotes the set of angles which parameterise the rotation taking the initial orientation of the

P-frame into coincidence with the L-frame; that is, a passive rotation formalism is used, and will be chosen as the formalism in all treatments hereafter. We see that the time-dependence of the time-correlation function in equation (3.42) is contained entirely in the Wigner functions. In fact, the time-correlation function is between the Wigner functions only. It follows from these considerations that the spectral density function for interactions Λ and Λ' is,

$$\begin{aligned} J^{\Lambda\Lambda'}_{kk'qq'}(\omega_{q'}) &= \mathrm{Re}\int_0^{+\infty} d\tau \overline{\Big[A^{\Lambda}_{k-q}(t)\Big]^{\mathrm{L}}\Big[A^{\Lambda'*}_{k'-q'}(t+\tau)\Big]^{\mathrm{L}}} e^{-i\omega_{q'}\tau} \\ &= \sum_{p,p'}\Big[A^{\Lambda}_{kp}\Big]^{\mathrm{P}}\Big[A^{\Lambda'*}_{k'p'}\Big]^{\mathrm{P}}\mathrm{Re}\int_0^{+\infty} d\tau \overline{D^{(k)*}_{-qp}(\Omega^{\mathrm{PL}}_0)D^{(k')}_{-q'p'}(\Omega^{\mathrm{PL}}_\tau)}e^{-i\omega_{q'}\tau}, \end{aligned} \tag{3.46}$$

where Ω_0 is the set of Euler angles describing the orientation of the molecular axis at time $t+0$, and Ω_τ the set of Euler angles describing molecular axis orientation at time $t+\tau$. In practice, the P-frame may differ between interactions. As such, with some hindsight, the reference frame which diagonalises the diffusion tensor (D-frame) is a convenient stop-off point since it is both molecule-fixed (transformations between the P- and D-frames are time-independent) and independent of interaction. The transformation from the P- to the D-frame, then the D-frame to the L-frame, means the spectral density function may be written,

$$J^{\Lambda\Lambda'}_{kk'qq'}(\omega_{q'}) = \sum_{m,m'}\Big[A^{\Lambda}_{km}\Big]^{\mathrm{D}}\Big[A^{\Lambda'*}_{k'm'}\Big]^{\mathrm{D}}\mathrm{Re}\int_0^{+\infty} d\tau G^{kk'}_{qq'mm'}(\tau)e^{-i\omega_{q'}\tau}, \tag{3.47}$$

with the correlation function given by,

$$G^{kk'}_{qq'mm'}(\tau) = \overline{D^{(k)*}_{-qm}(\Omega^{\mathrm{DL}}_0)D^{(k')}_{-q'm'}(\Omega^{\mathrm{DL}}_\tau)}, \tag{3.48}$$

and where,

$$\Big[A^{\Lambda}_{km}\Big]^{\mathrm{D}} = \sum_{p=-k}^{+k} D^{(k)*}_{mp}(\Omega^{\mathrm{PD}})\Big[A^{\Lambda}_{kp}\Big]^{\mathrm{P}}. \tag{3.49}$$

To find $G^{kk'}_{qq'mm'}(\tau)$, we write eq. (3.48) as,

$$G^{kk'}_{qq'mm'}(\tau) = \int\int d\Omega_0 d\Omega_\tau D^{(k)*}_{-qm}(\Omega_0)D^{(k')}_{-q'm'}(\Omega_\tau)P(\Omega_0)P(\Omega_\tau|\Omega_0), \tag{3.50}$$

where $P(\Omega_0)$ is the probability that the molecule will be at initial orientation Ω_0, and $P(\Omega_\tau|\Omega_0)$ is the conditional probability that the molecule is at orientation Ω_τ at time $t+\tau$, given that it was at orientation Ω_0 at time $t+0$. The DL superscripts have been dropped.

Right away, we know that for a rigid molecule in an isotropic liquid, $P(\Omega_0)$ is constant for all Ω_0, and is equal to,

$$P(\Omega_0) = \frac{1}{8\pi^2}. \tag{3.51}$$

The time-derivative of the probability that the molecule will be at orientation Ω_τ at time $t+\tau$, in the limit of a rigid molecule reorienting in random steps of small angular displacement, is given by the *Favro equation* [70],

$$\frac{\partial}{\partial\tau}P(\Omega_\tau) = -H_{\mathrm{rot-diff}}P(\Omega_\tau), \tag{3.52}$$

where $H_{\mathrm{rot-diff}}$ is the *rotational-diffusion Hamiltonian*, which may be written in the form,

$$\begin{aligned} H_{\mathrm{rot-diff}} &= \mathbf{J}\bullet\mathbf{D}\bullet\mathbf{J} \\ &= \mathbf{D}\bullet(\mathbf{J}\otimes\mathbf{J}), \end{aligned} \tag{3.53}$$

where $\mathbf{J}$ and $\mathbf{D}$ are the QM angular momentum operator and diffusion tensor, respectively. That is, the diffusion tensor describes the spatial aspect of the Hamiltonian in this case. Favro shows that the solution to equation (3.52) is,

$$P(\Omega_\tau) = \int d\Omega_0 P(\Omega_0)P(\Omega_0|\Omega_\tau), \tag{3.54}$$

for which $P(\Omega_0)$ is given by equation (3.51) and the conditional probability is,

$$P(\Omega_0|\Omega_\tau) = \sum_n \langle\psi_n(\Omega_0)|\psi_n(\Omega_\tau)\rangle\, e^{-E_n\tau}, \tag{3.55}$$

where $\psi_n(\Omega)$ are eigenfunctions of $H_{\mathrm{rot-diff}}$ with the associated eigenvalue E_n. This solution is reliant on the boundary condition $P(\Omega_0|\Omega_{\tau=0}) = \delta(\Omega_0,\Omega_\tau)$, where $\delta(\Omega_0,\Omega_\tau)$ is the Dirac delta function [2].

If eq. (3.53) is written in the D-frame, it takes the form $H_{\mathrm{rot-diff}} = \sum_i D_i J_i^2$ in which $i \in \{x, y, z\}$ and J_i have become the Cartesian angular momentum operators. This takes the form of the rigid-rotor Hamiltonian when considering the substitution $D_i \to \hbar^2/2I_i$, where I_i is the moment of inertia about principal axis i. Thus, (3.55) may be expanded in asymmetric-rotor eigenfunctions [13, 68, 69],

$$|\psi_n(\Omega)\rangle \to |nJM\rangle = \sum_K a_{n,K}^{(J)} |JKM\rangle, \tag{3.56}$$

with,

$$\begin{aligned} |JKM\rangle &= \sqrt{\frac{2J+1}{8\pi^2}} D_{MK}^{(J)*}(\Omega) \\ &= (-1)^{M-K} \sqrt{\frac{2J+1}{8\pi^2}} D_{-M-K}^{(J)}(\Omega), \end{aligned} \tag{3.57}$$

and $a_{n,K}^{(J)}$ constants which satisfy $\sum_K \left\{a_{n,K}^{(J)}\right\}^2 = 1$. Substitution into (3.55), and extending the sum over n, J, and M, the time-correlation function becomes,

$$\begin{aligned} G_{qq'mm'}^{kk'}(\tau) =& \frac{1}{(8\pi^2)^2} \sum_{n,J,M} (2J+1) e^{-E_n^{(J)}\tau} \sum_{K,K'} a_{n,K}^{(J)*} a_{n,K'}^{(J)} \\ & \times \int d\Omega_0 D_{-qm}^{(k)*}(\Omega_0) D_{MK}^{(J)}(\Omega_0) \int d\Omega_\tau D_{-q'm'}^{(k')}(\Omega_\tau) D_{MK'}^{(J)*}(\Omega_\tau). \end{aligned} \tag{3.58}$$

Using the orthogonality of Wigner functions,

$$\int d\Omega D_{pq}^{(j)}(\Omega) D_{p'q'}^{(j')}(\Omega) = \frac{8\pi^2}{2j+1} \delta_{jj'} \delta_{pp'} \delta_{qq'}, \tag{3.59}$$

gives us,

$$G_{qq'mm'}^{kk'}(\tau) = \delta_{kJ} \delta_{-qM} \delta_{mK} \delta_{k'J} \delta_{-q'M} \delta_{m'K'} \frac{1}{2J+1} \sum_n e^{-E_n^{(J)}\tau} \sum_{K,K'} a_{n,K}^{(J)*} a_{n,K'}^{(J)}. \tag{3.60}$$

We see that $k = J = k', -q = M = -q', m = K$, and $m' = K'$. Since $k = k'$ and $q = q'$, the above becomes,

$$\begin{aligned} G^{k}_{qmm'}(\tau) &= \overline{D^{(l)*}_{-qm}(\Omega^{\mathrm{DL}}_{0})D^{(l)}_{-q'm'}(\Omega^{\mathrm{DL}}_{\tau})} \\ &= \delta_{kk'}\delta_{qq'}G^{kk'}_{qq'mm'}(\tau) \\ &= \frac{1}{2k+1}\sum_{n} a^{(k)*}_{n,m}a^{(k)}_{n,m'}e^{-E^{(k)}_{n}\tau}. \end{aligned} \tag{3.61}$$

The strict requirement that $q = q'$ in eq. (3.61) removes non-secular terms from the relaxation superoperator in eq. (3.44), and yields,

$$\hat{\Gamma}\bullet = -\sum_{\Lambda,\Lambda'} c_{\Lambda}c_{\Lambda'}\sum_{k,q} J^{\Lambda\Lambda'}_{kq}(\omega_q)\hat{X}^{\Lambda}_{kq}\hat{X}^{\Lambda'\dagger}_{kq}\bullet \tag{3.62}$$

with,

$$J^{\Lambda\Lambda'}_{kq}(\omega_q) = \sum_{m,m'}\left[A^{\Lambda}_{km}\right]^{\mathrm{D}}\left[A^{\Lambda'*}_{km'}\right]^{\mathrm{D}}\mathrm{Re}\int_{0}^{+\infty} d\tau G^{k}_{qmm'}(\tau)e^{i\omega_q\tau}. \tag{3.63}$$

Note how the oscillating terms have vanished from the relaxation superoperator, and secularisation is a natural consequence, when stochastic molecular tumbling is mathematically described in a framework of anisotropic rotational diffusion of a rigid molecule.

3.2.3 Approximation to quantum spectral density functions

In contrast to the QM spectral density functions in section 3.1.4, the classical spectral density functions have the symmetry property,

$$J_{kq}(\omega_q) = J_{kq}(-\omega_q). \tag{3.64}$$

However, we have seen that,

$$\gamma_{jk}(\omega_j) = \gamma_{kj}(-\omega_j)e^{\beta\omega_j}, \tag{3.65}$$

for QM spectral density functions.

On considering interaction of the open system with its environment, Redfield [57] suggested that $J_{kq}(\omega_q) \propto e^{-\frac{1}{2}\hbar\beta\omega_q}$, which allows one to avoid to *ad hoc* correction in eq. (3.43), and is also presented

in Abragam's text [11]. Independently, various *ad hoc* corrections have been developed in order for semiclassical spectral density functions to display the same behaviour as their QM counterparts [71–77]. Importantly, the *detailed balance* condition must be satisfied; at thermal equilibrium, every transition out of a state in the system is *balanced* on average by a transition into said state [78].

A correction which has had success in applications to neutron scattering [71], vibrational relaxation [79], and recently in NMR spin relaxation processes [59, 60, 80], is the *Schofield correction* [71],

$$\gamma_{jk}(\omega_j) \to J_{kq}(\omega_q) e^{\frac{1}{2}\hbar\beta\omega_q}, \tag{3.66}$$

which happens to have the same convenient form as that proposed in Redfield and Abragam's work. Note that indices j and k in $\gamma_{jk}(\omega_j)$ refer to spins, whilst indices k and q in $J_{kq}(\omega_q)$ refer to the components of interaction in the L-frame.

3.3 Long-Lived States

One of the most prominent applications of WBR relaxation theory is that of *long-lived states* (LLS) [27, 81–93]. These are spin-orders which have a decay constant greatly exceeding their longitudinal relaxation constant T_1 [46, 88, 94, 95]. The most commonly accessed of these is *singlet-order*, which is defined as the operator whose expectation value is the population imbalance between the singlet- and triplet-manifolds of a two spin-1/2 system. Usually, $T_\mathrm{S} \gg T_1$, where T_S is the decay constant of singlet-order.

H_DD is given in eq. (2.81) and may be rewritten in terms of the trace over two rank-2 tensors as,

$$\begin{aligned} H_\mathrm{DD} &= \sum_{i<j} b_{ij} \mathbf{I}_i \cdot \mathbf{D}^{(ij)} \cdot \mathbf{I}_j \\ &= b_{ij} \mathrm{Tr}\left\{ \mathbf{D}^{(ij)} \mathbf{X}^{(ji)} \right\}, \end{aligned} \tag{3.67}$$

where $b_{ij} = \mu_0 \gamma_i \gamma_j \hbar / (4\pi r_{ij}^3)$ is the coupling constant, $\mathbf{D}^{(ij)}$ the spatial tensor, and $\mathbf{X}^{(ji)} = \mathbf{I}_j \otimes \mathbf{I}_i$ the spin tensor. As mentioned above, components of $\mathbf{X}^{(ji)}$ are inherently in the L-frame, whilst

components of $\mathbf{D}^{(ij)}$ are known in an arbitrary frame. However, we may express components of $\mathbf{D}^{(ij)}$ in the L-frame via those in the P-frame following diagonalisation to give,

$$\left[\mathbf{D}^{(ij)}\right]^{\mathrm{P}} = \begin{pmatrix} 1 & 0 & 0 \\ 0 & 1 & 0 \\ 0 & 0 & -2 \end{pmatrix}, \tag{3.68}$$

which may be decomposed in the IST operator basis as,

$$\left[\mathbf{D}^{(ij)}\right]^{\mathrm{P}} = -\sqrt{6}\mathbf{T}_{20}, \tag{3.69}$$

where only the rank-2 components survive. We then immediately obtain,

$$\hat{\Gamma}_{\mathrm{DD}}\bullet = -b_{ij}^2 \sum_q J_{2q}^{\mathrm{DD}}(\omega_q)\hat{X}_{2q}^{\mathrm{DD}}\hat{X}_{2q}^{\mathrm{DD}\dagger}\bullet, \tag{3.70}$$

where $\Lambda = \Lambda'$ since both spins are involved in the coupling.

Operators representing population configurations have zero quantum coherence. An eigenoperator of the *zero-quantum block* of $\hat{\Gamma}^{\mathrm{DD}}$, which describes the relevant population imbalance is,

$$|Q_{\mathrm{SO}}) = \frac{1}{2\sqrt{3}}\left(3\,|S_0\rangle\langle S_0| - \sum_{M=-1}^{+1}|T_M\rangle\langle T_M|\right), \tag{3.71}$$

and we write,

$$\begin{aligned}(Q_{\mathrm{SO}}|\,\hat{\Gamma}^{\mathrm{DD}}\,|Q_{\mathrm{SO}}) &\equiv \mathrm{Tr}\left\{\mathbf{Q}_{\mathrm{SO}}^{\dagger}\hat{\mathbf{\Gamma}}_{\mathrm{DD}}\mathbf{Q}_{\mathrm{SO}}\right\} \\ &= 0.\end{aligned} \tag{3.72}$$

This illustrates why singlet-order is very often long-lived; this particular spin-order does not evolve under the influence of the intrapair DD mechanism, which is the dominant mechanism in many cases [9, 88].

3.4 Spin Relaxation in solution NMR; practical considerations

In solution state NMR, a practical choice is to approximate the coherent Hamiltonian as the Zeeman Hamiltonian,

$$H_0 \approx H_{\mathrm{Z}} = \sum_i \omega_{0i} I_{iz}. \tag{3.73}$$

The reason being is that components X_{kq} have the commutation relation,

$$\left[I_z, X_{kq}\right] = qX_{kq}, \tag{3.74}$$

Thus, requirements,

$$\begin{aligned}\left[H_0, X_{kq}\right] &= \hat{H}_0 X_{kq} = \omega_q X_{kq} \\ \left[H_0, X_{kq}^\dagger\right] &= \hat{H}_0 X_{kq}^\dagger = -\omega_q X_{kq}^\dagger,\end{aligned}$$

are satisfied, while noting $X_{kq}^\dagger = (-1)^q X_{k-q}$, and $\omega_{-q} = -\omega_q$ holds. This gives a particularly simple spectral density function for simulation when considering a homonuclear two-spin system, since we may write,

$$J_{kq}(\omega_q) \rightarrow J_{kq}(q\omega_0) \propto e^{iq\omega_0\tau}. \tag{3.75}$$

This approximation presents a clear contradiction; H_0 is used to remove the unitary dynamics from the master equation via transformation to the interaction picture, and will not contain the Zeeman term only. However, we will see that this approximation allows for simple simulations which offer great insight into the spin dynamics and their consequences.

Further, since bath variables are unknown, when translating the WBR master equation to Lindblad form, the QM spectral density function will be substituted for the thermalised semiclassical form,

$$\gamma_{jk}(\omega_j) \rightarrow J_{kq}^{\theta\Lambda\Lambda'}(q\omega_0) = 2J_{kq}^{\Lambda\Lambda'}(q\omega_0)e^{\frac{1}{2}\beta q\omega_0} \tag{3.76}$$

where indices j and k in $\gamma_{jk}(\omega_j)$ refer to spins, whilst indices k and q on the RHS refer to the components of interaction in the L-frame. The factor of two is included to account for limits of integration in $\gamma_{jk}(\omega_j)$ ranging from $-\infty \rightarrow +\infty$, whilst those in $J_{kq}^{\Lambda\Lambda'}(q\omega_0)$ range only $0 \rightarrow +\infty$.

Attention must also be paid to the use of spin operators when moving through the two formalisms. The derivation of the Lindbladian master equation required that the open system operators S_j fulfill,

$$\begin{aligned}\big[H_0, S_j\big] &= -\omega_j S_j \\ \big[H_0, S_j^\dagger\big] &= +\omega_j S_j^\dagger,\end{aligned}$$

while the semiclassical master equation relied upon spin-system operators having the properties,

$$\begin{aligned}\big[H_0, X_{kq}\big] &= +\omega_q X_{kq} \\ \big[H_0, X_{kq}^\dagger\big] &= -\omega_q X_{kq}^\dagger.\end{aligned} \tag{3.77}$$

The above suggests the correspondence,

$$S_j \Leftrightarrow X_{kq}^\dagger \quad \text{and} \quad S_j^\dagger \Leftrightarrow X_{kq}. \tag{3.78}$$

Finally, as discussed in section 3.1.4, unitary dynamics contain Hamiltonian H_{shift}, which shifts the unperturbed energy levels and is absorbed into H_0, and analogy exists between H_{shift} and the dynamic frequency shift. In all treatments that follow, H_0 is written in terms of the Zeeman, chemical shift and spin-spin coupling interactions. Parameters which define the corresponding Hamiltonians are derived from experiment, and, thus, any perturbations in energy levels are indirectly accounted for. By comparing the WBR and Lindbladian formalisms, it is clear that there exists the correspondence,

$$H_0 \Leftrightarrow H_{\text{S}} + H_{\text{shift}} \quad \text{and} \quad H_1(t) \Leftrightarrow H_{\text{int}}(t), \tag{3.79}$$

where $H_1(t)$ and $H_{\text{shift}}(t)$ describe small time-dependent perturbations on the system which induce relaxation.

The resulting theory of this chapter and the practical considerations of this section will be used extensively throughout chapter 4, and in numerical simulations in chapter 5.

Chapter 4

The *Triyne* System; Cross-Correlated Lineshapes

After exhausting NMR and spin relaxation theory, we apply *all* of the above in an exposition of spectral line shape. In Redfield's 1965 paper, it is stated that the semiclassical theory, " ... *has found its greatest application in predicting line widths of complex spectra of molecules containing several spins.*" Here, we do just that, except the spectrum isn't *complex*, and we consider only a two-spin, rather than a *several-spin*, system. Nevertheless, we will see interesting effects from the *cross-correlation* between spin relaxation mechanisms.

The host of the spin system is a linear *triyne* derivative; that is, one may draw alternating single and triple bonds along a chain of carbon atoms as a representation. Initially, interest was stirred due to the innate symmetry of the molecule, which suggests the existence of very long-lived singlet-order if one were to label the two central carbons of the chain with ^{13}C isotopes. However, that is put-off for the time being, since a peculiar line shape materialised from a basic experiment. The investigation of this line shape self-constructed the material of this chapter.

The main body of this chapter describes the material in Whipham et al. (2022), "Cross-correlation effects in the solution NMR spectra of near-equivalent spin-1/2 pairs" [96], in detail. Figures 4.1, 4.2, 4.4, and 4.5 are identical to those found in the publication, whereas figure 4.3 is very similar to that published but with the addition of the chemical shift tensor.

4.1 Introduction

As written recently, if a nuclear spin system is perturbed from a thermal equilibrium, it slowly returns to equilibrium through nuclear spin relaxation. Relaxation processes are driven by fluctuations in the interactions between the nuclear spins and the thermal molecular environment, and these interactions may be correlated with each other. For example, in solution NMR, the fluctuations of nuclear spin interactions are caused by stochastic molecular tumbling, and since the rotation of a molecule modulates all intramolecular interactions at the same time, the fluctuations of these interactions are correlated. Such *cross-correlation* effects are well-documented in solution NMR [97–104]. Cross-correlation gives rise to differential line broadening and line narrowing, and differences in the longitudinal relaxation behaviour of individual multiplet components [97–100, 102, 104]. Cross-correlation effects have been used to estimate the relative orientations of nuclear spin interaction tensors, allowing the estimation of molecular torsional angles [105–107]. A particularly important set of cross-correlation effects is associated with the so-called TROSY techniques (transverse relaxation-optimized spectroscopy), which have important applications, especially in biomolecular NMR [108, 109].

Cross-correlation often takes place between the fluctuations of internuclear dipole-dipole (DD) couplings and chemical shift anisotropy (CSA) interactions. Such DD-CSA cross-correlation effects are well-known for heteronuclear spin pairs, and underpin important techniques (such as TROSY mentioned above) [100, 108, 109]. In this chapter, strong DD-CSA cross-correlation effects are demonstrated in the solution NMR of a system containing *homonuclear* pairs of ^{13}C nuclei, in the limit of *near-magnetic-equivalence*, implying that the chemical shift difference between the coupled nuclear sites is much smaller than the internuclear spin-spin (or J-) coupling.

The system in question is shown in fig. 4.1a. An analysis of cross-correlated relaxation must take into account the rod-like shape of the molecule, which causes strongly anisotropic rotational diffusion in solution. The theory of nuclear spin relaxation has been developed in the context of model-free treatments of biomolecules with anisotropic internal motions [110–115]. However, most

existing treatments of cross-correlated relaxation in small molecules assume approximately isotropic rotational diffusion, which is clearly not applicable here. In the following sections, the theory of cross-correlated relaxation in systems with anisotropic rotational diffusion is developed, and analytical formulae are provided which describe the NMR spectrum of a near-equivalent homonuclear spin pair undergoing cross-correlated relaxation in the presence of anisotropic rotational diffusion. The observed spectral asymmetry is reproduced, with good agreement between theory, experiment and numerical simulations.

Since near-equivalent spin-pairs are the most common subject in the field of long-lived states [88, 90, 95, 116, 117], the $^{13}C_{13}$-DAND system [95, 116] is considered to deduce the relationship between spectral lineshape and relative orientation of the principal axes of interaction. The "rules" deduced qualitatively agree with experiment, and numerical simulation of the spectrum using the theory described in this chapter agrees very well with experiment.

4.2 The triyne molecule and spin system

The system of interest is the $^{13}C_2$-labelled *triyne* derivative, with systematic name, 1-methoxy-4-((4-(methoxymethoxy)phenyl)hexa-1,3,5-triyn-1-yl)benzene... but here referred to as **I**. The molecular structure is shown in fig. 4.1a. Assuming a rigid geometry, each molecule of **I** has a rod-like shape, with two ^{13}C labels at the central pair of carbon atoms, in the centre of the triyne moiety. The end groups are different but far from the labelled nuclei, endowing the two ^{13}C nuclei with slightly different chemical shifts ($\Delta\delta_{\text{iso}} = 0.16$ ppm). Since the J-coupling is large ($J_{ij} = 214.15$ Hz) between the labelled nuclei, the ^{13}C pair is in the *near-equivalent* regime at all accessible magnetic fields [118].

4.3 Experimental

4.3.1 NMR spectrum

The experiments were performed on a 400 MHZ (9.4 T) Bruker Avance Neo spectrometer. The pulse sequence was a simple 90°pulse-acquire. The ^{13}C nutation frequency was 6.68 kHz and 1 scan was performed.

The ^{13}C NMR spectrum of a 0.3 M solution of **I** in $CDCl_3$ is shown in figure 4.2. This corresponds

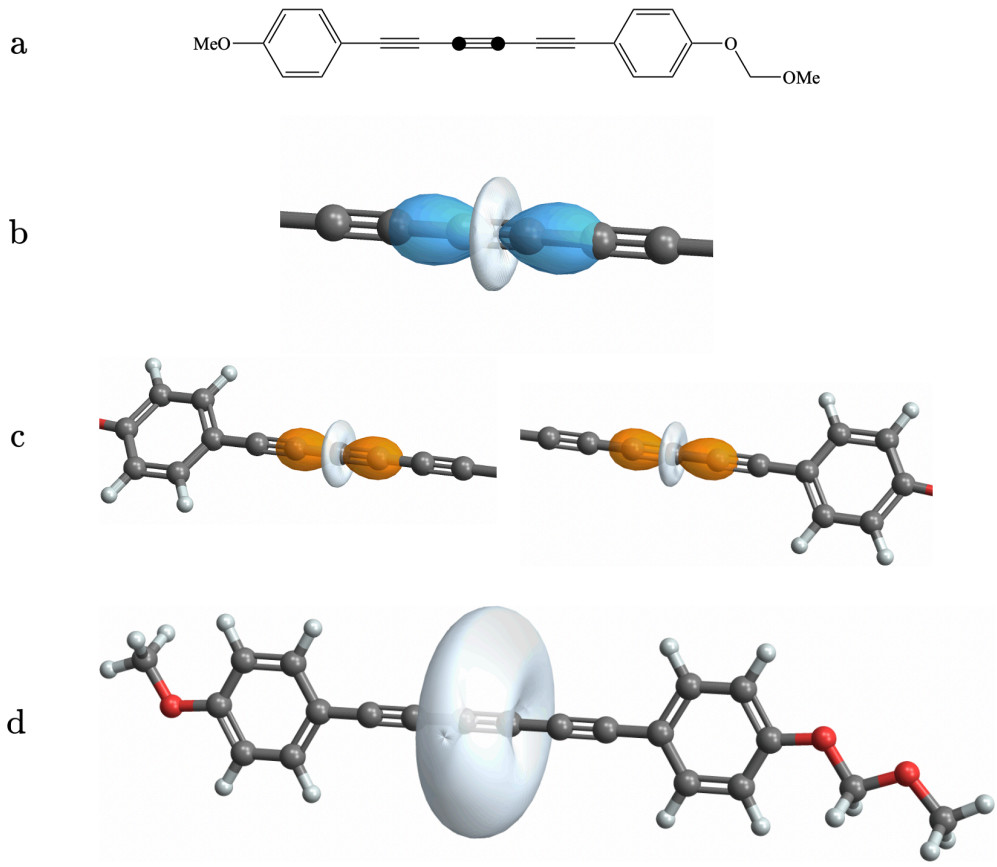

FIGURE 4.1: (a) Molecular structure of **I**, with ^{13}C labelled sites depicted by black circles; (b) The rank-2 part of the ^{13}C -^{13}C dipole-dipole coupling tensor, represented by an ovaloid [119, 120]; (c) The calculated ^{13}C CSA tensors of the ^{13}C labels represented by ovaloids; (d) The inertia tensor of the molecule, represented as an ovaloid, superimposed on the molecular structure. The grey atoms are C, the red atoms O, and white H. The graphics were generated in *SpinDynamica* [49].

to the expected AB four-peak structure, although the two outer peaks are too weak to be observed. The two strong central peaks are only partially resolved, and form a strongly asymmetric lineshape. As discussed below, the asymmetry of the central peak pair is due to strong DD-CSA cross-correlation effects.

4.3.2 Computation

Geometry optimisation and simulation of the magnetic shielding tensors of **I** were performed at the B3LYP/aug-cc-PVTZ [121–123] level of theory in the Gaussian 09 suite of programs [124]. After geometry optimisation, the dipole-dipole coupling tensor between the two ^{13}C nuclei was calculated from the internuclear distance. The parameters obtained from the computations are presented in table 4.1.

4.4 Interactions

4.4.1 Coherent Hamiltonian

The coherent spin Hamiltonian describes the interactions which are the same for identical members of the spin ensemble at a given point in time. For a homonuclear spin-1/2 pair in solution, it may be written in the rotating frame and in the absence of a radiofrequency field as,

$$H_0 = \frac{1}{2}\omega_\Sigma(I_{1z} + I_{2z}) + \frac{1}{2}\omega_\Delta(I_{1z} - I_{2z}) + \omega_J \mathbf{I}_1 \cdot \mathbf{I}_2, \tag{4.1}$$

with,

$$\omega_\Sigma = \omega_1 + \omega_2 \tag{4.2}$$

$$\omega_\Delta = \omega_1 - \omega_2 \tag{4.3}$$

$$\omega_J = 2\pi J_{12}, \tag{4.4}$$

where J_{12} is the isotropic part of the spin-spin coupling tensor, and ω_j is the precession frequency of spin j,

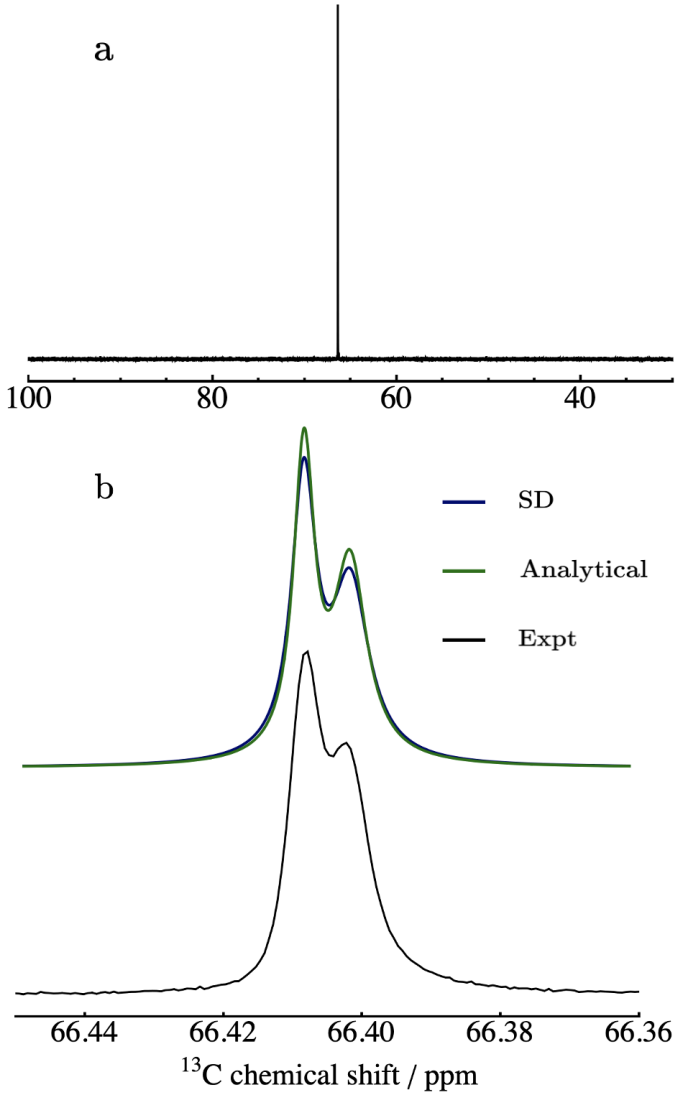

FIGURE 4.2: ^{13}C spectra of a 0.3 M solution of **I** in $CDCl_3$, at a magnetic field of 9.4 T. (a) Overview of the ^{13}C spectrum; (b) Black line: Expanded view of the central doublet, showing the strongly asymmetric linewidths of the doublet components. Dark blue line: Numerical *SpinDynamica* simulation [49], using the theory given in the text and parameters in table 4.1. Green line: Superposition of two Lorentzians with amplitudes, frequencies, and linewidths specified by table 4.5 and eq. (4.55) spectrum.

$$\omega_j = \omega_0(1 + \delta_j^{\text{iso}}) - \omega_{\text{rf}}. \tag{4.5}$$

Here, ω_0 is the Larmor frequency of the isotope, δ_j^{iso} is the isotropic chemical shift for the j^{th} spin, and ω_{rf} is the radiofrequency carrier frequency.

Generally, the Hamiltonian may be diagonalised by using the $\mathbb{B}'_{\text{ST}}$ basis, defined as,

$$\mathbb{B}'_{\text{ST}} = \left\{|S'_0\rangle, |T'_{+1}\rangle, |T'_0\rangle, |T'_{-1}\rangle\right\}, \tag{4.6}$$

with elements,

$$|S'_0\rangle = \cos\frac{\theta}{2}|S_0\rangle - \sin\frac{\theta}{2}|T_0\rangle \tag{4.7}$$

$$|T'_{+1}\rangle = |T_{+1}\rangle \tag{4.8}$$

$$|T'_0\rangle = \sin\frac{\theta}{2}|S_0\rangle + \cos\frac{\theta}{2}|T_0\rangle \tag{4.9}$$

$$|T'_{-1}\rangle = |T_{-1}\rangle, \tag{4.10}$$

where θ is the *singlet-triplet mixing angle*,

$$\tan\theta = \omega_\Delta/\omega_J. \tag{4.11}$$

Defining, $\omega_e^2 = \omega_\Delta^2 + \omega_J^2$, the eigenvalues of H_{coh} are

$$\omega_{S'_0} = -\frac{1}{4}\big(\omega_J + 2\omega_e\big) \tag{4.12}$$

$$\omega_{T'_{+1}} = +\frac{1}{4}\big(\omega_J + 2\omega_\Sigma\big) \tag{4.13}$$

$$\omega_{T'_0} = -\frac{1}{4}\big(\omega_J - 2\omega_e\big) \tag{4.14}$$

$$\omega_{T'_{-1}} = +\frac{1}{4}\big(\omega_J - 2\omega_\Sigma\big). \tag{4.15}$$

These eigenvalues are used in section 4.6 to analyse the signal, allowing assignment of coherence-peak correspondence.

4.4.2 Fluctuating Hamiltonian

As explained in section 2.4, the fluctuating Hamiltonian is a sum of contributions from the anisotropic spin interactions. These interactions differ between ensemble members at a given point in time due to random molecular tumbling. The current analysis is restricted to the intra-pair dipole-dipole (DD) and chemical shift anisotropy (CSA) interactions,

$$H_1(t) = H_{\mathrm{DD}}(t) + H_{\mathrm{CSA}}(t), \tag{4.16}$$

as well as the cross-correlation between the two mechanisms.

Intrapair dipole-dipole coupling

The case of the DD interaction between spins i and j was covered in section 3.3, but will briefly be recalled here.

The tensor components $\left[X^{\mathrm{DD}}_{2q}\right]^{\mathrm{L}}$ are equal to the rank-2 spherical tensor spin operators, as given in table 4.2. Assuming a rigid molecular geometry, the interaction constant for the DD coupling is given by $b_{ij} = \mu_0\gamma_i\gamma_j\hbar/(4\pi r_{ij}^3)$, where r_{ij} is the internuclear distance. In the current case, the ^{13}C -^{13}C internuclear distance of $r_{ij} = 122$ pm corresponds to a direct DD coupling of $b_{ij}/2\pi = -4152.84$ Hz. The only non-vanishing spatial component of the Cartesian tensor in the principal axis (P-)frame is $A_{20} = \sqrt{6}$.

The P-frame of the DD coupling tensor is aligned such that the z-axis is along the ^{13}C -^{13}C internuclear vector, as shown in figure 4.3. In general, the relative orientation of the DD P-frame and the molecular diffusion tensor is defined by Euler angles $\Omega^{\mathrm{DD}}_{\mathrm{PD}} = \{\alpha, \beta, \gamma\}$, as shown in figure 4.3. In the current case, the rod-like geometry of the molecule causes near-coincidence of the P-frames of the ^{13}C -^{13}C DD coupling and that of the inertia tensor, and in turn the D-frame, so that the angle β is small, while the angles α and γ may be taken as arbitrary.

Chemical shift anisotropy

An alternative way of forming the spin-part components of the Hamiltonian, is to first decompose the constituent vectors and couple the rank-1 spherical components. In the case of the CSA of spin

j, spin-field tensors X_{kq}^{CSA} of ranks $k = 1, 2$ are formed by coupling the rank-1 spherical tensor spin operators $T_{1q'}^{j}$ with the rank-1 spherical components of the external magnetic field [104]:

$$X_{kq}^{\mathrm{CSA}} = \sum_{q',q''} C_{qq'q''}^{k11} T_{1q'}^{j} B_{1q''} \tag{4.17}$$

where $C_{qq'q''}^{k11}$ are Clebsch-Gordan coefficients. Explicit expressions for the case $k = 2$ are given in the laboratory (L-) frame in table 4.2.

The computed magnetic shielding tensors $\boldsymbol{\sigma}$ are transformed to chemical shift tensors via the relation,

$$\boldsymbol{\delta} = \mathbb{1}\sigma_{\mathrm{iso}}^{\mathrm{TMS}} - \boldsymbol{\sigma}, \tag{4.18}$$

where $\mathbb{1}$ is the three-dimensional identity matrix, and $\sigma_{\mathrm{TMS}}^{\mathrm{iso}}$ is the isotropic component of the magnetic shielding tensor of tetramethylsilane acting as a reference. The chemical shift tensors are transformed to their P-frames by diagonalisation. Then, the *Haeberlen convention*[125] is used to define the anisotropy and biaxiality parameters, respectively, as,

$$\delta^{\mathrm{CSA}} = \delta_{zz}^{\mathrm{P}} - \delta_{\mathrm{iso}} \tag{4.19}$$

and,

$$\eta = \frac{\delta_{xx}^{\mathrm{P}} - \delta_{yy}^{\mathrm{P}}}{\delta^{\mathrm{CSA}}}, \tag{4.20}$$

with principal components arranged by,

$$|\delta_{zz}^{\mathrm{P}} - \delta_{\mathrm{iso}}| \geqslant |\delta_{xx}^{\mathrm{P}} - \delta_{\mathrm{iso}}| \geqslant |\delta_{yy}^{\mathrm{P}} - \delta_{\mathrm{iso}}|. \tag{4.21}$$

Values of these parameters are given in table 4.1, and the computed chemical shift tensors are,

$$\boldsymbol{\delta}_1 = \begin{pmatrix} 145.32 & 0 & 0 \\ 0 & 142.38 & 0 \\ 0 & 0 & -74.75 \end{pmatrix} \text{ ppm}, \tag{4.22}$$

and,

$$\boldsymbol{\delta}_2 = \begin{pmatrix} 145.32 & 0 & 0 \\ 0 & 142.38 & 0 \\ 0 & 0 & -74.66 \end{pmatrix} \text{ ppm.} \tag{4.23}$$

4.5 Relaxation via anisotropic rotational diffusion

4.5.1 Liouvillian

In Liouville space, the Liouville-von Neumann equation for the spin-sytem may be expressed as,

$$\frac{d}{dt} |\rho(t)) = \hat{L} |\rho(t)) , \tag{4.24}$$

where $|\rho(t))$ is the ensemble-averaged density operator of the spin-system, and $\hat{L}$ is the Liouvillian, itself given by,

$$\hat{L}\bullet = -i\hat{H}_0 \bullet + \hat{\Gamma}\bullet, \tag{4.25}$$

where $\hat{H}_0(t)$ is the coherent Hamiltonian commutation superoperator. By eq. (4.16), the relaxation superoperator may be written as a sum over auto- and cross-correlated mechanisms as,

$$\begin{aligned} \hat{\Gamma} &= \sum_{\Lambda,\Lambda'} \hat{\Gamma}_{\Lambda\Lambda'} \\ &= \hat{\Gamma}_{\text{DD}} + \hat{\Gamma}_{\text{CSA}} + \hat{\Gamma}_{\text{DD}\times\text{CSA}}, \end{aligned} \tag{4.26}$$

where $\Lambda = \Lambda'$ for the auto-correlated DD and CSA mechanisms.

If the Hilbert space $\mathcal{H}_d$ of the spin-system has dimension d, then the corresponding Liouville space $\mathcal{L}_D$ has dimension $D = d^2$. It follows that the Liouvillian has a set of D eigenvalues and eigenoperators,

$$\hat{L}|Q_q) = \Lambda_q|Q_q) \quad \forall q \in \{0, 1, \cdots, D-1\} , \tag{4.27}$$

Parameter	Value	Note
J_{ij}	214.15 Hz	Experimental[a]
$\Delta\delta_{\text{iso}}$	0.16 ppm	Experimental[b]
$b_{ij}/2\pi$	-4152.84 Hz	Estimated[c]
Ω_{PD}^{ij}	$\{\alpha, -2.5^\circ, \gamma\}$	Frames obtained by diagonalising calculated tensors
δ_i^{CSA}	-145.7 ppm	Calculated
η_i	0.020	Calculated
Ω_{PD}^{i}	$\{0, -2.6^\circ, 0\}$	Frames obtained by diagonalising calculated tensors
δ_j^{CSA}	-145.4 ppm	Calculated
η_j	0.023	Calculated
Ω_{PD}^{j}	$\{0, -2.6^\circ, 0\}$	Frames obtained by diagonalising calculated tensors
$\tau_\perp$	136.5 ps	Estimated from the parameters in this table and experimental T_1

TABLE 4.1: Spin system parameters for $\mathbf{I}$ in solution. [a]Obtained from 90° pulse-acquire spectrum on a 700 MHz spectrometer. [b]Estimated from the ^{13}C-spectrum of natural abundance material. [c]Estimated from the internuclear distance, $r_{ij} = 122$ pm, as determined from a computational geometry optimisation. The first two entries are coherent parameters, the next block of parameters are associated with the DD interaction. The next block of six entries contains parameters associated with the CSA interaction for each spin. The final entry is the correlation time, which is derived from the total relaxation superoperator.

Interaction, Λ	q	$\left[X^{\Lambda}_{2q}\right]^{\mathrm{L}}$
DD, spins i,j	0	$\frac{1}{2\sqrt{6}}(4I_{iz}I_{jz} - I_i^- I_j^+ - I_i^+ I_j^-)$
	±1	$\mp\frac{1}{2}(I_i^{\pm}I_{jz} + I_{iz}I_j^{\pm})$
	±2	$\frac{1}{2}(I_i^{\pm}I_j^{\pm})$
CSA, spin i	0	$\sqrt{\frac{2}{3}}B_0 I_{iz}$
	±1	$\mp\frac{1}{2}B_0 I_i^{\pm}$
	±2	0

TABLE 4.2: Irreducible spherical spin and spin-field tensor components for $l = 2$ in the L-frame [26].

Interaction, Λ	c_Λ	p	$\left[A^{\Lambda}_{2p}\right]^{\mathrm{P}}$
DD, spins i,j	b_{ij}	0	$\sqrt{6}$
CSA, spin i	$-\gamma_i$	0	$\sqrt{\frac{3}{2}}\delta_i^{\mathrm{CSA}}$
		±2	$\frac{1}{2}\delta_i^{\mathrm{CSA}}\eta_i$

TABLE 4.3: Non-vanishing spatial irreducible spherical tensor components for $l = 2$ in their P_Λ-frames [26].

with,

$$\Lambda_q = -\lambda_q + i\omega_q, \tag{4.28}$$

where λ_q and ω_q are both real. In the case where $\omega_q \neq 0$, the eigenoperators correspond to quantum coherences (QC) which decay with rate constant λ_q and oscillate at frequency ω_q. Eigenoperators with real eigenvalues ($\omega = 0$) represent a particular configuration of spin state populations with decay rate constant λ_q.

4.5.2 Spectral density function

The time-correlation function was derived for the case of completely anisotropic rotational diffusion in chapter 3. Here, by assuming molecular rigidity, **I** is treated as a symmetric rotor; that is, two principal axes of inertia are degenerate, and all principal axes are coincident with those of the diffusion tensor. To start, refer back to the Favro equation,

$$\frac{\partial}{\partial\tau}P(\Omega_\tau) = -H_{\mathrm{rot-diff}}P(\Omega_\tau), \tag{4.29}$$

with solution,

$$P(\Omega_0|\Omega_\tau) = \sum_n \langle\psi_n(\Omega_0)|\psi_n(\Omega_\tau)\rangle\, e^{-E_n\tau}, \tag{4.30}$$

where $|\psi_n(\Omega)\rangle$ and E_n are eigenfunctions and eigenvalues, respectively, of the rotational diffusion Hamiltonian, $H_{\mathrm{rot-diff}}$.

If we treat **I** as a rigid linear molecule, then $H_{\mathrm{rot-diff}}$ in the D-frame has the form,

$$H_{\mathrm{rot-diff}} = D_\perp\left(J_x^2 + J_y^2\right) + D_\parallel J_z^2, \tag{4.31}$$

where $D_\perp$ and $D_\parallel$ are rotational diffusion constants associated with axes perpendicular and parallel, respectively, with the z-axis, and hence the molecular long-axis. Eq. (4.31) is of the same form as the rigid-rotor Hamiltonian for a *symmetric top*. Eq. (4.30) is then given in terms of eigenfunctions and values of a symmetric-top, and we make the substitutions,

$$|\psi_n(\Omega)\rangle \rightarrow |JKM\rangle \equiv \sqrt{\frac{2J+1}{8\pi^2}} D^{(J)*}_{MK}(\Omega) \tag{4.32}$$

$$E_n \rightarrow E^{(J)}_K \equiv D_\perp J\,(J+1) + K^2\left(D_\parallel - D_\perp\right). \tag{4.33}$$

Following the derivation in section 3.2.2, the time-correlation function becomes,

$$G^k_{qm}(\tau) = \delta_{kk'}\delta_{qq'}\delta_{mm'}G^{kk'}_{qq'mm'}(\tau) \tag{4.34}$$

and the spectral density function becomes,

$$J^{\Lambda\Lambda'}_{kq}(q\omega_0) = \sum_m \left[A^\Lambda_{km}\right]^{\mathrm{D}}\left[A^{\Lambda'*}_{km}\right]^{\mathrm{D}} \mathrm{Re}\int_0^\infty d\tau G^k_{qm}(\tau)e^{iq\omega_0\tau}, \tag{4.35}$$

and we see that not only is the relaxation superoperator secularised, but spatial components in the D-frame of different order m do not *mix* in the limit of anisotropic tumbling of a symmetric rotor. Strictly, it is derived that, $k = J = k'$, $-q = M = -q'$, and $m = K = m'$.

Further, in this case, $J = k = 2$, and $K = m = 0$ in eq. (4.32). To see this, recall that the spatial components in the D-frame may be written,

$$\left[A^\Lambda_{km}\right]^{\mathrm{D}} = \sum_{p=-k}^{+k} D^{(k)*}_{mp}(\Omega^{\mathrm{PD}})\left[A^\Lambda_{kp}\right]^{\mathrm{P}}, \tag{4.36}$$

and for a passive rotation,

$$D^{(k)}_{mp}(\Omega) = e^{i\gamma m}e^{i\alpha p}d^{(k)}_{mp}(-\beta). \tag{4.37}$$

Firstly, consider the DD interaction, for which Euler angles α and γ are arbitrary and may be chosen to be zero, and since the z-axes between the P-and D-frames are approximated as parallel, $\beta = 0$. Thus, the components in the D-frame transform as,

$$\left[A^{\mathrm{DD}}_{2m}\right]^{\mathrm{D}} = \left[A^{\mathrm{DD}}_{20}\right]^{\mathrm{P}} d^{(2)*}_{m0}(\beta = 0), \tag{4.38}$$

where the knowledge that $\left[A_{20}^{\mathrm{DD}}\right]$ is the only non-vanishing component in the P-frame is used. Further, $d_{00}^{(k)}(\pm\beta) = \frac{3\cos^2\beta-1}{2}$ is the only non-vanishing reduced Wigner function, and equates to unity for $\beta = 0$. Then, the only surviving component in the D-frame is $\left[A_{20}^{\mathrm{DD}}\right]$, and $m = K = 0$. This is general for linear molecules.

The treatment of the CSA mechanism requires one further approximation; that of axial symmetry. For an axially symmetric rotor, the biaxiality parameter vanishes; $\eta_i = 0$. Then, an analogous relation to eq. (4.38) results.

The transformation described by eq. (4.36) may be repeated for a chain of any number of reference frames. Figure 4.3 depicts the transformations relevant here; from the P_Λ-frames to the L-frame via the D-frame. Since the P_Λ- and D-frames are molecule-fixed, while the L-frame is space-fixed, spatial components acquire a stochastic time-dependence through the motional modulation of the Euler angles $\Omega_{\mathrm{DL}}(t)$, representing the rotational diffusion of the molecules in solution.

4.6 The NMR spectrum

4.6.1 Signal

As explained in chapter 2, the signal may be written in terms of the eigenvalues of eq. (4.28) as,

$$s(t) = \sum_q a_q e^{\Lambda_q t}, \tag{4.39}$$

with a_q the peak amplitude given by,

$$a_q = (Q_{\mathrm{obs}}|Q_q)\,(Q_q|\,\hat{U}_{\mathrm{exc}}(t,t_0)\,|\rho_{\mathrm{eq}})\,, \tag{4.40}$$

where $\hat{U}_{\mathrm{exc}}(t,t_0)$ is the total propagator for the excitation sequence and $|\rho_{\mathrm{eq}})$ is the thermal equilibrium density operator. In quadrature detection, $|Q_{\mathrm{obs}}) \approx -\frac{1}{2}ie^{i\phi_{\mathrm{rec}}}\,|I_-)$ with ϕ_{rec} being the receiver phase [9]. Since the experiment here is a 90° pulse-acquire, we make the approximation,

$$\hat{U}_{\mathrm{exc}}\big|\rho_{\mathrm{eq}}\big) = \hat{R}_x(\pi/2)I_z = -I_y, \tag{4.41}$$

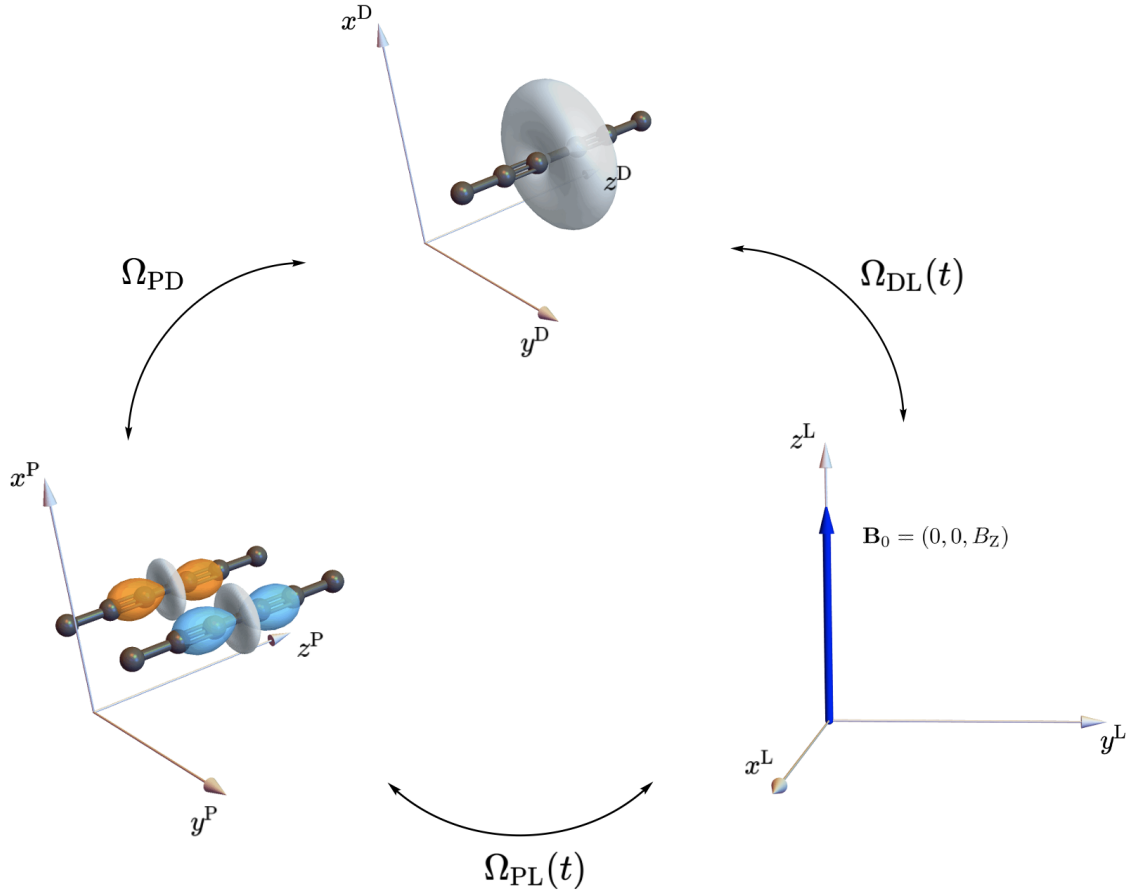

FIGURE 4.3: An illustration of the relevant frame transformations used here. On the left, the coordinate system is the molecule-fixed P-frame of the DD interaction, with the z-axis parallel to the internuclear vector. This is assumed to be coincident with the P-frame of the CSA interaction, and hence both tensors are depicted to illustrate this. The set of angles Ω_{PD} orientate the P- and D-frames. The molecule-fixed D-frame is given by the P-frame of the inertia tensor with its z-axis parallel to the molecular long axis. We may also approximate this as coincident with the P-frames of the DD and CSA interactions. The L-frame is defined such that its z-axis is parallel to the applied magnetic field. The angles $\Omega_{\mathrm{DL}}(t)$ orient the D- and L-frames with respect to each other. These angles are time-dependent, since the L-frame is space-fixed and stochastic molecular tumbling continuously alters the orientation of the D- and L-frames with respect to one another. The angles parameterising the transformation between the P- and L-frames will be time-dependent for the same reason.

ignoring constant numerical factors and relaxation.

Non-vanishing peak amplitudes are associated with (-1)-quantum eigenoperators $|Q_q)$, as defined by the eigenoperator equation,

$$\hat{I}_z \, |Q_q) = - \, |Q_q) \, , \tag{4.42}$$

where, as usual, $\hat{I}_z$ is the commutation superoperator of the spin operator I_z, and eigenvalue -1 defines the *coherence order* for operator $|Q_q)$. In the absence of relaxation, these observable operators are the (-1)-quantum eigenoperators of $\hat{H}_0$ and are given by elements of the basis,

$$\mathbb{B}_Q = \Big\{ \big||S_0'\rangle\langle T_{+1}'|\big), \big||T_{-1}'\rangle\langle S_0'|\big), \big||T_0'\rangle\langle T_{+1}'|\big), \big||T_{-1}'\rangle\langle T_0'|\big) \Big\}, \tag{4.43}$$

which is a subset of the 16-element basis of all outer products of elements in $\mathbb{B}'_{\mathrm{ST}}$.

In the absence of relaxation, the Liouvillian eigenvalues are purely imaginary, and are given by $\Lambda_q = +i\omega_q$, where ω_q are the peak frequencies. These are given in general by,

$$\omega_q = -(\omega_r - \omega_s), \tag{4.44}$$

with $r, s \in \{S_0', T_{+1}', T_0', T_{-1}'\}$, as given in table 4.4.

The two eigenoperators corresponding to (-1)-quantum coherences between the perturbed triplet states are particularly important in the current context, since these coherences give rise to the two components of the spectral doublet, as can be seen from their amplitudes in table 4.4. These two eigenoperators are denoted as follows:

$$\begin{aligned} Q_+ &= \big||T_0'\rangle\langle T_{+1}'|\big) \\ Q_- &= \big||T_{-1}'\rangle\langle T_0'|\big) \end{aligned} \tag{4.45}$$

The corresponding Liouvillian eigenvalues are,

$$\Lambda_\pm = -\lambda_\pm + i\omega_\pm. \tag{4.46}$$

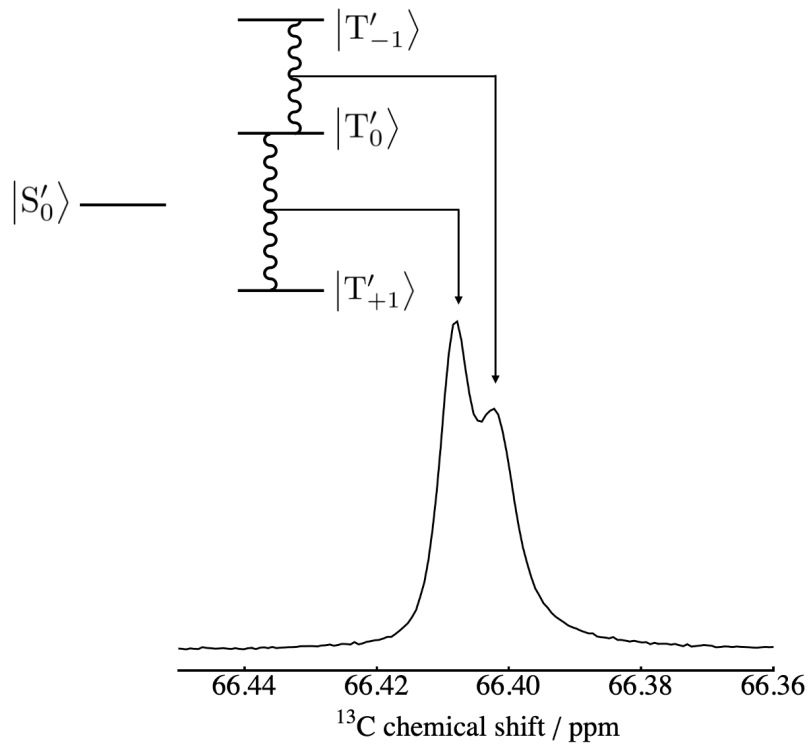

FIGURE 4.4: The correspondence between the single-quantum triplet-triplet coherences (wiggly lines) and the NMR spectrum. The coherence represented by the operator Q_+ is associated with the narrow peak while the coherence represented by Q_- is associated with the broad peak.

In general, the superoperators $\hat{H}_{\rm coh}$ and $\hat{\Gamma}$ do not commute. The presence of the relaxation superoperator $\hat{\Gamma}$ may therefore modify both the eigenvalues and the eigenoperators of the Liouvillian, $\hat{L}$. Indeed the modification of the peak frequencies by relaxation effects has been documented in the literature in a different context [126]. In the current case, the eigenvalues of the (-1)-quantum eigenoperators are only slightly modified by the relaxation superoperator, as shown by the agreement between theory and experiment. Hence, in the following discussion, we assume that the (-1)-quantum eigenoperators of the full Liouvillian, including relaxation, are given to a good approximation by the operators in eq. (4.43). The correspondence between the two triplet-triplet coherences and the NMR spectrum is depicted in figure 4.4.

.

$\big\vert Q_q\big)$	ω_q	a_q
$\big\vert\vert S_0'\rangle\langle T_{+1}'\vert\big)$	$\frac{1}{2}\big(\omega_\Sigma+\omega_J+\omega_e\big)$	$\frac{1}{2}\sin^2\frac{\theta}{2}$
$\big\vert\vert T_{-1}'\rangle\langle S_0'\vert\big)$	$\frac{1}{2}\big(\omega_\Sigma-\omega_J-\omega_e\big)$	$\frac{1}{2}\sin^2\frac{\theta}{2}$
$\big\vert\vert T_0'\rangle\langle T_{+1}'\vert\big)$	$\frac{1}{2}\big(\omega_\Sigma+\omega_J-\omega_e\big)$	$\frac{1}{2}\cos^2\frac{\theta}{2}$
$\big\vert\vert T_{-1}'\rangle\langle T_0'\vert\big)$	$\frac{1}{2}\big(\omega_\Sigma-\omega_J+\omega_e\big)$	$\frac{1}{2}\cos^2\frac{\theta}{2}$

TABLE 4.4: Coherence eigenoperators of $\hat{H}_{\text{coh}}$ along with the associated eigenfrequencies and peak amplitudes.

4.6.2 Frequencies

The coherence frequencies are given by the imaginary parts of the Liouvillian eigenvalues. As shown in eq. (4.49) below, the off-diagonal parts of the (-1)-quantum Liouvillian block may be ignored to a first approximation. With this, the coherence frequencies are as specified in Table 4.4. The frequencies of the two triplet-triplet coherences are given by,

$$\omega_\pm = \frac{1}{2}\big(\omega_\Sigma \pm \omega_J \mp \omega_e\big), \tag{4.47}$$

which are the coherences responsible for the two main peaks in the spectrum, as shown in fig. (4.4). Eq. (4.47) implies that the left peak corresponds to coherence Q_+, and the right peak to coherence Q_-. This is consistant with the treatment of linewidths below.

4.6.3 Linewidths

The correlation time was estimated using the experimental $T_1 = 2.23$ s value and the relation,

$$T_1^{-1} \simeq -\frac{\big(I_z\big\vert\hat{\Gamma}\big\vert I_z\big)}{\big(I_z\big\vert I_z\big)}, \tag{4.48}$$

and solving for $\tau_\perp$. Then, the (-1)-QC subspace of the Liouvillian is given by,

$$\hat{L}_{\mathbb{B}_Q} = \begin{array}{c} \\ \big||S_0'\rangle\langle T_{+1}'|\big) \\ \big||T_{-1}'\rangle\langle S_0'|\big) \\ \big||T_0'\rangle\langle T_{+1}'|\big) \\ \big||T_{-1}'\rangle\langle T_0'|\big) \end{array} \begin{array}{c} \begin{array}{cccc} \big||S_0'\rangle\langle T_{+1}'|\big) & \big||T_{-1}'\rangle\langle S_0'|\big) & \big||T_0'\rangle\langle T_{+1}'|\big) & \big||T_{-1}'\rangle\langle T_0'|\big) \end{array} \\ \begin{pmatrix} -0.294 + 1339.86i & 0.454 \times 10^{-3} & -0.0106 & 0.0123 \\ 0.454 \times 10^{-3} & -0.629 - 1339.86i & 0.0120 & -0.0210 \\ -0.0106 & 0.0120 & -0.578 + i5.68 & 0.324 \\ 0.0123 & -0.0210 & 0.325 & -1.182 - i5.68 \end{pmatrix} \end{array} \mathrm{s}^{-1}. \tag{4.49}$$

We see that the off-diagonal elements $(Q_\pm|\hat{\Gamma}|Q_\mp)$ are of the same order of magnitude as the real parts of the corresponding diagonal elements, and may contribute to relaxation [100]. Nevertheless, the operators $Q_\pm$ have a clear physical interpretation and use of this basis offers qualitative insight, as well as good agreement with experiment. Thus, the real parts of the Liouvillian eigenvalues are approximated by the Liouville bracket,

$$\mathrm{Re}(\Lambda_q) \simeq \frac{(Q_q|\,\hat{\Gamma}\,|Q_q)}{(Q_q|Q_q)}. \tag{4.50}$$

The real positive quantities $\lambda_q = -\mathrm{Re}(\Lambda_q)$ may be interpreted as the coherence decay rate constants for the eigenoperators $\big|Q_q\big)$. After Fourier transformation of the NMR spectrum, the peak associated with the eigenoperator $\big|Q_q\big)$ has amplitude a_q, centre frequency ω_q, and has a Lorentzian shape with half-width-at-half-height equal to λ_q, in units of rad s^{-1}. Its full-width-at-half-height is given by λ_q/π in units of Hz.

The relaxation superoperator $\hat{\Gamma}$ may be written as a sum of auto-correlation terms for the DD and CSA interactions, and a DD×CSA cross-correlation term (eq. (4.26)). The coherence decay rate constants λ_q may therefore be written as a superposition of terms as,

$$\lambda_q = \lambda_q^{\mathrm{DD}} + \lambda_q^{\mathrm{CSA}} + \lambda_q^{\mathrm{DD\times CSA}}. \tag{4.51}$$

For the two triplet-triplet coherences, each term in eq (4.51) is given by,

$$\lambda_\pm^{\mathrm{DD}} = \frac{3}{20} b_{ij}^2 \tau_\perp \left(3 + \frac{3}{1+\omega_0^2\tau_\perp^2} + \frac{2}{1+4\omega_0^2\tau_\perp^2}\right), \tag{4.52}$$

$$\lambda_\pm^{\mathrm{CSA}} = \frac{1}{20}\omega_0^2\tau_\perp \left\{ \left(\left[\delta_i^{\mathrm{CSA}}\right]^2 + \left[\delta_j^{\mathrm{CSA}}\right]^2\right) \frac{5+2\omega_0^2\tau_\perp^2}{1+\omega_0^2\tau_\perp^2} + \delta_i^{\mathrm{CSA}}\delta_j^{\mathrm{CSA}} \frac{3}{1+\omega_0^2\tau_\perp^2} \right\}, \tag{4.53}$$

and,

$$\lambda_{\pm}^{\mathrm{DD}\times\mathrm{CSA}} = \pm\frac{3}{20}\omega_0 b_{ij}\tau_{\perp}\left(\delta_i^{\mathrm{CSA}} + \delta_j^{\mathrm{CSA}}\right)\frac{3+2\omega_0^2\tau_{\perp}^2}{1+\omega_0^2\tau_{\perp}^2}, \tag{4.54}$$

Equations (4.52)-(4.54) depend on the correlation time $\tau_{\perp}$ for molecular rotation around an axis perpendicular to the long axis of the molecule. Rotational diffusion around the molecular long axis does not modulate the spin interactions, under the approximation of a rigid symmetric top undergoing rotational diffusion, and does not lead to spin relaxation. In the current case, the chemical shift anisotropies of the two spins are very similar, allowing the simplification $\delta^{\mathrm{CSA}} \simeq \delta_i^{\mathrm{CSA}} \simeq \delta_j^{\mathrm{CSA}}$.

The limiting regimes of the correlation time $\tau_{\perp}$ are as follows:

1. In the *extreme narrowing limit*, eq. (4.51) may be written,

$$\lambda_{\pm} \simeq \frac{3}{10}\left(4b_{jk} \pm 3\omega_0\delta^{\mathrm{CSA}}\right)b_{jk}\tau_{\perp} + \lambda^{\mathrm{CSA}}, \tag{4.55}$$

   where the CSA-induced decay rate constant λ^{CSA} is given by,

$$\lambda^{\mathrm{CSA}} \simeq \frac{13}{20}\omega_0^2\left[\delta^{\mathrm{CSA}}\right]^2\tau_{\perp}. \tag{4.56}$$

   The field-dependence of the two rate constants $\lambda_{\pm}$ is illustrated in figure 4.5a. The decay rate constant λ_+ is minimized at a magnetic field such that $|4b_{jk}| = \left|3\omega_0\delta^{\mathrm{CSA}}\right|$, in which case the first term in eq. (4.55) cancels out. At this field, the dipole-dipole contribution to the decay rate constant vanishes, and λ_+ becomes equal to the limiting CSA relaxation rate constant λ^{CSA} (eq. (4.56)). The decay rate constant λ_+, on the other hand, increases monotonically with increasing magnetic field.

2. In the *long correlation time limit*, $|\omega_0\tau_{\perp}| \gg 1$, eq. (4.51) may be written as,

$$\lambda_{\pm} \simeq \frac{1}{20}\left(3b_{jk} \pm 2\omega_0\delta^{\mathrm{CSA}}\right)^2\tau_{\perp}. \tag{4.57}$$

   The field-dependence of the two rate constants $\lambda_{\pm}$ is illustrated in figure 4.5b. In this regime, the linewidth parameter λ_+ goes to zero at a magnetic field such that $|3b_{ij}| = \left|2\omega_0\delta^{\mathrm{CSA}}\right|$. The strong narrowing of one of the two doublet components resembles the TROSY effects exploited in biomolecular NMR [108, 109].

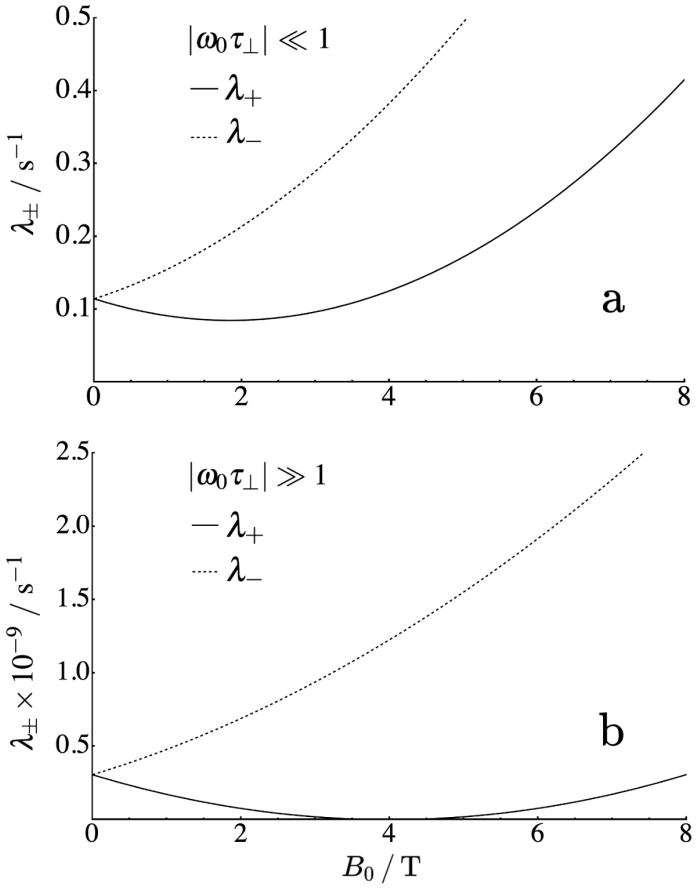

FIGURE 4.5: Plots of the linewidth parameters $\lambda_\pm$ against external static field, for the parameters in table 4.1. (a) The extreme-narrowing limit, based on eq. (4.55), showing the minimum $\lambda_+ = 8.47 \times 10^{-2}$ s^{-1} at $B_0 = 1.84$ T. (b) The long-$\tau_\perp$ limit, with a minimum $\lambda_+ = 0$ at $B_0 = 4.0$ T. The DD and CSA mechanisms cancel in the long-$\tau_\perp$ limit at this magnetic field. The cancellation is incomplete in the extreme-narrowing limit.

Using eq. (4.40), the peak amplitudes associated with the (-1)-quantum singlet-triplet coherences are $\propto \sin^2(\theta/2)$, while those associated with the (-1)-quantum triplet-triplet coherences are $\propto \cos^2(\theta/2)$. In the current case, the singlet-triplet mixing angle is small ($\theta = -0.0750 = -4.30^\circ$), and the amplitudes are,

$$\begin{aligned} a_{S'_0 \rightarrow T'_{+1}} &= a_{T'_{-1} \rightarrow S'_0} \simeq 0.686 \times 10^{-3} \\ a_{T'_0 \rightarrow T'_{+1}} &= a_{T'_{-1} \rightarrow T'_0} \simeq 0.499, \end{aligned} \tag{4.58}$$

with the sum over all amplitudes equal to 1. The spectrum is therefore dominated by the strong peaks from the two triplet-triplet coherences.

From eq. (4.47), $\omega_+ < \omega_-$. This indicates that the left peak of the doublet is associated with the Q_+ coherence, while the right-hand peak is associated with the Q_- coherence, after taking into account the sign of the Larmor frequency [127]. This assignment is shown in figure 4.4. The splitting between the peaks is given by $\Delta\omega/(2\pi) = 0.60\,\text{Hz}$.

From eqs. (4.52)-(4.54), since b_{jk}, ω_0, δ_j^{CSA} and δ_k^{CSA} are all negative, we see that the cross-correlation contributions reduce the value of λ_+ while increasing the value of λ_-. For the experimental parameters, the coherence decay rate constants are given by $\lambda_+ \simeq 0.583\ \text{s}^{-1}$ and $\lambda_- \simeq 1.190\ \text{s}^{-1}$. These correspond to full peakwidths at half-height of 0.186 Hz and 0.379 Hz, for the left-hand and right-hand doublet components, respectively.

The green curve in figure 4.2 is a plot of the analytical spectral function,

$$S(\omega) = a_+ \frac{\lambda_+}{\lambda_+^2 + (\omega - \omega_+)^2} + a_- \frac{\lambda_-}{\lambda_-^2 + (\omega - \omega_-)^2}, \tag{4.59}$$

using the parameters in table 4.5. There is good agreement with the experimental ^{13}C NMR spectrum (black).

The blue curve in figure 4.2 shows the result of a numerical calculation using *SpinDynamica* [49], in which the full Liouvillian is diagonalized. There is good qualitative agreement between the numerical simulations, the analytical theory and the experimental result. The minor differences between the *SpinDynamica* simulation and the analytical theory may be attributed to the neglect of the off-diagonal Liouvillian elements in the analytical theory, since the $\mathbb{B}_Q$ is not strictly an eigenbasis of the Liouvillian.

Parameter	Value	Note
λ_+	0.583 s^{-1}	eq. (4.55)
λ_-	1.19 s^{-1}	eq. (4.55)
$a_\pm$	0.499	eq. (4.40)
$\omega_\pm$	$\mp$1.90 rad s^{-1}	eq. (4.47)

TABLE 4.5: Parameters used to plot the analytical spectral function in fig. 4.2b. Each of these parameters are fed into eq. (4.59). The first two entries are the peak linewidths, calculated using eq. (4.55), which uses parameters b_{jk} and δ^{CSA} ultimately derived from computation (see Table 4.1).

4.7 Related systems

The effects of cross-correlated relaxation on lineshape in homonuclear spin pairs crops up more often than one might anticipate, since these are the most commonly studied type of system in the field of long-lived states (LLS)[88, 90, 95, 116, 117].

4.7.1 $^{13}C_2$-DAND

The effects of cross-correlation on lineshape in a homonuclear system crops up often in the field of long-lived states. This is because many systems studied involve nuclei only one bond apart. An interesting example is in the case of $^{13}C_2-$DAND, shown in fig. 4.6a. This is another *near-equivalent* system with $\Delta\delta_{\mathrm{iso}} = 0.075$ ppm and $J_{ij} = 54.39$ Hz, giving a mixing-angle of $\theta = 7.85°$.

Relaxation via *isotropic* rotational diffusion

$^{13}C_2$-DAND is locally planar about the relevant spins, and will tumble anisotropically about the three principal axes of the D-frame. However, for an asymmetric top such as this, the D-frame is not necessarily coincident with the principal axes of inertia. With some hindsight, though, it becomes convenient to treat $^{13}C_2$-DAND as a spherical molecule undergoing isotropic rotational diffusion. The reason for this is two-fold:

1. By inspection, the DD and CSA tensors in fig. 4.6b and 4.6c, respectively, are expected to

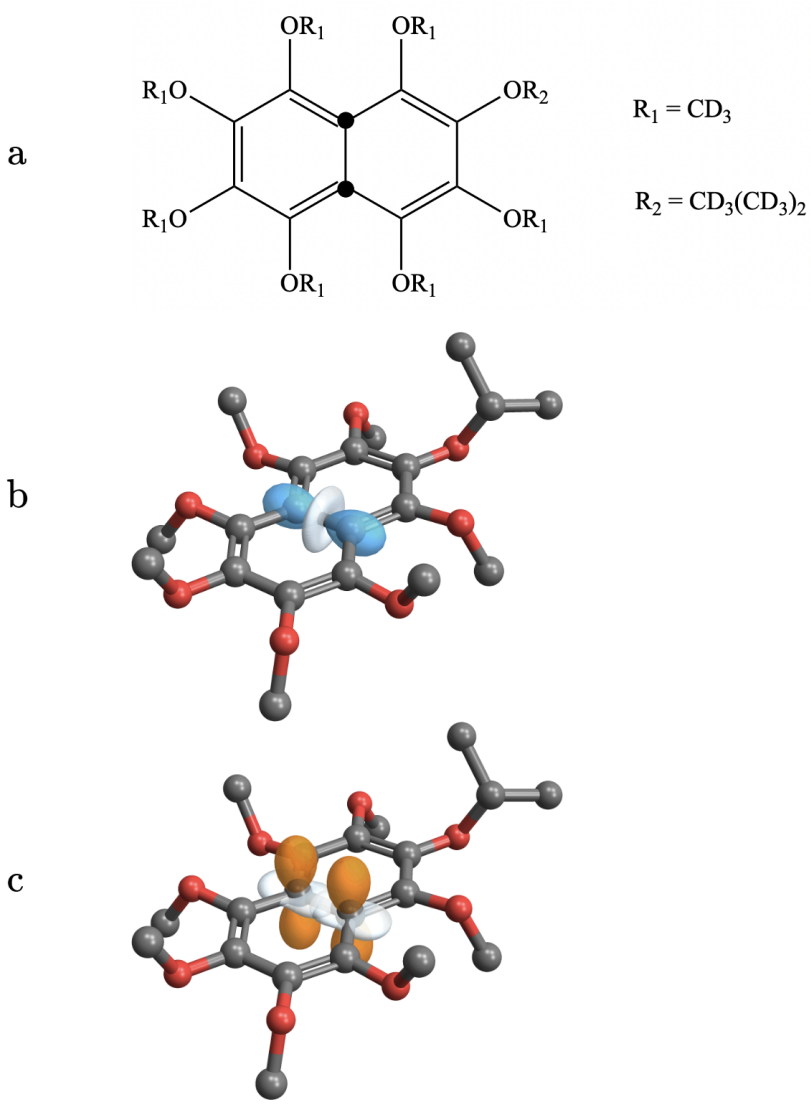

FIGURE 4.6: (a) Molecular structure of $^{13}C_2$-DAND (1,2,3,4,5,6,8-heptakis(methoxy-d_3)-7-((propan-2-yl-d_7)oxy)naphthalene-4a,8a-[$^{13}C_2$]), with ^{13}C labelled sites depicted by black circles; (b) The rank-2 part of the ^{13}C -^{13}C DD coupling tensor; (c) The calculated ^{13}C CSA tensors of the ^{13}C labels represented by ovaloids. The grey atoms are C, and the red atoms O. The H atoms are not shown for clarity.

have perpendicular z-principal axes.

2. Since no axis system in a spherical geometry is unique, we may arbitrarily choose an interaction-independent axis system to be where is most convenient, henceforth referred to as the *molecular* (M-) *frame*.

Taken together, by choosing the M-frame to be that with z-principal axis parallel with the internuclear vector, it is coincident with the P-frame of the DD interaction. Then, since the z-principal axes of the DD and CSA mechanisms are expected to be perdendicular, that of the M-frame is also perpendicular to the z-axis of the CSA P-frame. The trigonometric Wigner transformations between the M-frame and P-frames will be greatly simplified, since $\Omega_{\mathrm{PM}} = \{0, 0, 0\}$ for transformation of components $\left[A_{kq}^{\mathrm{DD}}(t)\right]^{\mathrm{P}}$, and $\Omega_{\mathrm{PM}} = \{\alpha, \pi/2, \gamma\}$ for $\left[A_{kq}^{\mathrm{CSA}}(t)\right]^{\mathrm{P}}$, which allows one to derive a simple spectral density function for what would otherwise be a complicated case. This in turn offers qualitative insight into the cross-correlation effects on NMR spectra, with respect to relative orientation of the principal axes of interaction.

For this case, we have,

$$\begin{aligned} H_{\mathrm{rot-diff}} &= D\left(J_x^2 + J_y^2 + J_z^2\right) \\ &= D\mathbf{J}^2, \end{aligned} \tag{4.60}$$

which is of the same form as the Hamiltonian of a *spherical top*. The eigenvalues are then,

$$E_J = DJ\left(J+1\right), \tag{4.61}$$

which is evident both from the theory of angular momentum and the limiting case of $D_{\parallel} = D_{\perp}$ in eq. (4.32).

We find ourselves in an analogous position to when a symmetric top was considered, since $|JKM\rangle$ are eigenfunctions of $\mathbf{J}^2$ and J_z,[1] and spherical and symmetric tops share eigenfunctions. Here, though, K may not necessarily vanish, and a correlation time τ_c is considered, which corresponds with the rotation of the molecule as a whole, rather than about perpendicular axes only.

The spectral density function becomes,

[1] As required by eq. (4.60) and general angular momentum theory

$$J^{\Lambda\Lambda'}_{kq}(q\omega_0) = \sum_m \Big[A^{\Lambda}_{km}\Big]^{\mathrm{M}}\Big[A^{\Lambda'}_{km}\Big]^{\mathrm{M}} \mathrm{Re}\int_0^\infty d\tau G^k_q(\tau)e^{iq\omega_0\tau}, \tag{4.62}$$

where $G^k_q(\tau)$ is given by,

$$G^k_q(\tau) = \frac{1}{2J+1}\delta_{qq'}\delta_{kk'}e^{\tau/\tau_c}, \tag{4.63}$$

with $\tau_c = (6D)^{-1}$. By definition,

$$\Big[A^{\mathrm{DD}}_{km}\Big]^{\mathrm{M}} \equiv \Big[A^{\mathrm{DD}}_{kp}\Big]^{\mathrm{P}}, \tag{4.64}$$

and the only non-vanishing component is $k = 2$ and $m = q = 0$. From table 4.3, $\Big[A^{\mathrm{DD}}_{20}\Big]^{\mathrm{M}} = \sqrt{6}$.

For components $\Big[A^{\mathrm{CSA}}_{2\pm2}\Big]^{\mathrm{P}}$, we cannot make the approximation $\eta_i = 0$ for each spin, since $^{13}\mathrm{C}_2$-DAND does not have axial symmetry. In fact, from computation, $\eta_i = 0.30$ and $\eta_j = 0.31$. Also from computation and utilising routines in *SpinDynamica*, $\Omega^i_{\mathrm{PM}} = \{\alpha, 89.80^\circ, \gamma\}$ and $\Omega^j_{\mathrm{PM}} = \{\alpha, 89.84^\circ, \gamma\}$; i.e. the z-principal axes associated with the individual spins for the CSA interaction are essentially perpendicular to the z-principal axis of the M-frame, and will be approximated as being so. The spatial components in the M-frame for the CSA interaction may be decomposed by,

$$\begin{aligned}
\Big[A^{\mathrm{CSA}}_{20}\Big]^{\mathrm{M}} &= \sum_{p=-2}^{+2} D^{(k)*}_{0p}(\Omega_{\mathrm{PM}})\Big[A^{\mathrm{CSA}}_{2p}\Big]^{\mathrm{P}} \\
&= -\sqrt{\frac{3}{8}}\Big[A^{\mathrm{CSA}}_{2+2}\Big]^{\mathrm{P}} - \frac{1}{2}\Big[A^{\mathrm{CSA}}_{20}\Big]^{\mathrm{P}} - \sqrt{\frac{3}{8}}\Big[A^{\mathrm{CSA}}_{2-2}\Big]^{\mathrm{P}} \\
&= -\sqrt{\frac{3}{8}}\delta^{\mathrm{CSA}}_i\left(\eta_i + 1\right),
\end{aligned} \tag{4.65}$$

where $\alpha = \gamma = 0$ is chosen arbitrarily, $\beta = \pi/2$, and $d^{(k)}_{0p}(-\beta)$ is used for a passive rotation. By the same process one may also derive,

$$\Big[A^{\mathrm{CSA}}_{2\pm2}\Big]^{\mathrm{M}} = \frac{1}{4}\delta^{\mathrm{CSA}}_i\eta_i. \tag{4.66}$$

Consider the limit, $\left|\Big[A^{\mathrm{CSA}}_{20}\Big]^{\mathrm{P}}\right| \gg \left|\Big[A^{\mathrm{CSA}}_{2\pm2}\Big]^{\mathrm{P}}\right|$, to the extent that $\left|\Big[A^{\mathrm{CSA}}_{2\pm2}\Big]^{\mathrm{P}}\right|$ are qualitatively negligible. This is the limit we found ourselves in previously when considering the symmetry of $\mathbf{I}$.

From eq. (4.65), $\lambda_{\pm}^{\mathrm{DD}\times\mathrm{CSA}}$ given by eq. (4.54) will change sign, while being reduced by one-half. We find then that,

1. The asymmetric broadening/narrowing is *reversed*.
2. The effect is *less exaggerated*.

The case of perfect axial symmetry is recovered immediately by setting $\eta_i = 0$ in the last line of eq. (4.65) and in eq. (4.66), and the above two points are applicable.

When the three components are of similar magnitude, $\left|\left[A_{20}^{\mathrm{CSA}}\right]^{\mathrm{P}}\right| \sim \left|\left[A_{2\pm2}^{\mathrm{CSA}}\right]^{\mathrm{P}}\right|$, eq. (4.65) and (4.66) show that,

1. The asymmetric broadening/narrowing is reversed.
2. The extent of broadening/narrowing is determined by extent of biaxiality, η_i.

Simulations and experiment agree with these findings, as shown in fig. 4.7, with the line shape reproduced in the literature [116]. In the above analysis, it is assumed that the sign of δ^{CSA} is unchanged.

The algorithm

The algorithm used to predict spectra using the relaxation framework outlined thus far was implemented in *Mathematica* [128], using the *SpinDynamica* package, and is as follows:

1. Input atomic coordinates from a computational geometry optimisation.
   - From coordinates, deduce b_{ij}, and in turn the DD-tensor using expression 2.82 given in section 2.4
   - From coordinates, define the M-frame as that with its z-axis parallel to the internuclear vector connecting the labelled nuclei
   - Diagonalise the DD tensor and find Euler angles between the P_{DD}- and M-frames, which should be $\alpha = \beta = \gamma = 0$.
2. Input magnetic shielding $\boldsymbol{\sigma}_i$ tensors for labelled nuclei from computation.

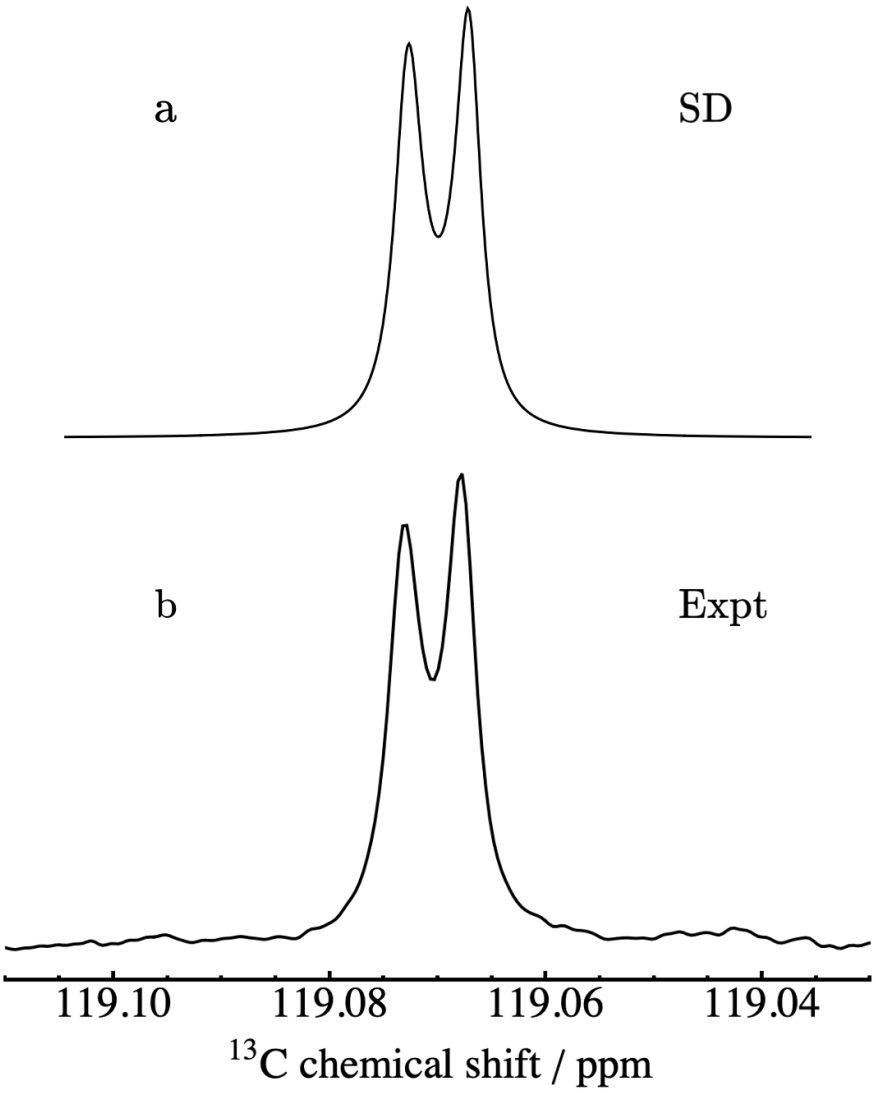

FIGURE 4.7: a: $^{13}C_2$-DAND spectrum simpulated in *SpinDynamica*. b: Experimental spectrum at 9.4 T. We see the asymmetric broadening/narrowing is reversed, and less exaggerated than in the case of **I**.

- Transform $\boldsymbol{\sigma}_i$ to chemical shift tensors, $\boldsymbol{\delta}_i$, using computational tetramethylsilane tensors as a reference (all tensors obtained at the same computational level of theory).
- Diagonalise the chemical shift tensors of the labelled carbons.
- Order diagonal elements based on the Haeberlen convention (see eq. (4.21)).
- Deduce Euler angles parameterising the orientation of the P_{CSA}-frame in the M-frame, which has $\beta \simeq 90^\circ$ for $^{13}C_2$-DAND.

3. Define the relaxation superoperator as a function which takes two interactions, ω_0, and τ_c as arguments, $\hat{\Gamma}(\Lambda, \Lambda', \omega_0, \tau_c)$.
   - $\Lambda = \Lambda'$ for auto-correlated, and $\Lambda \neq \Lambda'$ for cross-correlated mechanisms
   - Define $\hat{\Gamma}(\Lambda, \Lambda', \omega_0, \tau_c)$ for auto-correlated and cross-correlated mechanisms individually; the complete operator is the sum of these.
   - τ_c is approximated using $1/T_1 \simeq (I_z|\,\hat{\Gamma}(\Lambda, \Lambda', \omega_0, \tau_c)\,|I_z)\,/\,(I_z|I_z)$, and solving for τ_c.
4. Define $\hat{H}_{\text{coh}}$.
   - Coherent parameters $\Delta\delta_{\text{iso}}$ and J_{jk} are obtained from experiment
5. Define the Liouvillian as $\hat{L} = -i\hat{H}_0 + \hat{\Gamma}(\Lambda, \Lambda', \omega_0, \tau_c)$
6. Simulate the spectrum as a Fourier Transformed signal using routines implemented in *Spin-Dynamica*
   - Routines are FT[ ], Signal1D[ ], and BackgroundGenerator[ ]

The above algorithm may be extended to **I** by making the substitutions, M- → D-frame, and $\tau_c \rightarrow \tau_\perp$, and the process is simplified immensely by approximating the coincidence of P_{DD}-, P_{CSA}-, and D-frames. *Mathematica* notebooks are available for both cases.

4.8 Conclusion

The results and theory reported here show that cross-correlated relaxation can have a strong effect on the NMR spectra of homonuclear spin-1/2 pairs in the near-equivalence regime. This has strong relevance to NMR experiments on long-lived states, which are often performed on spin systems of this kind [88, 90, 95, 116, 117]. We also saw that the degree of cross-correlation effects is dependent

on the relative orientation of the DD and CSA tensors. In two cases, the lineshape is reproduced using the theoretical framework described in chapter 3, with good agreement with experiment. After understanding the origin of the peculiar lineshape, we are able to study **I** in the manner originally intended; how *long-lived* is its *long-lived state?*...

Chapter 5

The *Triyne* System; Spin Relaxation Studies

We end this thesis with a chapter largely experimental; the theory creeping in seeks to aid experimental understanding, and numerical simulations solidify confidence in the theoretical model. As such, for those experimentally inclined readers, we cannot leave analytical acrobatics at the door. As mentioned in the prelude to chapter 4, the triyne molecule has the potential to host a long-lived singlet-order, with a lifetime greatly exceeding that of inverted longitudinal-order. We do, infact, uncover a remarkable result, justifying the intense interest in this simple system thus far.

5.1 Introduction

In this chapter, we continue investigations of the spin relaxation of **I** in isotropic solution and the consequent effects on NMR spectra. In the current paper, we consider the relaxation of the spin state populations, as investigated by inversion-recovery NMR experiments. As shown below, inversion-recovery NMR experiments display a strong asymmetry between the recovery trajectories of the different spectral peaks after an initial population-inversion pulse. These effects are dependent on the flip-angle of the pulse used to induce the NMR signal following some delay post-inversion. The asymmetry in the recovery to thermal equilibrium is associated with the cross-correlation of the chemical shift anisotropy (CSA) and dipole-dipole (DD) interactions.

Singlet NMR experiments are also presented, demonstrating the long lifetime of $^{13}C_2$ singlet-order for **I** in solution. In particular, the singlet-order decay time constant T_S is found to exceed the magnetization relaxation time constant T_1 by a factor a little above 120 at an approximate field of 2 T. The slow decay of nuclear singlet-order is due, in this case, to the strong cross-correlation of the chemical shift anisotropy interactions for the two ^{13}C sites, as well as the immunity of singlet order to relaxation caused by dipole-dipole interactions within the spin pair.

I became an attractive candidate to study the singlet-order relaxation behaviour of for three reasons; the lifetime of singlet-order will be prolonged due to,

- The small chemical shift difference (0.16 ppm) allows access to singlet-order, but minimises relaxation via coherent interactions [90, 118, 129]
- By symmetry, singlet-order should have some immunity to relaxation via the symmetric CSA mechanism [27, 84]
- The high local symmetry about the ^{13}C nuclei may cause the antisymmetric CSA contribution to singlet-order to be negligible [130]

To elaborate on these points, a symmetry-breaking mechanism is required for coherent mixing between the singlet- and triplet-manifolds to allow population transfer [118, 129]. One such mechanism is a chemical shift difference. This does, however, cause relaxation, but the shift difference is small enough for this to potentially be an insignificant effect.

Further, if **I** is treated as a symmetric rotor, we may approximate the local symmetry about the labelled nuclei axially and having that of $D_{\infty h}$ point-group symmetry, as well as the z-principle

axes parallel. Pileio [27] showed from symmetry arguments that for a spin system with high local symmetry such as this one, with parallel principle axes, and identical chemical shift anisotropies for the two spins, the contribution to singlet relaxation rate is zero.

The last point above is also related to the local point-group symmetry about the spins; Buckingham and Malm [130] showed that for a molecule of $D_{\infty h}$ symmetry, all components of the antisymmetric CSA tensor vanish. Thus, if **I** was to be treated as a rigid rotor the contribution to singlet-order relaxation would be zero for the antisymmetric CSA. In reality, **I** will exhibit random fluctuations in geometry and divert from $D_{\infty h}$ geometry. However, to a first approximation, we assume the local geometry about the spins offers some protection to singlet-order.

The linewidths are related to the decay of coherences, and T_S to the decay of singlet-order via equilibration of populations. A natural progression is to study the longitudinal relaxation, and in particular the ratio T_S/T_1. Further, this ratio is determined as a function of static field.

5.2 Methods

5.2.1 Sample

19 mg of **I** was made up to a 200 μL 0.3 M solution in $CDCl_3$. 5 freeze-thaw degassing cycles were performed on the solution.

5.2.2 Equipment and pulse sequences

Spectrometers

All experiments were performed on a 400 MHz (9.4 T) Bruker Avance Neo spectrometer. A custom-built *shuttle* was used to shuttle the sample to a field as low as 5 mT, and anywhere between.

Estimation of T_1

T_1 was estimated by the inversion-recovery process, where by the inversion of spin populations was achieved via a $90^\circ_y - 180^\circ_x - 90^\circ_y$ composite pulse [131], followed by a delay τ, and then by a 90°_x-pulse. This process is repeated while varying the delay τ to give a longitudinal recovery curve. To estimate

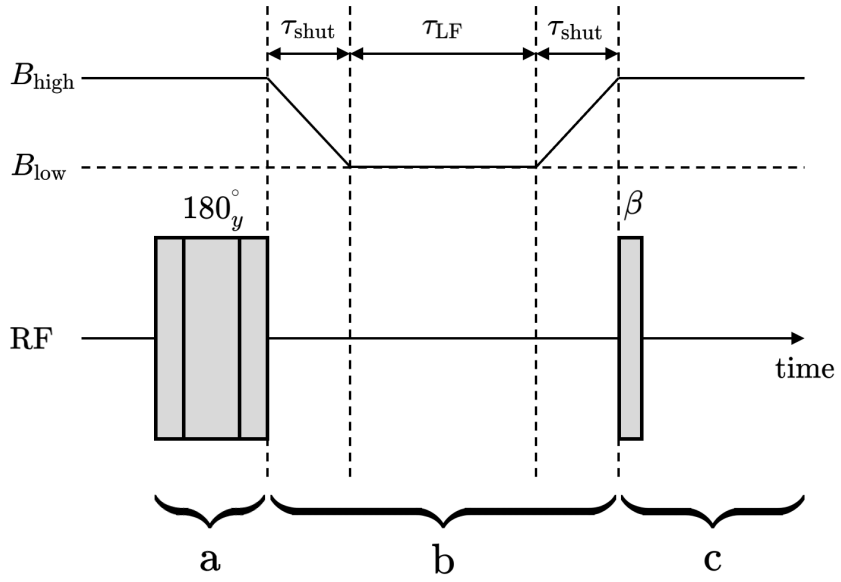

FIGURE 5.1: Pulse sequence for each stage of the experiment inversion-recovery experiments. In (a), a 180°_{y} composite pulse $90^{\circ}_{y} - 180^{\circ}_{x} - 90^{\circ}_{y}$ inverts the thermal equilibrium populations of the spin system. In (b), the sample is *shuttled* to low field for a time τ_{LF} and the spin system evolves freely. Note that there is a delay of τ_{shut} while shuttling is taking place. This delay is constant for all experiments in the measurement, and this experimental artefact should not affect results. In (c), a pulse with flip-angle β creates measurable coherences before acquisition of the signal.

T_1 as a function of static field, the process is repeated with the sample shuttled to a lower field for time τ_{LF} during the delay (see fig. 5.1).

Variable flip-angle experiments

Inversion-recovery experiments are repeated with the final pulse flip-angle (β) varied with values 10°, 50°, and 90° chosen (see fig. 5.1).

Estimation of T_{S}

T_{S} was measured using the M2S-S2M pulse-sequence, shown in figure 5.2. This was implemented with the shuttling device as depicted in figure 5.3. A singlet-order destruction (SOD-) filter [132] was used prior to the initial 90_x pulse, followed by an M2S block, and a T_{00}-filter [133] was used after the relaxation delay and upon shuttling the sample back into high field. Singlet-order was transformed to measurable coherences via an S2M block.

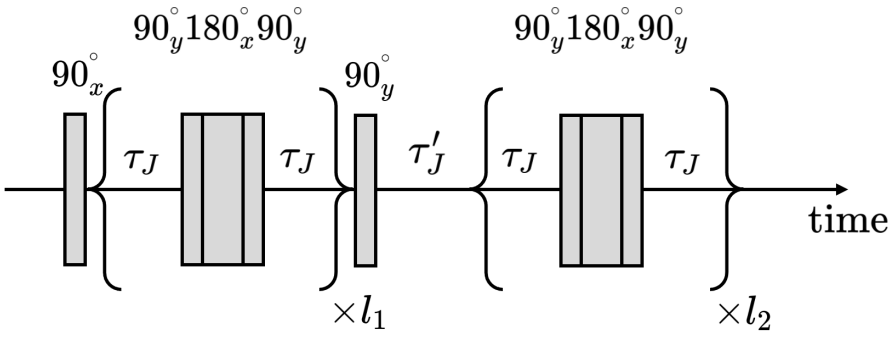

FIGURE 5.2: M2S block of an M2S-S2M pulse sequence. J-synchronised spin-echo trains are utilised to create singlet-order. The number of carriages in the train is specified by loop number l_i. delays are given analytically by, $\tau_J = \tau'_J = 1/4J$, and optimised along with l_1 and l_2 in experiment. Optimised values are, $\tau_\mathrm{J} = 1.155$ ms, $\tau'_J = 1.099$ ms, $l_1 = 20$, and $l_2 = 9$. The S2M block is the chronological reverse of M2S.

Analytically, $\tau_J = \tau'_J = 1/4J$ and $l_1 = 2l_2$, where J is the J-coupling between the two spins. Practically, however, these parameters must be optimised, and are, $\tau_\mathrm{J} = 1.155$ ms, $\tau'_J = 1.099$ ms, $l_1 = 20$, and $l_2 = 9$.

5.3 Experimental results

5.3.1 Inversion-recovery

$\pi/2$ read-out

T_1 values at fields ranging from 5 mT to 9.39 T are given in table 5.1. T_1 was estimated at each field by integrating over both peaks in a spectrum at a given delay, fitting each spectrum in the experiment to the function,

$$f(\tau_\mathrm{LF}) = A_0 e^{-\tau_\mathrm{LF}/T_1} + A_\infty \left(1 - e^{-\tau_\mathrm{LF}/T_1}\right), \tag{5.1}$$

where A_0 and A_∞ are coefficients at $\tau_\mathrm{LF} = 0$ and $\tau_\mathrm{LF} \to \infty$, respectively.

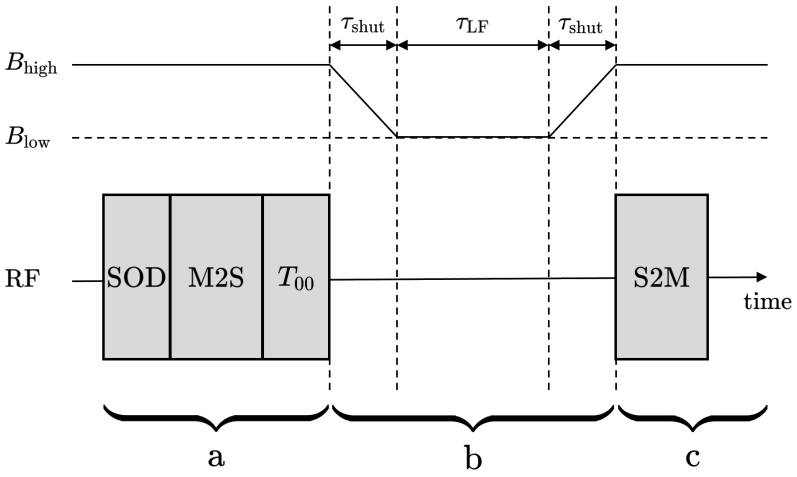

FIGURE 5.3: Pulse sequence used to measure the singlet decay time constant T_{S} as a function of field strength. (a) A singlet-order destruction (SOD) filter removes residual singlet-order, before singlet-order is created via the M2S pulse sequence [118]. A T_{00}-filter removes residues spin-orders other than singlet-order. (b) The sample is shuttled to low-field in the interval τ_{shut} and evolves freely during the interval τ_{LF} before being shuttled to high-field in the second τ_{shut} interval. (c) Singlet order is converted back to measurable magnetisation via the S2M pulse sequence; i.e. chronological reverse of M2S, with an additional 90°pulse.

Variable flip-angle experiments

The amplitude of each peak at a given value of τ for a given experiment was obtained by fitting the spectrum in this region to a superposition of absorption Lorentzians of the form,

$$L(\omega) = a_{\text{a}} \frac{\lambda_{\text{a}}}{\lambda_{\text{a}}^2 + (\omega - \omega_{\text{a}})^2} + a_{\text{b}} \frac{\lambda_{\text{b}}}{\lambda_{\text{b}}^2 + (\omega - \omega_{\text{b}})^2}, \tag{5.2}$$

where $a_{\text{a(b)}}$ is the peak amplitude, $\lambda_{\text{a(b)}}$ the linewidth, and $\omega_{\text{a(b)}}$ the position for peak a(b). The fitting for the 90° pulse-acquire spectrum is shown in figure 5.4. Experimental and simulated peak trajectories are shown in figure 5.5, showing very close agreement between numerical simulations and experiment.

Fittings were implemented in *Mathematica* and the details of the process for the $\beta = \pi/2$ experiment are,

1. Import the high-field $\pi/2$ pulse-acquire (or fully relaxed) spectrum and fit parameters.
    - Import spectrum in ASCII file format.

B_0 / T	T_1 / s	T_S / s	T_S/T_1
9.39	2.23 ± 0.04	208.80 ± 1.8	93.63 ± 1.8
7.96	2.45 ± 0.1	271.86 ± 6.5	110.96 ± 5.2
5.11	4.20 ± 0.1	459.09 ± 15.4	109.31 ± 4.5
1.94	$\mathbf{6.54 \pm 0.2}$	$\mathbf{789.49 \pm 22.5}$	$\mathbf{120.72 \pm 5.0}$
0.845	$\mathbf{6.21 \pm 0.3}$	$\mathbf{789.41 \pm 22.5}$	$\mathbf{127.12 \pm 7.1}$
0.409	6.11 ± 0.03	607.56 ± 13.8	99.44 ± 2.3
0.218	5.92 ± 0.03	508.56 ± 37.5	85.91 ± 6.3
0.126	5.70 ± 0.2	–	–
0.0428	5.58 ± 0.2	–	–
0.0210	5.78 ± 0.1	–	–
0.0116	5.80 ± 0.03	–	–
0.00695	5.82 ± 0.03	536.92 ± 50.1	92.25 ± 8.6
0.005	5.48 ± 0.2	549.18 ± 57.4	100.22 ± 11.1

TABLE 5.1: Values of T_1 and T_S, along with the magnitude of the static magnetic field in which the measurements were taken. In bold are the two rows with the largest T_S/T_1 ratios of 120.72 ± 5.0 and 127.21 ± 7.1. Both are highlighted since there is an overlap of error.

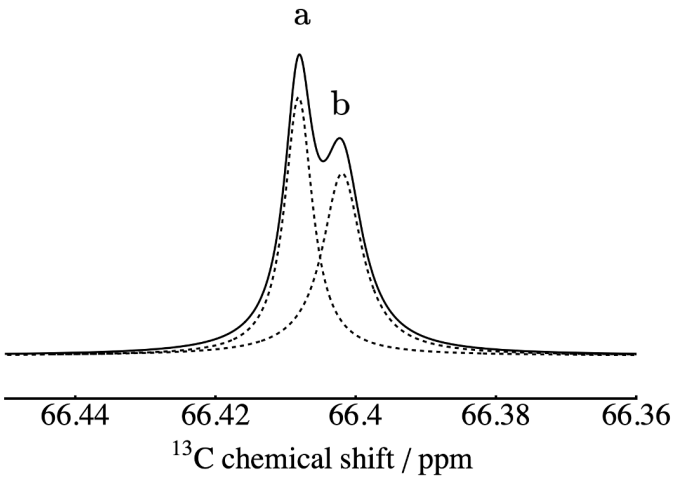

FIGURE 5.4: The NMR spectrum of **I** fitted as a sum of two absorption Lorentzian functions, given by eq. (5.2). The dashed lines are individual Lorentzians, and the solid line is the sum of them.

- With restriction $a_\mathrm{a} = a_\mathrm{b} \equiv a$, fit parameters a, λ_a, λ_b, ω_a, and ω_b to the experimental spectrum using eq. (5.2) (these are henceforth denoted a^f, $\lambda_\mathrm{a}^\mathrm{f}$, etc.).

2. Import spectra from the inversion-recovery experiment and fit a_a and a_b.

   - Each spectrum corresponds to that obtained for a different delay τ.
   - Fit $a_\mathrm{a}^{(1)}$ and $a_\mathrm{b}^{(1)}$ independently, with $\lambda_\mathrm{a}^\mathrm{f}$, $\lambda_\mathrm{b}^\mathrm{f}$, $\omega_\mathrm{a}^\mathrm{f}$, and $\omega_\mathrm{b}^\mathrm{f}$ fixed, and $-a^\mathrm{f}$ as initial guess for both a_a and a_b.
   - Fit $a_\mathrm{a}^{(i)}$ and $a_\mathrm{b}^{(i)}$ independently, with $\lambda_\mathrm{a}^\mathrm{f}$, $\lambda_\mathrm{b}^\mathrm{f}$, $\omega_\mathrm{a}^\mathrm{f}$, and $\omega_\mathrm{b}^\mathrm{f}$ fixed, and $a_\mathrm{a}^{(i-1)}$ and $a_\mathrm{b}^{(i-1)}$ as initial guesses for $a_\mathrm{a}^{(i)}$ and $a_\mathrm{b}^{(i)}$, respectively.
   - For each amplitude $a_\mathrm{a}^{(i)}$ and $a_\mathrm{b}^{(i)}$ corresponds a delay $\tau^{(i)}$
   - The couples $\left\{a_\mathrm{a}^{(i)}, \tau^{(i)}\right\}$ and $\left\{a_\mathrm{b}^{(i)}, \tau^{(i)}\right\}$ provide peak amplitude trajectories over the course of the experiment and may be plotted as in figure 5.5.

The $\beta < \pi/2$ fittings are somewhat more nuanced, and follow the process,

1. Fit parameters to the $\beta < \pi/2$ fully relaxed spectrum

   - Define $\lambda_\mathrm{a} = \lambda_\mathrm{a}^\mathrm{f} + \lambda'$, where λ' accounts for any perturbation from $\lambda_\mathrm{a}^\mathrm{f}$, with similar definitions for λ_b, ω_a, and ω_b, with perturbations assumed equal for both peaks.
   - Fit the parameters a_a, a_b, λ', and ω', where $a_\mathrm{a} \neq a_\mathrm{b}$ in this case

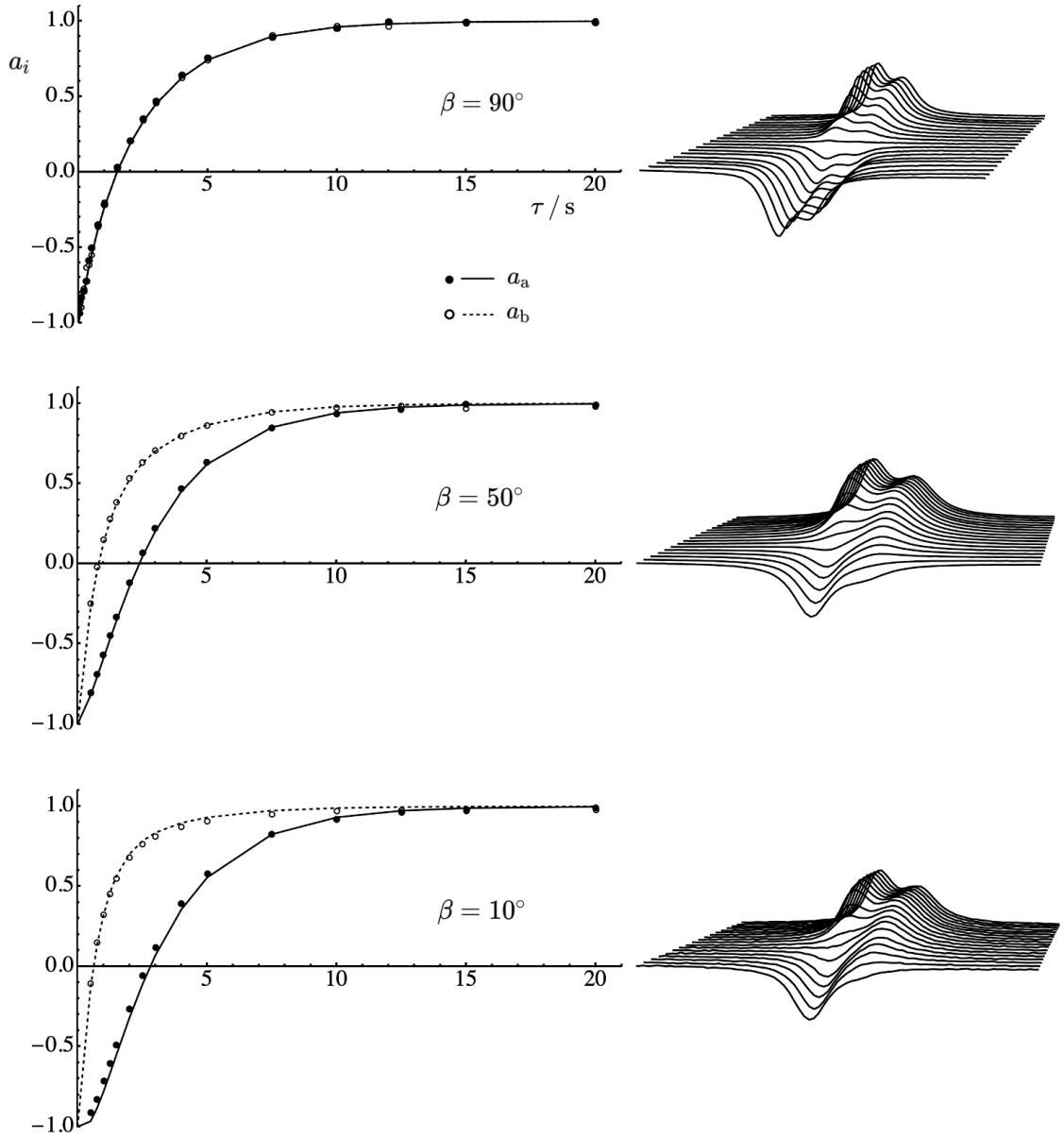

FIGURE 5.5: Left: Experimental (points) and peak trajectories (curves) for the variable flip-angle experiments at 9.4 T. Simulations were performed in Mathematica using the SpinDynamica package [49] using the theory outlined in section 5.5. Parameters: $\tau_\perp = 160$ ps, $r_{jk} = 122$ pm, $\Delta\delta_{\text{iso}} = 0.16$ ppm, $J_{jk} = 214.15$ Hz. Right: Experimental spectra obtained during the associated experiments to illustrate differential recovery of peaks.

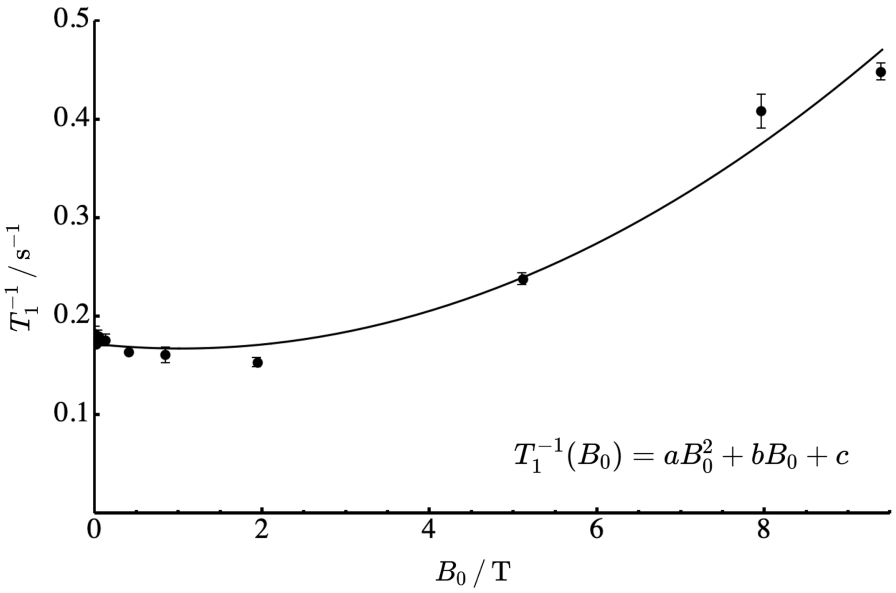

FIGURE 5.6: Plot of T_1^{-1} against B_0, with the polynomial $T_1^{-1}(B_0) = aB_0^2 + bB_0 + c$ fitted to the data. Parameters: $a = 4.70 \times 10^{-3} \pm 3 \times 10^{-4}$ s^{-1} T^{-2}, $b = -8.86 \times 10^{-3} \pm 6.1 \times 10^{-3}$ s^{-1} T^{-1}, $c = 0.17 \pm 5.8 \times 10^{-3}$ s^{-1}. The fit suggests the CSA$^{(\pm)}$ mechanisms to be active with a quadratic dependence on B_0, the DD-CSA cross-correlation to be active with a linear dependence on B_0, and the DD interaction active since the field-dependence is very small outside of the extreme-narrowing limit at 298 K, and may be approximated as field-independent and contained in $c \neq 0$.

2. Load in remaining spectra from the inversion-recovery experiment

   - Spectra are in ASCII file format
   - Fit $a_{\mathrm{a}}^{(1)}$ and $a_{\mathrm{b}}^{(1)}$ independently, with λ_{a}, λ_{b}, ω_{a}, and ω_{b} fixed, and $-a_{\mathrm{a}}$ and $-a_{\mathrm{b}}$ as initial guesses for $a_{\mathrm{a}}^{(1)}$ and $a_{\mathrm{b}}^{(1)}$, respectively.
   - Fit $a_{\mathrm{a}}^{(i)}$ and $a_{\mathrm{b}}^{(i)}$ independently, with λ_{a}, λ_{b}, ω_{a}, and ω_{b} fixed, and $a_{\mathrm{a}}^{(i-1)}$ and $a_{\mathrm{b}}^{(i-1)}$ as initial guesses for $a_{\mathrm{a}}^{(i)}$ and $a_{\mathrm{b}}^{(i)}$, respectively.
   - The couples $\left\{a_{\mathrm{a}}^{(i)}, \tau^{(i)}\right\}$ and $\left\{a_{\mathrm{b}}^{(i)}, \tau^{(i)}\right\}$ provide peak amplitude trajectories over the course of the experiment and may be plotted as in figure 5.5.

The values of T_1 as a function of static field are given in table 5.1, and plotted in fig. 5.6

5.3.2 Singlet-order

Both peaks in figure 5.8 were integrated over and peak area was fitted to the biexponential decay,

$$f(\tau_{\mathrm{LF}}) = A_1 e^{-\tau_{\mathrm{LF}}/T_1} + A_{\mathrm{S}} e^{-\tau_{\mathrm{LF}}/T_{\mathrm{S}}}, \tag{5.3}$$

with T_1 given in table 5.1. Integration was performed in *Topspin* and fitting in *Mathematica*. T_{S} with respect to field is also given in table 5.1, and plotted in fig. 5.7.

5.4 Numerical Simulations

Figure 5.9 compares fitted experimental spectra with those simulated for the variable flip-angle experiments. All simulations were performed in Mathematica, using SpinDynamica [49]. Section 5.4.3 offers details on implementation into Mathematica, and a notebook is presented alongside the thesis.

5.4.1 Lindbladian relaxation superoperator

Since the relaxation of spin-state populations are considered here, a Lindbladian-type relaxation superoperator is utilised. All the way back in chapter 3, the derivation of the relaxation superoperator required that the open system operators S_j fulfill,

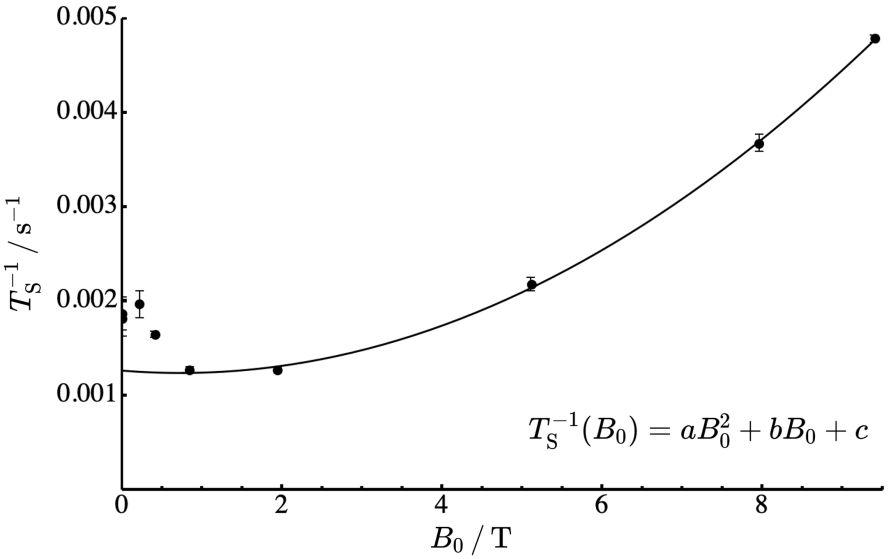

FIGURE 5.7: Plot of T_S^{-1} against B_0. The polynomial $T_S^{-1}(B_0) = aB_0^2 + bB_0 + c$ is fitted to the data from 0.845 to 9.39 T. Parameters: $a = 4.70 \times 10^{-5} \pm 3 \times 10^{-6}$ s^{-1} T^{-2}, $b = -6.80 \times 10^{-5} \pm 3.1 \times 10^{-5}$ s^{-1} T^{-1}, $c = 1.27 \times 10^{-3} \pm 5.9 \times 10^{-5}$ s^{-1}. The fit suggests the CSA$^{(\pm)}$ mechanisms to be active with a quadratic dependence on B_0, and the DD-CSA cross-correlation to be active with a linear dependence on B_0. Field-independent interactions are also active as illustrated by $c \neq 0$. The behaviour below 0.845 T has been attributed to geometry fluctuations in the literature [95], allowing for interactions such as the antisymmetric CSA and paramagnetic relaxation to dominate at low fields.

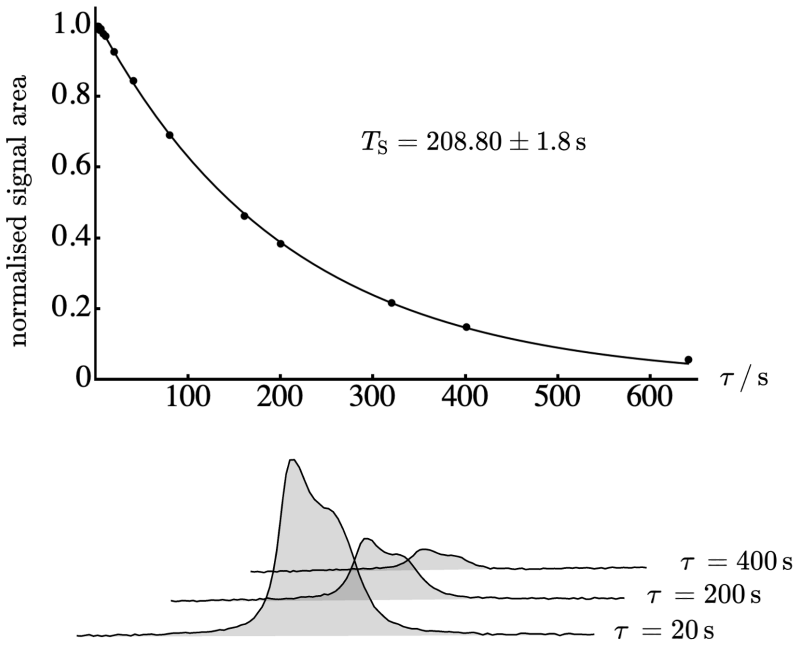

FIGURE 5.8: The T_S decay curve at 9.4 T is shown, with its exponential nature illustrated with spectra obtained at time τ = 20 s, 200 s, and 400 s after the M2S block. The ratio T_S/T_1 = 93.63 ± 1.8 at this field is exceptionally large, owing not only to the immunity of SO to DD relaxation, but also the small contributions of the $CSA^{(\pm)}$ and all cross-correlations due to the high local symmetry about the spin pair.

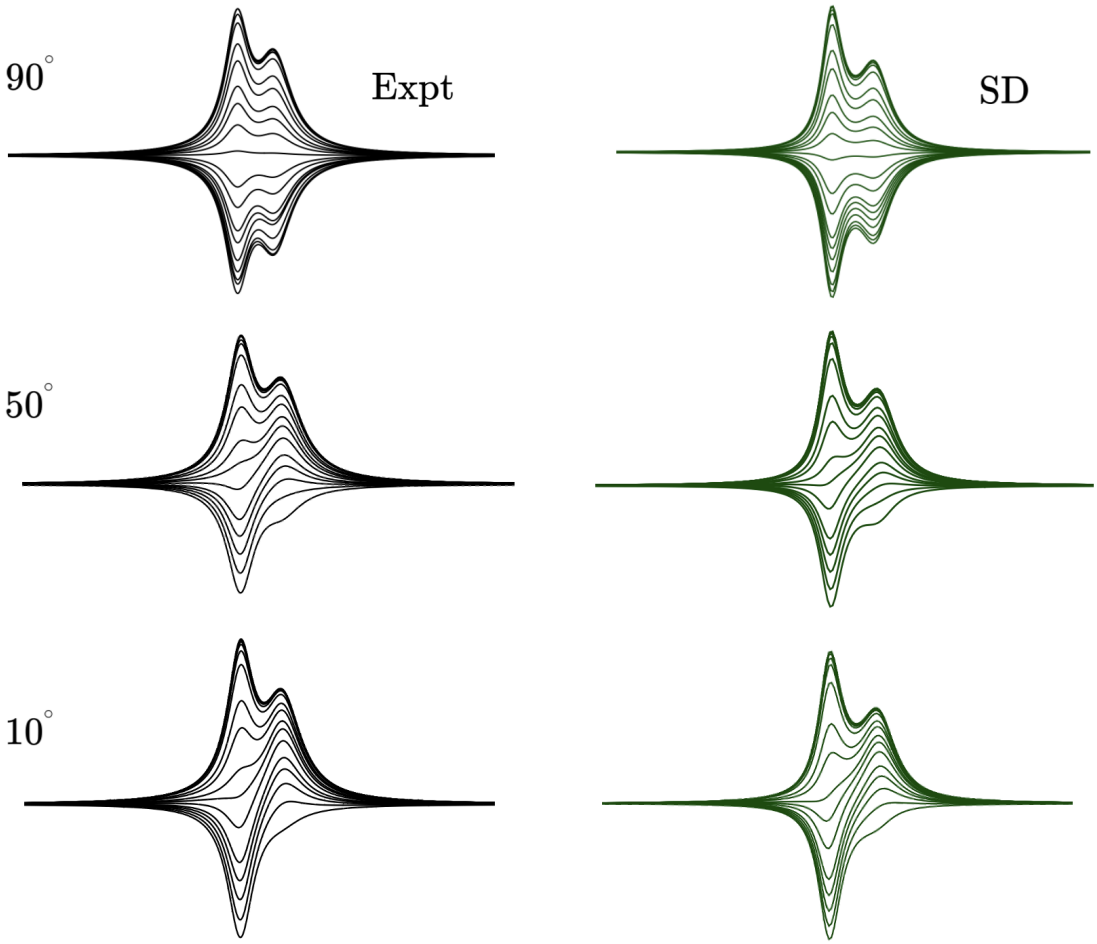

FIGURE 5.9: Experimental and simulated inversion-recovery spectra at 9.4 T, for $\beta = 10^\circ, 50^\circ, 90^\circ$, with all spectra from an inversion-recovery experiment superimposed. One can imagine the inverted peak with amplitude of the greatest magnitude being that which is obtained at the shortest delay τ. This corresponds to the first point in a recovery-curve plot. Moving vertically upwards, each spectrum follows τ chronologically. The thermalised relaxation superoperator in Lindbladian form was used to describe the incoherent interactions active during the delay and acquisition period. There is a one-to-one correspondence between each spectrum on the left with one on the right, since the list of delays implemented in experiment was replicated in simulation. The experimental plots are those of the fitted spectra using the process outlined in section 5.3. The plots were generated in *SpinDynamica* [49]. The only input required for the simulations are the magnetic shielding tensors and the internuclear bond length, $r_{ij} = 122$ pm. Details of implementation from here are given in section 5.4.3.

$$\begin{aligned}\big[H_0, S_j\big] &= -\omega_j S_j \\ \big[H_0, S_j^\dagger\big] &= +\omega_j S_j^\dagger,\end{aligned} \tag{5.4}$$

while the semiclassical master equation relied upon,

$$\begin{aligned}\big[H_0, X_{kq}\big] &= +\omega_q X_{kq} \\ \big[H_0, X_{kq}^\dagger\big] &= -\omega_j X_{kq}^\dagger.\end{aligned} \tag{5.5}$$

When casting the semiclassical master equation used in chapter 4 to Lindbladian form, the above suggests the correspondence,

$$S_j \Leftrightarrow X_{kq}^\dagger \quad \text{and} \quad S_j^\dagger \Leftrightarrow X_{kq}. \tag{5.6}$$

However, one must remember that we are utilising a covariant basis of irreducible spherical tensors as described in section 2.5.3 in chapter 2, and we instead end up with the correspondence,

$$S_j \Leftrightarrow X_{kq} \quad \text{and} \quad S_j^\dagger \Leftrightarrow X_{kq}^\dagger. \tag{5.7}$$

The relaxation superoperator for rank-k interactions Λ and Λ' becomes,

$$\hat{\Gamma}_k^{\theta\Lambda\Lambda'}\bullet = c_\Lambda c_{\Lambda'} \sum_q J_{kq}^{\theta\Lambda\Lambda'}(q\omega_0)\hat{\mathcal{D}}\big[X_{kq}^\Lambda, X_{kq}^{\Lambda'}\big]\bullet, \tag{5.8}$$

where $J_{kq}^{\theta\Lambda\Lambda'}(q\omega_0) = J_{kq}^{\Lambda\Lambda'}(q\omega_0)e^{\frac{1}{2}\theta q\omega_0}$ is the *thermalised* spectral density function, with $J_{kq}^{\Lambda\Lambda'}(q\omega_0)$ the classical spectral density function used throughout chapter 4, and $\theta = \hbar/k_\mathrm{B}T$ is the inverse temperature. In eq. (5.8), the spectral density function has been written separately from the dissipator, and the latter is now given by,

$$\hat{\mathcal{D}}\big[X_{kq}^\Lambda, X_{kq}^\Lambda\big]\bullet = X_{kq}^\Lambda \bullet X_{kq}^{\Lambda'\dagger} - \frac{1}{2}\left\{X_{kq}^{\Lambda'\dagger}X_{kq}^\Lambda, \bullet\right\}. \tag{5.9}$$

We find that in all simulations, the spectral density function of chapter 4, section 4.5.2 may be used, with a simple thermalisation, and the double commutator in the relaxation superoperator may be substituted for the dissipator in eq. (5.9).

5.4.2 Interactions

The interactions considered are largely the same as in chapter 4; coherently we consider the Zeeman, isotropic chemical shift, and scalar coupling interactions, and incoherently we consider the DD, CSA, and cross-correlation between the two. However, the rank-1 *antisymmetric* CSA is also considered here. Although the argument that it should vanish due to symmetry was put forward, a molecule of **I** isn't perfectly symmetrical, and – as shown below – has an associated correlation time three times that of a rank-2 interaction.

The antisymmetric chemical shift anisotropy

The CSA mechanism involves both rank-1 antisymmetric ($\mathrm{CSA}^{(-)}$) and rank-2 symmetric ($\mathrm{CSA}^{(+)}$) contributions. The antisymmetric and symmetric tensors are, respectively, defined as,

$$\boldsymbol{\delta}^{(-)} = \frac{1}{2}\left(\boldsymbol{\delta} - \boldsymbol{\delta}^{\mathrm{T}}\right) \tag{5.10}$$

and,

$$\boldsymbol{\delta}^{(+)} = \frac{1}{2}\left(\boldsymbol{\delta} + \boldsymbol{\delta}^{\mathrm{T}}\right) - \delta_{\mathrm{iso}}, \tag{5.11}$$

where $\boldsymbol{\delta}$ is the chemical shift tensor, and δ_{iso} is the isotropic chemical shift.

For a symmetric rotor, $\left[\tau_{\perp}^{(k)}\right]^{-1} = k\,(k+1)\,D_{\perp}$. From this, we have the relation,

$$\tau_{\perp}^{(1)} = 3\tau_{\perp}^{(2)}. \tag{5.12}$$

Thus, even if the components of the antisymmetric tensor are small compared to the symmetric tensor components, this may be offset by the much longer correlation time.

Upon diagonalisation of $\boldsymbol{\delta}$, rank-1 components vanish. However, we may work in the P-frame of the rank-2 tensor (P_2). That is, we use the eigenvectors of the rank-2 tensor to transform the rank-1 tensor; i.e.,

$$\left[\mathbf{A}^{(1)}\right]^{\mathrm{P}_2} = \mathbf{S}^{-1}\left[\mathbf{A}^{(1)}\right]^{\mathrm{AAS}}\mathbf{S}, \tag{5.13}$$

q, p	$\left[X_{kq}^{\mathrm{CSA}^-}\right]^{\mathrm{L}}$	$\left[A_{kp}^{\mathrm{CSA}^-}\right]^{\mathrm{P}_2}$
0	0	$-\frac{i}{\sqrt{2}}\left(\delta_{xy}-\delta_{yx}\right)$
± 1	$\frac{1}{2}B_0 I_j^{\pm}$	$\frac{1}{2}\{\delta_{xz}-\delta_{zx}\mp i(\delta_{zy}-\delta_{yz})\}$

TABLE 5.2: Irreducible spherical spin and spatial tensor components for the $\mathrm{CSA}^{(-)}$ interaction.

where $\mathbf{S}$ is a matrix whose columns are the eigenvectors of $\mathbf{A}^{(2)}$, and $\left[\mathbf{A}^{(1)}\right]^{\mathrm{AAS}}$ is the rank-1 tensor expressed in an *arbitrary axis system*. Since there is no cross-correlation between interactions of different rank, the is no cross-correlation between the $\mathrm{CSA}^{(-)}$ and $\mathrm{CSA}^{(+)}$, or $\mathrm{CSA}^{(-)}$ and DD mechanisms. Irreducible spherical spin and spatial tensor components for the $\mathrm{CSA}^{(-)}$ interaction are given in table 5.2.

5.4.3 The algorithm

The algorithm which allowed prediction of spectra for each delay in these T_1 experiments is very similar in structure to that used to simulate lineshapes, but with significant changes. A Mathematica notebook is provided illustrating its use, and follows the structure,

1. Input atomic coordinates from a computational geometry optimisation.
   - From coordinates, deduce b_{jk}, and in turn the DD-tensor using expression 2.82 in section 2.4
   - Diagonalise the DD tensor to express it in the $\mathrm{P_{DD}}$-frame
2. Input computed magnetic shielding $\boldsymbol{\sigma}_j$ tensors for labelled nuclei.
   - Transform $\boldsymbol{\sigma}_j$ to chemical shift tensors, $\boldsymbol{\delta}_j$, using computational tetramethylsilane tensors as a reference (all tensors obtained at the same computational level of theory).
   - Form $\boldsymbol{\delta}^{(-)}$ and $\boldsymbol{\delta}^{(+)}$ using eq. (5.10) and (5.11), respectively.
   - Use the eigenvectors of $\boldsymbol{\delta}^{(+)}$ to put $\boldsymbol{\delta}^{(-)}$ and $\boldsymbol{\delta}^{(+)}$ in the $\mathrm{P_2}$-frame.
   - Order diagonal elements of $\boldsymbol{\delta}^{(+)}$ using the Haeberlen convention, and use this to order the off-diagonal elements of $\boldsymbol{\delta}^{(-)}$.

3. Define the Lindbladian relaxation superoperator as a function which takes two interactions, ω_0, and $\tau_\perp$ as arguments, $\hat{\Gamma}^\theta(\Lambda, \Lambda', \omega_0, \tau_\perp^{(k)})$.

    - $\Lambda = \Lambda'$ for auto-correlated, and $\Lambda \neq \Lambda'$ for cross-correlated mechanisms
    - Define $\hat{\Gamma}^\theta(\Lambda, \Lambda', \omega_0, \tau_\perp^{(k)})$ for auto-correlated and cross-correlated mechanisms individually; the complete operator is the sum of these.
    - $\tau_\perp$ is approximated using $1/T_1 \simeq (I_z|\,\hat{\Gamma}^\theta(\Lambda, \Lambda', \omega_0, \tau_\perp^{(k)})\,|I_z)\,/\,(I_z|I_z)$, and solving for $\tau_\perp$.
    - Set $\tau_\perp^{(1)} = 3\tau_\perp^{(2)}$.

4. Define $\hat{H}_{\text{coh}}$.

    - Coherent parameters $\Delta\delta_{\text{iso}}$ and J_{jk} are obtained from experiment

5. Define the Liouvillian, $\hat{L} = -i\hat{H}_0 + \hat{\Gamma}^\theta(\Lambda, \Lambda', \omega_0, \tau_\perp^{(k)})$

6. Define the thermal equilibrium density operator.

    - The Hamiltonian is approximated as H_{Z} and temperature is $T = 300$ K.

7. Simulate the spectrum as the real part of a Fourier transformed signal using routines implemented in *SpinDynamica*

    - Routines used are FT[ ], Signal1D[ ] with the Preparation option, and BackgroundGenerator[ ].

The Preparation option allows one to specify the pulse sequence in the experiment. To simulate an inversion-recovery experiment with the 10° final pulse flip-angle, the syntax is,

$$\text{Preparation} \rightarrow \{\text{Pulse}[\{\pi, \pi/2\}], \{\text{None}, \#\}, \text{Pulse}[\{10^\circ, \pi/2\}]\}, \tag{5.14}$$

whereby the first pulse has flip-angle π of phase $\pi/2$, and the delay is the placeholder #, which is fed the sequence of delays implemented in experiment. Figure 5.9, where simulations for the variable flip-angle experiments are compared to experiment. We see excellent agreement between experiment and theory.

5.5 Theory

5.5.1 Operator basis

In chapter 4, the spectral lineshape was understood by considering the spin dynamics described by (-1)-quantum operators. To understand the dynamics during population equilibration during inversion-recovery and singlet-order experiments, the (0)-quantum operators must be considered. The set of 0-quantum operators of an appropriate basis is,

$$\mathbb{ST}_0 = \left\{ \frac{1}{2}\mathbb{1}, \mathbb{T}_{00}^{jk}, \mathbb{T}_{10}^{g}, \mathbb{T}_{10}^{u}, \mathbb{T}_{10}^{u'}, \mathbb{T}_{20}^{jk} \right\}, \tag{5.15}$$

where the normalised spherical tensor operators [60] are,

$$\begin{aligned}
\mathbb{T}_{00}^{jk} &= -\frac{2}{\sqrt{3}}\mathbf{I}_j \cdot \mathbf{I}_k \\
&= -\frac{1}{2\sqrt{3}}\left(3|S_0\rangle\langle S_0| - |T_{+1}\rangle\langle T_{+1}| - |T_0\rangle\langle T_0| - |T_{-1}\rangle\langle T_{-1}|\right), \\
\\
\mathbb{T}_{10}^{g} &= \frac{1}{\sqrt{2}}(I_{jz} + I_{kz}) \\
&= \frac{1}{\sqrt{2}}\left(|T_{+1}\rangle\langle T_{+1}| - |T_{-1}\rangle\langle T_{-1}|\right), \\
\\
\mathbb{T}_{10}^{u} &= \frac{1}{\sqrt{2}}(I_{jz} - I_{kz}) \\
&= \frac{1}{\sqrt{2}}\left(|T_0\rangle\langle S_0| + |S_0\rangle\langle T_0|\right) \\
\\
\mathbb{T}_{10}^{u'} &= \frac{1}{\sqrt{2}}\left(I_j^- I_k^+ - I_j^+ I_k^-\right) \\
&= \frac{1}{\sqrt{2}}\left(|T_0\rangle\langle S_0| - |S_0\rangle\langle T_0|\right) \\
\\
\mathbb{T}_{20}^{jk} &= \sqrt{\frac{2}{3}}\left(3I_{jz}I_{kz} - \mathbf{I}_j \cdot \mathbf{I}_k\right) \\
&= \frac{1}{\sqrt{6}}\left(|T_{+1}\rangle\langle T_{+1}| - 2|T_0\rangle\langle T_0| + |T_{-1}\rangle\langle T_{-1}|\right).
\end{aligned} \tag{5.16}$$

The $\mathbb{T}_{00}^{jk}$ operator has an expectation value proportional to the population imbalance between

the singlet and triplet manifolds, and referred to as *singlet-order* (SO). The $\mathbb{T}^g_{10}$ operator has an expectation value proportional to longitudinal magnetisation, and referred to as *longitudinal-order* (LO), with the g ("*gerade*") superscript referring to the symmetric permutation symmetry of the operator with respect to spin labels. The antisymmetic operators $\mathbb{T}^u_{10}$ and $\mathbb{T}^{u'}_{10}$ ("*ungerade*") represent ZQ-coherences via their expectation values. The $\mathbb{T}^{jk}_{20}$ operator has an expectation value proportional to a population imbalance in the triplet manifold, and since $\mathbb{1} = |S_0\rangle\langle S_0| + |T_{+1}\rangle\langle T_{+1}| + |T_0\rangle\langle T_0| + |T_{-1}\rangle\langle T_{-1}|$, the $\frac{1}{2}\mathbb{1}$ operator represents the sum of populations over all states, and is conserved under relaxation.

The basis in eq. (5.16) is convenient for our purposes since it is an eigenbasis of the relaxation superoperator describing DD relaxation, and may be approximated as an eigenbasis for the relaxation superoperator describing the rank-2 CSA relaxation. Rank-1 CSA components are negligibly small in the rigid model (recall section 5.1), and will not be considered in this analytical treatment. We find that SO is immune to relaxation by the DD mechanism, and largely unaffected by the CSA$^{(+)}$ mechanism in the rigid-rotor limit. However, the cross-correlation between the two mechanisms induces transitions between SO and the ZQ-coherences $|S_0\rangle\langle T_0|$ and $|T_0\rangle\langle S_0|$.

5.5.2 Observable trajectories: inversion-recovery experiments

Matrix elements and spin dynamics

Since Longitudinal order is approximately an eigenorder of the full Liouvillian involving the DD and CSA mechanisms, we may write,

$$\begin{aligned}\Lambda^{\mathrm{DD}}_{\mathrm{LO}} &= -\frac{(\mathbb{T}^g_{10}|\hat{\Gamma}^{\theta}_{\mathrm{DD}}|\mathbb{T}^g_{10})}{(\mathbb{T}^g_{10}|\mathbb{T}^g_{10})} \\ &= \frac{3}{10} b^2_{jk}\tau_{\perp}\left\{\frac{\cosh(\frac{\omega_0\theta}{2})}{1+\tau^2_{\perp}\omega^2_0} + \frac{4\cosh(\omega_0\theta)}{1+4\tau^2_{\perp}\omega^2_0}\right\},\end{aligned} \tag{5.17}$$

and,

$$\begin{aligned}\Lambda^{\mathrm{CSA}}_{\mathrm{LO}} &= -\frac{(\mathbb{T}^g_{10}|\hat{\Gamma}^{\theta}_{\mathrm{CSA}}|\mathbb{T}^g_{10})}{(\mathbb{T}^g_{10}|\mathbb{T}^g_{10})} \\ &= \frac{3}{20}\omega^2_0\tau_{\perp}\left(\left[\delta^{\mathrm{CSA}}_j\right]^2 + \left[\delta^{\mathrm{CSA}}_k\right]^2\right)\frac{\cosh(\frac{\omega_0\theta}{2})}{1+\tau^2_{\perp}\omega^2_0},\end{aligned} \tag{5.18}$$

where axial symmetry is assumed ($\eta_{j(k)} = 0$).

$\mathbb{T}_{10}^{g}$ is not an eigenorder of the Liouvillian when cross-correlation between the DD and CSA mechanisms are considered, and is connected to the $\mathbb{T}_{20}^{jk}$ operator by,

$$-\frac{(\mathbb{T}_{10}^{g}|\hat{\Gamma}_{\mathrm{DD}\times\mathrm{CSA}}^{\theta}|\mathbb{T}_{20}^{jk})}{(\mathbb{T}_{10}^{g}|\mathbb{T}_{20}^{jk})} = -\frac{3\sqrt{3}}{10}\omega_0 b_{jk}\tau_{\perp}\left(\delta_j^{\mathrm{CSA}} + \delta_k^{\mathrm{CSA}}\right)\frac{\cosh(\frac{\omega_0\theta}{2})}{1+\tau_{\perp}^2\omega_0^2}. \tag{5.19}$$

That is, the $|T_0\rangle$ state population is in excess relative to $|T_{\pm}\rangle$. This in turn is loosely connected to the ZQ-coherences, $\mathbb{T}_{10}^{u}$. The off-diagonal matrix element $\mathbb{T}_{20}^{jk} \rightarrow \mathbb{T}_{10}^{u}$ is given by,

$$-\frac{(\mathbb{T}_{20}^{jk}|\hat{\Gamma}_{\mathrm{DD}\times\mathrm{CSA}}^{\theta}|\mathbb{T}_{10}^{u})}{(\mathbb{T}_{20}^{jk}|\mathbb{T}_{10}^{u})} = \frac{1}{5\sqrt{3}}\omega_0 b_{jk}\tau_{\perp}\left(\delta_j^{\mathrm{CSA}} - \delta_k^{\mathrm{CSA}}\right)\left\{1 - \frac{3\cosh(\frac{\omega_0\theta}{2})}{1+\tau_{\perp}^2\omega_0^2}\right\}. \tag{5.20}$$

However, this matrix element is small compared to that in eq. (5.19) due to being proportional to the difference in CSA of the two sites, which are very similar in our model. The matrix representation of the relaxation superoperator and the dominant dynamics responsible for the observed peak trajectories are shown in fig. 5.10 and 5.11, respectively.

From here, we may use the material from chapter 2, section 2.6, to mathematically describe the effect of a small β on the observed peak amplitudes. For a time-independent $\hat{L}$, the spin dynamics of the system may be described in the period t_0 to t by the solution of the Liouville-von Neumann equation as,

$$\begin{aligned} |\rho(t)) &= e^{(t-t_0)\hat{L}}\,|\rho(t_0)) \\ &= \sum_q |Q_q)\,(Q_q|\,\rho(t_0))e^{(t-t_0)\Lambda_q}, \end{aligned} \tag{5.21}$$

where $\sum_q |Q_q)(Q_q| = \mathbb{1}$ is used, and $\{|Q_q)\}_{q=0}^{\mathcal{L}_D-1}$ is a complete and orthonormal operator basis. As shown in chapter 4, the (-1)-quantum block is approximately diagonal in the $\mathbb{B}_Q$ basis, and a basis may be constructed for which $\mathbb{B}_Q$ is a subset of $\mathbb{ST}$ ($\mathbb{B}_Q \in \mathbb{ST}$). Thus, the set of Λ_q are here considered eigenvalues if $|Q_q)$ are restricted to (-1)-quantum operators. The signal may then be written as [6, 9, 96],

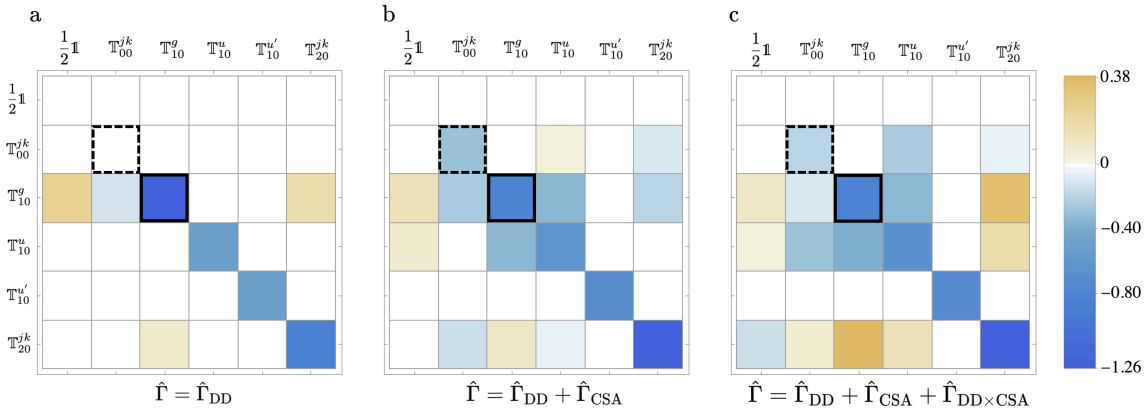

FIGURE 5.10: Matrix representations of the relaxation superoperator. The element outlined by with a solid black line correspinds to LO, $\mathbb{T}_{10}^{g}$. The element outlined by a dashed black line corresponds to SO, $\mathbb{T}_{00}^{jk}$. a) LO shows strong relaxation under the DD mechanism, whilst SO is immune. Off-diagonal elements are five- and six-orders of magnitude smaller than those on the diagonal, and the $\mathbb{ST}_0$ operators in eq. (5.15) are considered eigenoperators of Γ when considering only the DD interaction. b) Inclusion of the CSA mechanism. Off-diagonal elements are still very small compared to those along the diagonal, and although SO is not immune to the CSA mechanism, the contribution to T_{S}^{-1} is proportional to the square of the difference in anisotropy parameters of the two spins. Since these parameters are very similar, this matrix element is on the order of 1×10^{-5}. c) Inclusion of the DD-CSA cross-correlation. Inclusion of the correlated mechanisms contributes little to the diagonal elements. However, operators are mixed as illustrated by the larger off-diagonal elements.

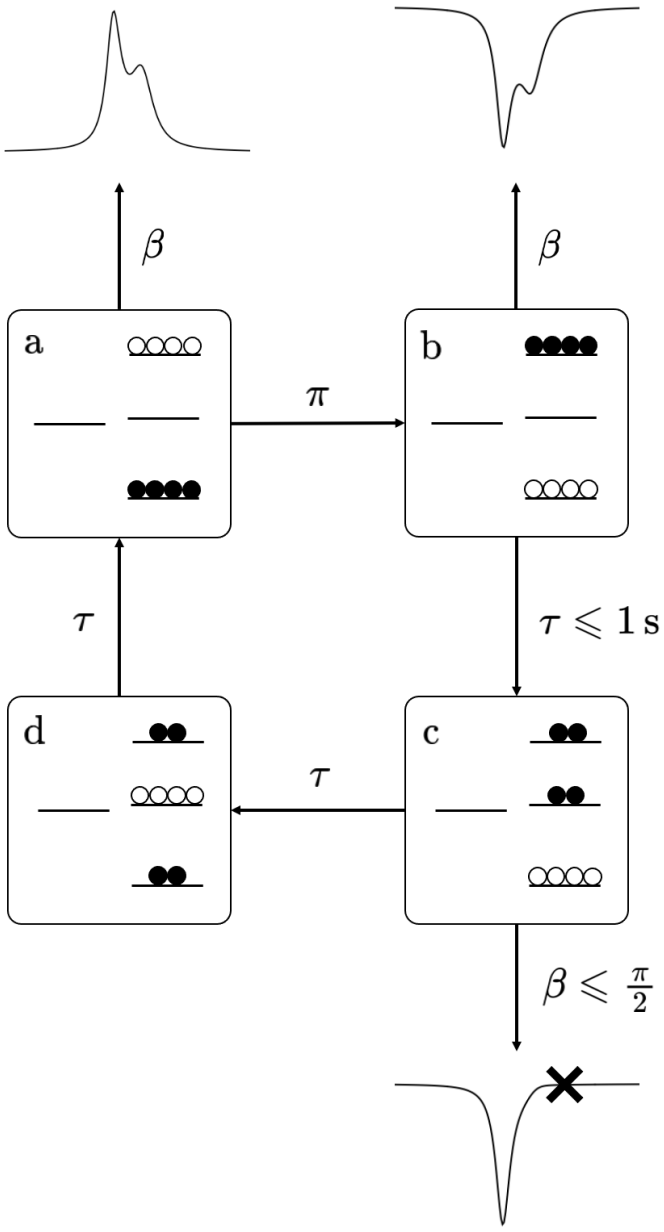

FIGURE 5.11: Energy level diagram illustrating the spin dynamics and how they describe the differential recovery effects of the peaks in the spectrum. The filled circles represent positive populations, and the open circles represent negative populations. a) The spin system at thermal equilibrium may be approximated by longitudinal-order, $\mathbb{T}^{+}_{10}$. b) A π-pulse inverts populations, and a pulse with arbitrary β gives an inverted spectrum. c) After a small delay $\tau \ll 1$ s, the density operator is approximated by an operator intermediate between $-\mathbb{T}^{+}_{10}$ and $\mathbb{T}^{jk}_{20}$. Relaxation is assumed to have taken place significantly between states $|T_0\rangle$ and $|T_{-1}\rangle$ only. A pulse with small β leads to a spectrum in which only the Q_+ operator is measurable. d) The density operator evolves into $\mathbb{T}^{jk}_{20}$. A delay returns thermal equilibrium and a pulse of arbitrary β returns the recovered spectrum.

$$\begin{aligned} s(t) &= \frac{1}{2} i \left(I_- | \, \rho(t) \right) \\ &= \sum_q a_q e^{(t-t_0)\Lambda_q}, \end{aligned} \tag{5.22}$$

where a_q is the complex amplitude associated with the coherence represented by operator $\big|Q_q\big)$, and using eq. (5.21) and (5.22) is given by,

$$a_q = \frac{1}{2} i \big(I_- \big| Q_q \big) \big(Q_q \big| \rho(t_0) \big). \tag{5.23}$$

If t_0 is defined as the start of acquisition,

$$\big| \rho(t_0) \big) = \hat{V}_{\text{exc}} \big| \rho_{\text{eq}} \big), \tag{5.24}$$

where $\hat{V}_{\text{exc}}$ is the excitation sequence. In our case, this corresponds to an inversion-recovery experiment and is,

$$\begin{aligned} \hat{V}_{\text{exc}} &\equiv \hat{V}_{\text{exc}}(\beta, \tau) \\ &= \hat{R}_\phi(\beta) e^{\hat{L}\tau} \hat{R}_\phi(\pi), \end{aligned} \tag{5.25}$$

where $\hat{R}_\phi(\beta)$ and $\hat{R}_\phi(\pi)$ are rotation superoperators of phase ϕ and with angles β and π as argument. The complex amplitude in eq. (5.23) may then be written,

$$\begin{aligned} a_q &\equiv a_q(\beta, \tau) \\ &= \frac{1}{2} i \big(I_- \big| Q_q \big) \big(Q_q \big| \hat{R}_\phi(\beta) e^{\hat{L}\tau} \hat{R}_\phi(\pi) \big| \rho_{\text{eq}} \big). \end{aligned} \tag{5.26}$$

If approximating $\big|\rho_{\text{eq}}\big)$ as longitudinal order as in chapter 4 we may write,

$$\big| \rho_{\text{eq}} \big) \approx \sqrt{2} \big| \mathbb{T}^g_{10} \big), \tag{5.27}$$

a π-pulse leads to,

$$\hat{R}_\phi(\pi)\big|\rho_{\mathrm{eq}}\big) \approx -\sqrt{2}\big|\mathbb{T}^g_{10}\big), \tag{5.28}$$

and eq. (5.26) may be written,

$$a_q(\beta,\tau) = \frac{1}{\sqrt{2}} i\big(I_-\big|Q_q\big)\big(Q_q\big|\hat{R}_\phi(\beta)e^{\hat{\mathcal{L}}\tau}\hat{R}_\phi(\pi)\big|\mathbb{T}^g_{10}\big), \tag{5.29}$$

The amplitudes of the individual peaks are then,

$$a_\pm(\beta,\tau) = \frac{1}{\sqrt{2}} i\big(I_-\big|Q_\pm\big)\big(Q_\pm\big|\hat{R}_\phi(\beta)e^{\hat{\mathcal{L}}\tau}\hat{R}_\phi(\pi)\big|\mathbb{T}^g_{10}\big). \tag{5.30}$$

Considering the dynamics deduced in eq. (5.17)-(5.20) and depicted in fig. 5.11, the peak amplitudes may be deduced at each point in the inversion-recovery process.

Following the inversion pulse and at $\tau = 0$ s and with $\phi = 0$, we have,

$$\begin{aligned} a_\pm(\beta,0) &= -\frac{1}{\sqrt{2}} i\big(I_-\big|Q_\pm\big)\big(Q_\pm\big|\hat{R}_0(\beta)\big|\mathbb{T}^g_{10}\big) \\ &= -\frac{1}{2}\sin\beta. \end{aligned} \tag{5.31}$$

We see that the (0)- and (−1)-quantum operators are connected by the rotation superoperator, with an amplitude of transformation depending on β. In this limit, both peaks have equal amplitude.

The normalised density operator after free evolution for a small delay ($\tau \ll 1$ s) as depicted in fig. 5.11c is given by,

$$\rho_{\mathrm{c}} = \frac{1}{8}\mathbb{1} - \frac{1}{4\sqrt{3}}\mathbb{T}^{jk}_{00} - \frac{3}{2\sqrt{2}}\mathbb{T}^g_{10} - \frac{5}{2\sqrt{6}}\mathbb{T}^{jk}_{20}. \tag{5.32}$$

The amplitudes become,

$$\begin{aligned} \lim_{\tau\to 0} a_\pm(\beta,\tau) &= \frac{1}{2} i\big(I_-\big|Q_\pm\big)\big(Q_\pm\big|\hat{R}_0(\beta)\big|\rho_{\mathrm{c}}\big) \\ &= -\frac{1}{8}\left(3 \pm 5\cos\beta\right)\sin\beta. \end{aligned} \tag{5.33}$$

Following this, the cases $\beta = \pi/2$ and $\beta \ll \pi/2$ are considered to explain the experimental findings above.

$\pi/2$ read-out

At point depicted in figure 5.11b, no relaxation has occurred and both peaks have equal amplitude upon excitation of transverse magnetisation, as deduced by eq. (5.31). $a_{\pm}(\pi/2, 0)$ becomes,

$$a_{\pm}(\pi/2, 0) = -\frac{1}{2}, \tag{5.34}$$

and is in greement with that deduced in chapter 4, section 4.6, in the limit of chemical equivalence and taking into account inversion of spin polarisation. When τ is small (see fig. 5.11c) we have,

$$\lim_{\tau \to 0} a_{\pm}(\pi/2, \tau) = -\frac{3}{8}, \tag{5.35}$$

and we see that both peaks have equal amplitude again, as observed experimentally.

Small flip-angle read-out

The theory thus far may be used to explain the differential recovery effects observed experimentally. For small τ and β, when the spin-system resembles fig. 5.11c, eq. (5.33) shows that the Q_+ peak amplitude remains negative, whilst the Q_- peak amplitude is positive but tends to zero as $\beta \to 0$. For example, a $\beta = 10^{\circ}$ pulse at this point in the experiment gives the following theoretical amplitudes:

$$\begin{aligned} \lim_{\tau \to 0} a_{+}(10^{\circ}, \tau) &= -0.172 \\ \lim_{\tau \to 0} a_{-}(10^{\circ}, \tau) &= 0.0418. \end{aligned} \tag{5.36}$$

Overall we have,

$$\begin{aligned} \lim_{\tau \to 0} a_{+}(\beta \ll \pi/2, \tau) &< 0 \\ \lim_{\tau \to 0} a_{-}(\beta \ll \pi/2, \tau) &\simeq 0, \end{aligned} \tag{5.37}$$

which qualitatively describes the experimental results obtained in figure 5.5 correctly.

5.5.3 Singlet-order relaxation

The same process can be used to study SO. We find that SO is immune to DD relaxation, which is known and the fundamental property which makes it long-lived [27, 81, 82]. Also, $\Lambda_{\mathrm{SO}}^{\mathrm{CSA}}$ is proportional to the square of the difference in chemical shift anisotropy of the two sites:

$$\begin{aligned}\Lambda_{\mathrm{SO}}^{\mathrm{CSA}} &= -\frac{(\mathbb{T}_{00}^{jk}|\hat{\Gamma}_{\mathrm{CSA}}^{\theta}|\mathbb{T}_{00}^{jk})}{(\mathbb{T}_{00}^{jk}|\mathbb{T}_{00}^{jk})} \\ &= \frac{1}{15}\omega_0^2\tau_\perp\left(\delta_j^{\mathrm{CSA}}-\delta_k^{\mathrm{CSA}}\right)^2\left\{2+\frac{3\cosh(\frac{\omega_0\theta}{2})}{1+\tau_\perp^2\omega_0^2}\right\}.\end{aligned} \tag{5.38}$$

Since δ^{CSA} is very similar for each spin, this suggests SO will be largely immune to the CSA mechanism if a rigid molecule is assumed.

Like $\mathbb{T}_{10}^{g}$, $\mathbb{T}_{00}^{jk}$ is not an eigenoperator of the Liouvillian involving the DD-CSA cross-correlation. We find that under this influence, $\mathbb{T}_{00}^{jk}$ is connected to the operator $\mathbb{T}_{10}^{u}$ (ZQ-coherences), which are in turn connected to $\mathbb{T}_{20}^{jk}$ and, ultimately, $\mathbb{T}_{10}^{g}$ as descibed at the beginning of section 5.5.2. We find that the limiting step is,

$$\begin{aligned}&-\frac{(\mathbb{T}_{00}^{jk}|\Gamma_{\mathrm{DD}\times\mathrm{CSA}}^{\theta}|\mathbb{T}_{10}^{u})}{(\mathbb{T}_{00}^{jk}|\mathbb{T}_{10}^{u})} \\ &=-\frac{1}{20\sqrt{2}}\omega_0 b_{jk}\tau_\perp\left(\delta_j^{\mathrm{CSA}}-3\delta_k^{\mathrm{CSA}}\right)\left\{2+\frac{3\cosh(\frac{\omega_0\theta}{2})}{1+\tau_\perp^2\omega_0^2}\right\}.\end{aligned} \tag{5.39}$$

That is, cross-correlation between the DD and CSA mechanisms relaxes singlet-order by transforming it to the ZQ-coherences, which connects the manifolds and allows for population equilibration. The dominant spin dynamics are depicted in fig. 5.12.

5.6 Discussion and conclusions

Taken together, the field-dependence and β-dependence experiments show interesting relaxation behaviour. The SO experiments are simpler to interpret, yet offer remarkable results and a natural direction for future work.

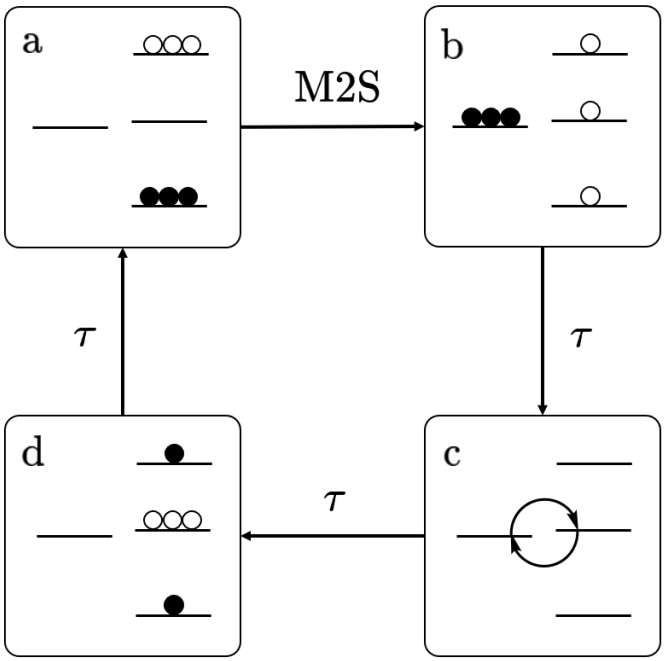

FIGURE 5.12: Energy level diagram illustrating the dominant spin dynamics of SO relaxation in molecule **I**. The filled circles represent positive populations, the open circles negative populations, and the curly arrows represent coherences. In going from (a) to (b), the M2S pulse-sequence (see fig. 5.2) creates SO from LO. c) After some delay, coherences connecting the singlet- and triplet-manifolds are created, with facilitates relaxation back to LO via population transfer between manifolds as depicted in (d) and (a).

5.6.1 Inversion-recovery experiments

Inversion-recovery experiments for which $\beta = \pi/2$ show a field dependence where by T_1 increases with decreasing field to a maximum of 5.82 ± 0.03 s at $B_0 \approx 7$ mT. This small T_1 may be attributed to the large DD coupling between the spins, and the large $\text{CSA}^{(+)}$ mechanism, which is the dominant relaxation mechanism active in the system. The variable flip-angle experiments show differential recovery trajectories of the two main peaks. The numerical simulations show excellent agreement with these experiment, and were based on the theory presented in chapters 3, 4, and section 5.4 here. Further, analytical theory is presented which accounts for the spin dynamics and successfully describes the differential recovery effects qualitatively.

5.6.2 Singlet-order relaxation

The T_S of 208.80 s at 9.4 T does not seem hugely impressive on its own. However, an arguably more important quantity is the ratio T_S/T_1, which is approximately 120-fold for the triyne derivative at fields $B_0 = 1.94$ T and 0.845 T. This ratio is exceptionally high, and is attributed to the immunity of SO to the large DD couplings, as well as the consequences of high local symmetry about the labelled nuclei.

To elaborate, the analytical theory presented shows that $\Lambda_\text{SO}^\text{CSA}$ is proportional to the square of the difference in CSA parameters of the two spins. These parameters are $\delta_j^\text{CSA} = -145.7$ ppm and $\delta_k^\text{CSA} = -145.4$ ppm. As such, the contribution to T_S is very small. Further, analysis of the relaxation superoperator allows one to trace the spin dynamics induced by the DD-CSA cross correlated mechanisms. Taken together, the theory outlined in section 5.5.3 offers some understanding of what makes $T_\text{S} \gg T_1$ in this system. However, not all limits, regimes, and mechanisms were considered, which offers avenues for future work.

For example, the small contribution from the $\text{CSA}^{(+)}$ mechanism, and neglect of the $\text{CSA}^{(-)}$ mechanism, assumes a rigid geometry. This is unlikely, and the triyne derivative will undergo instantaneous conformational fluctuations at any point in time. These changes will affect the degree to which interactions and the cross-correlation between them contribute to relaxation. For example, Pileio [27] showed that the contribution of the symmetric CSA mechanisms to T_S^{-1} is dependent not only on the difference in chemical shift anisotropies of the two spins, but also the relative orientation of the P_CSA-frames; if the two z-axes are parallel, and anisotropies equal, then there is no contribution. The treatment in of $\mathbf{I}$ in this thesis relied on assuming a rigid geometry, which in

turn allows one to approximate the P_{CSA}-frames as parallel. Yet, at any instant in time, it is likely that conformational flexibility means we deviate from this ideal.

Of foremost significance is the contribution from the $CSA^{(-)}$ mechanism. In section 4.7, the molecule $^{13}C_2$-DAND was considered. Intuitively, one would expect the ring structure to be rigid, with little flexibility. However, it has been shown by molecular dynamics that the conformational fluctuations are significant [95]. Further computations also implied that these fluctuations allowed for $CSA^{(-)}$ to be the dominant mechanism at low fields. It is reasonable to believe that the triyne derivative is subject to greater conformational fluctuations in the vicinity of the labelled nuclei, than is $^{13}C_2$-DAND, and this mechanism may offer a large contribution to T_S^{-1}.

Future work would explore the use of molecular dynamics to predict the relaxation behaviour in different limits. For example, to predict the peculiar behaviour of T_1 and T_S at low-fields, illustrated by figures 5.6 and 5.7, respectively; in both cases, there is a minimum in the inverse constants when the field is very low, followed by an increase in the inverse constants. This behaviour has been predicted by Klauda et al. (2008) in the context of lipids rotating in membranes [134], which also rotate anisotropically.

As it stands, the vast majority of the work presented in this thesis is analytical, offering results which are relevant in strict regimes; the model of a rigid symmetric top, tumbling anisotropically in an isotropic medium. Although this may appear to be a limitation, it has allowed one to derive significant and meaningful results throughout, describing the spin dynamics of a misleadingly simple system.

References

[1] N. Jeevanjee, *An Introduction to Tensors and Group Theory for Physicists*, 2nd ed. 2015, Springer International Publishing : Imprint: Birkhäuser, Cham, **2015**.

[2] P. A. M. Dirac, *The Principles of Quantum Mechanics*, 4. ed. (rev.), repr, Clarendon Press, Oxford University Press, Oxford, **2010**.

[3] J. Audretsch, *Entangled Systems: New Directions in Quantum Physics*, Wiley-VCH, Weinheim, **2007**.

[4] J. von Neumann, *Mathematical Foundations of Quantum Mechanics: New Edition*, First, (Ed.: R. T. Beyer), Princeton University Press, **2018**.

[5] P. A. M. Dirac, *Math. Proc. Camb. Phil. Soc.* **1939**, *35*, 416–418.

[6] R. R. Ernst, G. Bodenhausen, A. Wokaun, *Principles of Nuclear Magnetic Resonance in One and Two Dimensions*, Clarendon press, Oxford, **1992**.

[7] U. Fano, *Rev. Mod. Phys.* **1957**, *29*, 74–93.

[8] J. Jeener, *J. Magn. Reson.* **1982**, *10*, 1–51.

[9] M. H. Levitt, *Spin Dynamics: Basics of Nuclear Magnetic Resonance*, 2nd ed, John Wiley & Sons, Chichester, England ; Hoboken, NJ, **2008**.

[10] O. Sørensen, G. Eich, M. Levitt, G. Bodenhausen, R. Ernst, *Prog. Nucl. Mag. Res. Sp.* **1984**, *16*, 163–192.

[11] A. Abragam, *The Principles of Nuclear Magnetism*, Repr, Oxford Univ. Pr, Oxford, **2011**.

[12] R. Shankar, *Principles of Quantum Mechanics*, Second edition, Springer New York, Boston, MA, **1994**.

[13] R. N. Zare, *Angular Momentum: Understanding Spatial Aspects in Chemistry and Physics*, Wiley, New York, **1988**.

[14] A. R. Edmonds, *Angular Momentum in Quantum Mechanics*, Princeton University Press, Princeton, **1996**.

[15] D. A. Varshalovich, A. N. Moskalev, V. K. Kheronskii, *Quantum Theory of Angular Momentum*, World Scientific, Singapore, **1988**.

[16] J. J. Sakurai, J. Napolitano, *Modern Quantum Mechanics:* Second, Cambridge University Press, **2017**.

[17] E. P. Wigner, *Group Theory and Its Application to the Quantum Mechanics of Atomic Spectra*, Expanded and improved ed, Academic Press, New York, **1959**.

[18] W. Gerlach, O. Stern, *Z. Physik* **1922**, *9*, 349–352.

[19] W. Gerlach, O. Stern, *Z. Physik* **1922**, *9*, 353–355.

[20] H. C. Ohanian, *Am. J. Phys.* **1986**, *54*, 500–505.

[21] J. H. Van Vleck, *J. Chem. Phys.* **1939**, *7*, 72–84.

[22] J. H. Van Vleck, *Phys. Rev.* **1940**, *57*, 426–447.

[23] M. H. L. Pryce, *Proc. Phys. Soc. A* **1950**, *63*, 25–29.

[24] A. Abragam, M. H. L. Pryce, *Proc. R. Soc. Lond. A* **1951**, *205*, 135–153.

[25] S. A. Smith, W. E. Palke, J. T. Gerig, *Concepts Magn. Reson.* **1992**, *4*, 107–144.

[26] S. A. Smith, W. E. Palke, J. T. Gerig, *Concepts Magn. Reson.* **1992**, *4*, 181–204.

[27] G. Pileio, *Prog. Nucl. Mag. Res. Sp.* **2010**, *56*, 217–231.

[28] E. L. Hahn, D. E. Maxwell, *Phys. Rev.* **1952**, *88*, 1070–1084.

[29] P. S. Hubbard, *Phys. Rev.* **1963**, *131*, 1155–1165.

[30] J. Blicharski, *Z. Naturforsch. A* **1972**, *27*, 1456–1458.

[31] F. A. L. Anet, D. J. O'Leary, *Concepts Magn. Reson.* **1991**, *3*, 193–214.

[32] F. A. L. Anet, D. J. O'leary, *Concepts Magn. Reson.* **1992**, *4*, 35–52.

[33] J. P. King, T. F. Sjolander, J. W. Blanchard, *J. Phys. Chem. Lett.* **2017**, *8*, 710–714.

[34] N. Bloembergen, E. M. Purcell, R. V. Pound, *Phys. Rev.* **1948**, *73*, 679–712.

[35] I. Solomon, *Phys. Rev.* **1955**, *99*, 559–565.

[36] N. Bloembergen, *J. Chem. Phys.* **1957**, *27*, 572–573.

[37] N. Bloembergen, L. O. Morgan, *J. Chem. Phys.* **1961**, *34*, 842–850.

[38] J. Kowalewski, L. Nordenskiöld, N. Benetis, P.-O. Westlund, *Prog. Nucl. Mag. Res. Sp.* **1985**, *17*, 141–185.

[39] A. J. Pell, G. Pintacuda, C. P. Grey, *Prog. Nucl. Mag. Res. Sp.* **2019**, *111*, 1–271.

[40] R. V. Pound, *Phys. Rev.* **1950**, *79*, 685–702.

[41] J. Pople, *Mol. Phys.* **1958**, *1*, 168–174.

[42] L. Werbelow, G. Pouzard, *J. Phys. Chem.* **1981**, *85*, 3887–3891.

[43] P. P. Man, *Concepts Magn. Reson.* **2013**, *42*, 197–244.

[44] L. J. Mueller, *Concepts Magn. Reson.* **2011**, *38A*, 221–235.

[45] E. Vinogradov, A. K. Grant, *J. Magn. Reson.* **2007**, *188*, 176–182.

[46] M. Carravetta, O. G. Johannessen, M. H. Levitt, *Phys. Rev. Lett.* **2004**, *92*, 153003.

[47] M. Bouten, *Physica* **1969**, *42*, 572–580.

[48] Y. Millot, P. P. Man, *Concepts Magn. Reson.* **2012**, *40A*, 215–252.

[49] C. Bengs, M. H. Levitt, *Magn. Reson. Chem.* **2018**, *56*, 374–414.

[50] M. Mehring, *Principles of High Resolution NMR in Solids*, Second, revised and enlarged edition, softcover reprint of the hardcover 2nd edition 1983, Springer, Berlin Heidelberg New York, **1983**.

[51] L. Gengying, X. Haibin, *Rev. Sci. Instrum.* **1999**, *70*, 1511–1513.

[52] H.-P. Breuer, F. Petruccione, *The Theory of Open Quantum Systems*, Clarendon, Oxford, **2007**.

[53] D. Manzano, *AIP Adv.* **2020**, *10*, 025106.

[54] R. K. Wangsness, F. Bloch, *Phys. Rev.* **1953**, *89*, 728–739.

[55] F. Bloch, *Phys. Rev.* **1956**, *102*, 104–135.

[56] A. G. Redfield, *IBM J. Res. Dev.* **1957**, *1*, 19–31.

[57] A. Redfield, *Adv. Magn. Reson.* **1965**, *1*, 1–32.

[58] M. Goldman, *J. Magn. Reson.* **2001**, *149*, 160–187.

[59] C. Bengs, M. H. Levitt, *J. Magn. Reson.* **2020**, *310*, 106645.

[60] M. H. Levitt, C. Bengs, *Magn. Reson.* **2021**, *2*, 395–407.

[61] R. Dümcke, H. Spohn, *Z Physik B* **1979**, *34*, 419–422.

[62] H. Spohn, *Rev. Mod. Phys.* **1980**, *52*, 569–615.

[63] A. Suárez, R. Silbey, I. Oppenheim, *J. Chem. Phys.* **1992**, *97*, 5101–5107.

[64] P. Pechukas, *Phys. Rev. Lett.* **1994**, *73*, 1060–1062.

[65] L. G. Werbelow, R. E. London, *J. Chem. Phys.* **1995**, *102*, 5181–5189.

[66] L. Werbelow, R. E. London, *Concepts Magn. Reson.* **1996**, *8*, 325–338.

[67] L. G. Werbelow in *Encyclopedia of Magnetic Resonance*, (Ed.: R. K. Harris), John Wiley & Sons, Ltd, Chichester, UK, **2011**, emrstm0138.pub2.

[68] W. T. Huntress, *J. Chem. Phys.* **1968**, *48*, 3524–3533.

[69] W. T. Huntress, *Adv. Magn. Reson.* **1970**, *4*, (Ed.: J. S. Waugh), 1–37.

[70] L. D. Favro, *Phys. Rev.* **1960**, *119*, 53–62.

[71] P. Schofield, *Phys. Rev. Lett.* **1960**, *4*, 239–240.

[72] B. J. Berne, R. G. Gordon, V. F. Sears, *J. Chem. Phys.* **1968**, *49*, 475–476.

[73] S.-C. An, C. J. Montrose, T. A. Litovitz, *J. Chem. Phys.* **1976**, *64*, 3717–3719.

[74] P. H. Berens, D. H. J. Mackay, G. M. White, K. R. Wilson, *J. Chem. Phys.* **1983**, *79*, 2375–2389.

[75] J. S. Bader, B. J. Berne, *J. Chem. Phys.* **1994**, *100*, 8359–8366.

[76] J. L. Skinner, *J. Chem. Phys.* **1997**, *107*, 8717–8718.

[77] D. W. Oxtoby in *Advances in Chemical Physics*, (Eds.: J. Jortner, R. D. Levine, S. A. Rice), John Wiley & Sons, Inc., Hoboken, NJ, USA, **2007**, pp. 487–519.

[78] B. J. Berne, G. D. Harp in *Advances in Chemical Physics*, (Eds.: I. Prigogine, S. A. Rice), John Wiley & Sons, Inc., Hoboken, NJ, USA, **2007**, pp. 63–227.

[79] S. Egorov, J. Skinner, *Chem. Phys. Lett.* **1998**, *293*, 469–476.

[80] B. A. Rodin, C. Bengs, A. S. Kiryutin, K. F. Sheberstov, L. J. Brown, R. C. D. Brown, A. V. Yurkovskaya, K. L. Ivanov, M. H. Levitt, *J. Chem. Phys.* **2020**, *152*, 164201.

[81] M. Carravetta, M. H. Levitt, *J. Chem. Phys.* **2005**, *122*, 214505.

[82] G. Pileio, M. H. Levitt, *J. Chem. Phys.* **2009**, *130*, 214501.

[83] G. Pileio, *J. Chem. Phys.* **2011**, *134*, 214505.

[84] G. Pileio, J. T. Hill-Cousins, S. Mitchell, I. Kuprov, L. J. Brown, R. C. D. Brown, M. H. Levitt, *J. Am. Chem. Soc.* **2012**, *134*, 17494–17497.

[85] B. Meier, J.-N. Dumez, G. Stevanato, J. T. Hill-Cousins, S. S. Roy, P. Håkansson, S. Mamone, R. C. D. Brown, G. Pileio, M. H. Levitt, *J. Am. Chem. Soc.* **2013**, *135*, 18746–18749.

[86] J.-N. Dumez, P. Håkansson, S. Mamone, B. Meier, G. Stevanato, J. T. Hill-Cousins, S. S. Roy, R. C. D. Brown, G. Pileio, M. H. Levitt, *J. Chem. Phys.* **2015**, *142*, 044506.

[87] G. Stevanato, S. Singha Roy, J. Hill-Cousins, I. Kuprov, L. J. Brown, R. C. D. Brown, G. Pileio, M. H. Levitt, *Phys. Chem. Chem. Phys.* **2015**, *17*, 5913–5922.

[88] M. H. Levitt, *J. Magn. Reson.* **2019**, *306*, 69–74.

[89] S. J. Elliott, C. Bengs, L. J. Brown, J. T. Hill-Cousins, D. J. O'Leary, G. Pileio, M. H. Levitt, *J. Chem. Phys.* **2019**, *150*, 064315.

[90] *Long-Lived Nuclear Spin Order: Theory and Applications*, 1 edition, (Ed.: G. Pileio), Royal Society of Chemistry, S.l., **2020**.

[91] C. Bengs, *J. Chem. Phys.* **2020**, *152*, 054106.

[92] C. Bengs, L. Dagys, G. A. I. Moustafa, J. W. Whipham, M. Sabba, A. S. Kiryutin, K. L. Ivanov, M. H. Levitt, *J. Chem. Phys.* **2021**, *155*, 124311.

[93] D. E. Korenchan, J. Lu, M. Sabba, L. Dagys, L. J. Brown, M. H. Levitt, A. Jerschow, *Phys. Chem. Chem. Phys.* **2022**, *24*, 24238–24245.

[94] M. Carravetta, M. H. Levitt, *J. Am. Chem. Soc.* **2004**, *126*, 6228–6229.

[95] G. Stevanato, J. T. Hill-Cousins, P. Håkansson, S. S. Roy, L. J. Brown, R. C. D. Brown, G. Pileio, M. H. Levitt, *Angew. Chem. Int. Ed.* **2015**, *54*, 3740–3743.

[96] J. W. Whipham, G. A. I. Moustafa, M. Sabba, W. Gong, C. Bengs, M. H. Levitt, *J. Chem. Phys.* **2022**, *157*, 104112.

[97] H. M. McConnell, *J. Chem. Phys.* **1956**, *25*, 709–711.

[98] H. Shimizu, *J. Chem. Phys.* **1964**, *40*, 3357–3364.

[99] L. G. Werbelow, D. M. Grant, *Adv. Magn. Reson.* **1977**, *9*, 189.

[100] M. Goldman, *J. Magn. Reson.* **1984**, *60*, 437–452.

[101] L. Di Bari, J. Kowalewski, G. Bodenhausen, *J. Chem. Phys.* **1990**, *93*, 7698–7705.

[102] A. Kumar, R. Christy Rani Grace, P. K. Madhu, *Prog. Nucl. Mag. Res. Sp.* **2000**, *37*, 191–319.

[103] P. K. Madhu, P. K. Mandal, N. Müller, *J. Magn. Reson.* **2002**, *155*, 29–38.

[104] J. Kowalewski, L. Mäler, *Nuclear Spin Relaxation in Liquids Theory, Experiments, and Applications*, Second, CRC Press, Taylor & Francis Group, Boca Raton, FL, **2018**.

[105] B. Reif, M. Hennig, C. Griesinger, *Science* **1997**, *276*, 1230–1233.

[106] B. Reif, H. Steinhagen, B. Junker, M. Reggelin, C. Griesinger, *Angew. Chem. Int. Ed.* **1998**, *37*, 1903–1906.

[107] S. Ravindranathan, X. Feng, T. Karlsson, G. Widmalm, M. H. Levitt, *J. Am. Chem. Soc.* **2000**, *122*, 1102–1115.

[108] K. Pervushin, R. Riek, G. Wider, K. Wüthrich, *Proc. Natl. Acad. Sci. USA* **1997**, *94*, 12366–12371.

[109] V. Tugarinov, P. M. Hwang, J. E. Ollerenshaw, L. E. Kay, *J. Am. Chem. Soc.* **2003**, *125*, 10420–10428.

[110] G. Lipari, A. Szabo, *J. Am. Chem. Soc.* **1982**, *104*, 4546–4559.

[111] G. Lipari, A. Szabo, *J. Am. Chem. Soc.* **1982**, *104*, 4559–4570.

[112] L. K. Lee, M. Rance, W. J. Chazin, A. G. Palmer, *J. Biomol. NMR* **1997**, *9*, 287–298.

[113] M. Marcellini, M.-H. Nguyen, M. Martin, M. Hologne, O. Walker, *J. Phys. Chem. B* **2020**, *124*, 5103–5112.

[114] N. Tjandra, P. Wingfield, S. Stahl, A. Bax, *J. Biomol. NMR* **1996**, *8*, 273–284.

[115] M. J. Osborne, P. E. Wright, *J. Biomol. NMR* **2001**, *19*, 209–230.

[116] M. Sabba, N. Wili, C. Bengs, J. W. Whipham, L. J. Brown, M. H. Levitt, *J. Chem. Phys.* **2022**, *157*, 134302.

[117] M. H. Levitt, *Annu. Rev. Phys. Chem.* **2012**, *63*, 89–105.

[118] M. C. D. Tayler, M. H. Levitt, *Phys. Chem. Chem. Phys.* **2011**, *13*, 5556–5560.

[119] R. Radeglia, *Solid State Nucl. Mag.* **1995**, *4*, 317–321.

[120] R. P. Young, C. R. Lewis, C. Yang, L. Wang, J. K. Harper, L. J. Mueller, *Magn. Reson. Chem.* **2019**, *57*, 211–223.

[121] A. D. Becke, *J. Chem. Phys.* **1992**, *96*, 2155–2160.

[122] T. H. Dunning, *J. Chem. Phys.* **1989**, *90*, 1007–1023.

[123] R. A. Kendall, T. H. Dunning, R. J. Harrison, *J. Chem. Phys.* **1992**, *96*, 6796–6806.

[124] M. J. Frisch, G. W. Trucks, H. B. Schlegel, G. E. Scuseria, M. A. Robb, J. R. Cheeseman, G. Scalmani, V. Barone, G. A. Petersson, H. Nakatsuji, X. Li, M. Caricato, A. V. Marenich, J. Bloino, B. G. Janesko, R. Gomperts, B. Mennucci, H. P. Hratchian, J. V. Ortiz, A. F. Izmaylov, J. L. Sonnenberg, D. Williams-Young, F. Ding, F. Lipparini, F. Egidi, J. Goings, B. Peng, A. Petrone, T. Henderson, D. Ranasinghe, V. G. Zakrzewski, J. Gao, N. Rega, G. Zheng, W. Liang, M. Hada, M. Ehara, K. Toyota, R. Fukuda, J. Hasegawa, M. Ishida, T. Nakajima, Y. Honda, O. Kitao, H. Nakai, T. Vreven, K. Throssell, J. A. Montgomery, Jr., J. E. Peralta, F. Ogliaro, M. J. Bearpark, J. J. Heyd, E. N. Brothers, K. N. Kudin, V. N.

Staroverov, T. A. Keith, R. Kobayashi, J. Normand, K. Raghavachari, A. P. Rendell, J. C. Burant, S. S. Iyengar, J. Tomasi, M. Cossi, J. M. Millam, M. Klene, C. Adamo, R. Cammi, J. W. Ochterski, R. L. Martin, K. Morokuma, O. Farkas, J. B. Foresman, D. J. Fox, Gaussian 09, Gaussian, Inc. Wallingford CT, **2016**.

[125] U. Haeberlen, *High Resolution NMR in Solids: Selective Averaging*, Academic Press, New York, **1976**.

[126] G. S. Harbison, *J. Am. Chem. Soc.* **1993**, *115*, 3026–3027.

[127] M. H. Levitt, *J. Magn. Reson.* **1997**, *126*, 164–182.

[128] Mathematica, Version 12.3.1.0, Wolram Research, Inc., Champaign, IL, 2021.

[129] G. Pileio, *Prog. Nucl. Mag. Res. Sp.* **2017**, *98–99*, 1–19.

[130] A. Buckingham, S. Malm, *Mol. Phys.* **1971**, *22*, 1127–1130.

[131] M. H. Levitt, *Prog. Nucl. Mag. Res. Sp.* **1986**, *18*, 61–122.

[132] B. A. Rodin, K. F. Sheberstov, A. S. Kiryutin, L. J. Brown, R. C. D. Brown, M. Sabba, M. H. Levitt, A. V. Yurkovskaya, K. L. Ivanov, *J. Chem. Phys.* **2019**, *151*, 234203.

[133] G. Pileio, M. H. Levitt, *J. Magn. Reson.* **2008**, *191*, 148–155.

[134] J. B. Klauda, M. F. Roberts, A. G. Redfield, B. R. Brooks, R. W. Pastor, *Biophys. J.* **2008**, *94*, 3074–3083.